THE ROLE OF MEMBRANE LIPID COMPOSITION ON SKELETAL MUSCLE DAMAGE IN THE RODENT MODEL OF DUCHENNE MUSCULAR DYSTROPHY

MARAL ZIBAMANZARMOFRAD, MD

Submitted in partial fulfilment of the requirements for the degree of
Masters of Science in Applied Health Sciences
(Health Sciences)

Under the supervision of Dr. Paul J. LeBlanc

Faculty of Applied Health Sciences, Brock University
St. Catharines, Ontario

ABSTRACT

Duchenne muscular dystrophy is a X-linked muscle disease, which leads to alterations in membrane phospholipid fatty acid (FA) composition and skeletal muscle damage. Increased membrane saturated FA in muscular dystrophy may suggest its association with increased susceptibility (as being the cause or consequence) to muscle damage. It was hypothesised that increased saturation is positively correlated to increased muscle damage. Correlations were hypothesized to be greater in extensor digitorum longus (EDL) at 20 weeks compared to soleus (SOL) at 10 weeks in dystrophin deficient (*mdx*) mice. Increased saturation was correlated to damage in EDL at both 10 and 20 weeks, with stronger correlations at 10 weeks. The results suggest that membrane PL FA composition may be associated with damage through two possible means. Increased saturation may be a cause or consequence of membrane damage. Association of membrane composition with eccentric induced damage has underscored the importance of saturated PL FA compositions in damage to dystrophic myofibres.

Keywords: Muscular dystrophy, mdx, membrane damage, fatty acids

ACKNOWLEDGEMENTS

First of all, I would like to express my sincerest gratitude to my supervisor, Dr. Paul LeBlanc. His continuous support and inspiration enable me to move forward smoothly through every step of my research. His illuminating instruction and guidance have laid a solid foundation on my research experience, which benefit me throughout the program.

I feel very grateful to receive the supports from my committee member, Dr. Rob Grange and Dr. Rene Vandenboom, who offer splendid and constructive suggestions during the entire process of my thesis development. I would like to extend my appreciation to my external examiner, Dr. Thad Harroun, for his valuable suggestions and insightful comments on my thesis.

A great deal of thanks is owed to William Gittings for taking time out of his busy schedules to accommodate this research with his great experience and knowledge.

I would like to thank my husband Arash, my parents and Tanaby for their infinite supports throughout my entire education, and encouragement, without whom I would not have made it this far.

CONTRIBUTIONS

This thesis incorporates the outcome of a joint research project undertaken in collaboration with William Gittings under the supervision of Dr. Rene Vandenboom. In all cases, the key ideas, primary contributions, experimental designs, data analysis and interpretation, were performed by the author, and the contribution of W. Gittings was primarily through the provision of skeletal muscle isolation, stretch injury, functional and contractile parameters.

LIST OF ABBREVIATION

ABC: avidin biotin complex

ATP: adenosine triphosphate

BSA: bovine serum albumin

BMD: Becker muscular dystrophy

Ca^{2+} ATPase: calcium ATPase

CK: creatine kinase

CL: cardiolipin

DAB: diaminobenzidine

DDW: double distilled water

DGC: dystrophin glycoprotein complex

DHPR: dihydropiridine receptor

DMD: Duchenne muscular dystrophy

EDL: extensor digitorum longus

FA: fatty acid

FG: fast glycolytic

FOG: fast oxidative glycolytic

GC: gas chromatography

HRP: horseradish peroxidase

MUFA: mono unsaturated fatty acid

Na^{+}/K^{+} ATPase: sodium potassium ATPase

OCT: optimized cryo temperature

PBS: phosphate base solution

PC: phosphatidylcholine

PE: phosphatidylethanolamine

PFA: paraformaldehyde

PI: phosphatidylinositol

PL: phospholipid

PS: phosphatidylserine

PUFA: polyunsaturated fatty acid

RT: room temperature

SAC: stretch activated channels

SERCA: sarco(endo)plasmic reticulum calcium ATPase

SFA: saturated fatty acid

SL: sarcolemma

SM: sphingomyelin

SO: slow oxidative

SOL: soleus

SR: sarcoplasmic reticulum

TBS: tris base solution

TLC: thin layer chromatography

TnC: troponin C

WT: wild type

TABLE OF CONTENTS

LIST OF FIGURES

LIST OF TABLES

CHAPTER 1: INTRODUCTION

Biological membranes

Biological membranes are barriers surrounding the cell that define the boundary between the intracellular and extracellular environment. Moreover, biological membranes are semi-permeable, allowing movement of macromolecules essential in cell metabolism, differentiation and regulation (Keren, 2011). Furthermore, ion channels in membranes facilitate the production of excitation contraction coupling (ECC) by conducting action potentials along the membrane. As a result, considering the central roles of biological membranes in cell signalling, regulation, and metabolism, understanding its constituents (lipids, carbohydrates and proteins) is of significant importance.

Biological membranes are composed of different compounds, which vary among cells according to their function. Biological membranes are assembled in a bilayer which is comprised mainly of lipids, in addition to proteins and carbohydrates (Alberts, *et al.*, 2002). Proteins in biological membranes are located peripheral to the membrane or integral by spanning across the membrane. Carbohydrates are associated with lipids and proteins, forming glycolipids and glycoproteins, respectively (Voet & Voet, 2004).

Membrane composition

Membrane lipids

There are three major types of lipids found in cell membranes; phospholipids, glycolipids, and cholesterol. These main classes of membrane lipids are amphipathic and the orientation of their hydrophobic and hydrophilic regions directs their location within the membrane bilayer (Alberts *et al.*, 2002). Within these three classes of membrane

lipids, vast diversity in phospholipids is due to various combinations of head groups and/or fatty acyl tails.

Phospholipids

Phospholipids make up 80-85% of biological membrane structure (Dufourc *et al.*, 1992). The main structure of a phospholipid contains either a glycerol (1, 2- diacyl- sn-glycerol) or sphingosine (N-acyl-sphingosine) backbone to which 2-4 fatty acyl chains (hydrophobic) and a phosphate head group are attached, thus forming glycerophospholipids or sphingophospholipids, respectively (Cooper, 1977; Dannenberger *et al.*, 2007). The head group varies between phospholipids, resulting in different phospholipid species. Head groups that contain choline, serine, ethanolamine or inositol result in phosphotidylcholine (PC), phosphatidylserine (PS), phosphatidylethanolamine (PE), and phosphatidylinositol (PI), respectively. Cardiolipin (CL) is known to be a double glycerophospholipid and consists of two phosphatidylglycerols connected with a glycerol backbone, forming a dimeric structure with four fatty acyl chains (Ritov *et al.*, 2006). Sphingomyelin (SM) is a sphingophospholipid having a unique structure with a sphingosine backbone, choline head group, and 2 fatty acyl chains. One of the SM FA tails is ceramide, which is comprised of an amide group and fatty acyl chain attached to a sphingosine molecule (Brown, 1998). Two forms of SM have been identified in cell membranes; sphingosile-1 phosphorylcholine and sphingosile-1 phosphorylethanolamine (Ramstedt *et al.*, 2002). Altogether, these phospholipids are present in differing biological cell membranes and in differing amounts (Table 1.1).

Glycolipids

The glycolipids constitute 5% of lipids in biological membrane, exclusively located on the outer surface of membrane (Voet, 2004). Glycolipids have a carbohydrate head group instead of phosphate as seen in phospholipids (Yamomoto *et al.*, 1998). However, similar to phospholipids, the backbone structure could be glycerol or sphingosine, creating glyceroglycolipids and sphingoglycolipids, respectively.

Cholesterol

Cholesterol is a lipid molecule with a unique four linked hydrocarbon ring structure, hydrocarbon side chains and a hydroxyl group (Bell *et al.*, 1976). Cholesterol is also amphipathic where its hydroxyl group aligns with the phosphate head of phospholipids and its hydrophobic steroid rings stays adjacent to the fatty acyl tail. Cholesterol preferentially interacts with SM compare to other phospholipids due to interactive forces between its rigid ring structure and saturated fatty acids of SM (Yeagle, 1990; Ramstedt & Slotte, 2002). Moreover, cholesterol is more abundant in micro-domains, named lipid rafts, enriched with SM (Ramstedt & Slotte, 2002).

Table 1.1. Characteristics of the main lipids found in biological membranes.

Lipid	Composition	Charge	Primary fatty acids	Location
PC	30-35%[2]	Neutral[1]	↑ 16:0, 18:2n6 and ↓ 22:6n3[2]	Outer monolayer (66%)[3]
PE	15-25%[4,5]	Neutral[4,5]	↑18:0[3], 20:4n6[3], and 18:2n6[6]	Inner monolayer (~20%)[3,6]
SM	2-15%[8,9]	Neutral [8]	↑ 16:0 and 18:0, ↓ UFA, 24:1 and 22:0[1,8]	Outer monolayer[8,9]
PI	10-15%[1]	Acidic[1]	18:0 in sn-1, 20:4 in sn-2[1]	Inner monolayer
PS	2-10%	Acidic[1]	↑22:6n3	Inner monolayer
CL	2-5%[9]	Acidic	18:2n6[6], ↑ levels (80%) of unsaturation[7]	Matrix facing leaflet of mitochondria[6]
Cholesterol	10%	Neutral		Inner and outer monolayer
Glycolipids	2-5%	Neutral		Outer monolayer

Original data obtained from: [1](Voet, 2004), [2](Mitchell, *et al.*, 2007), [3] (Clore, *et al.*, 1998), [4] (Bell GH, 1976), [5] (Bleijerveld, *et al.*, 2007), [6] (Ritov, *et al.*, 2006), [7] (Tsalouhidou, *et al.*, 2006),[8] (Ramstedt & Slotte, 2002), [9] (Tsalouhidou, *et al.*, 2006). PL, phospholipids; SM, sphingomyelin; PC, phosphatidylcholine; PS, phosphatidylserine; PI, phosphatidylinositol; PE, phosphatidylethanolamine; sn stereospecific numbering; UFA, unsaturated fatty acid.

Fatty acids

Fatty acids are long chain carboxylic acids (mostly 14-20 carbons), containing a long alkyl chain with a carboxyl group at one end. Normally FAs have an even number of carbon atoms and can be saturated (SFA), with no double bonds, or unsaturated, with one or more double bonds. Unsaturated fatty acids are classified as monounsaturated fatty acids (MUFA, one double bond) and polyunsaturated fatty acids (PUFA, more than one double bond) (Hamilton, 2003). PUFAs are further subclassified as n3 or n6, where the position of first double bond occurs on the 3^{rd} or 6^{th} carbon relative to the methyl end, respectively (Lauritzen *et al.*, 2001). Additional classification of FAs is according to their configuration. Fatty acids with double bonds have two types of configuration, known as *cis* and *trans*. The *cis* configuration has the hydrogen atoms on the same side as the carbon-carbon double bond causing a 30˚kink in the chain (Whitney *et al.*, 1998) while the *trans* configuration has the hydrogen on opposite sides (Figure 1.1). Spatial configuration of FAs is important since it dictates how close FAs can associate with their adjacent FAs.

The nomenclature of fatty acids is according to their carbon length, number of double bonds and the location of the first double bond. For example, 18:2n6 refers to an 18 carbon long fatty acid with two double bonds with the first double bond at the 6^{th} carbon from the methyl end. Both 18:2n6 and 18:3n3 PUFA are regarded as essential fatty acids due to the inability of mammals to introduce double bonds beyond carbon 9 and 10 from the methyl end (Berg, 2002; Gurr, 2002; Pelley, 2011) therefore, they must obtain these fatty acids from their diet (Connor, 2000).

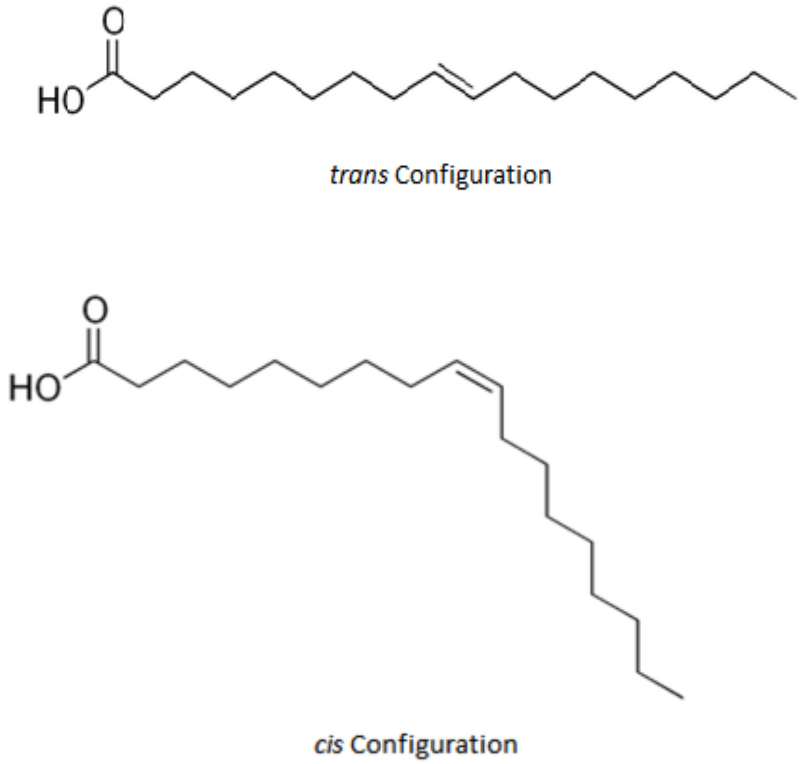

Figure 1.1 .View of cis and trans configurations of fatty acids.

Membrane proteins

Membrane proteins carry out dynamic processes associated with the cell. These processes include enzyme activity, transportation across the membrane, cellular attachments, cell to cell communication, and signal transduction. These processes are important in cellular function and its response to the environment (Houston, 2006). Membrane proteins are classified according to their association with the membrane into integral or intrinsic and peripheral or extrinsic proteins (Voet, 2004). Integral or intrinsic proteins are embedded within the membrane and may be exposed on one side of a membrane or span the membrane, being exposed on both sides of the membrane. Peripheral or extrinsic proteins are loosely bound to the head group of phospholipids or other integral proteins.

Membrane fluidity

The organization and interaction of the components of the membrane is said to be fluid, as explained by the fluid mosaic model. In this model of cell membrane structure, the membrane is envisioned as an assortment of individually inserted protein molecules drifting laterally in a fluid bilayer of phospholipids. This model best explains the fluidity and function of the membrane by modulating the interactions between lipids and proteins (Singer & Nicolson, 1972). Membrane fluidity is defined as the viscosity of the membrane and is characterized by ease of motion within the bilayer. Fluidity is an important factor in membrane function that influences many biological and biochemical processes within the cell such as metabolism, transportation of chemicals, cell fusion, and protein rotation and diffusion. Membrane fluidity is determined by the phospholipid

species, fatty acid composition and cholesterol content of the membrane (Garzetti *et al.*, 1993).

Phospholipid species

Phospholipids may adopt different molecular shapes according to their head group. PC, SM and PS adopt cylindrical shapes, whereas PE and CL have cone shapes. PI possesses a large polar head in compare to its fatty acids which formulates an inverted cone shape (Alberts, 2002; Ramstedt & Slotte, 2002; Figure 1.2). Molecular shapes of PLs predict the packing nature of PL within a membrane. PLs with cone or inverse cone shapes are able to pack closely to each other, decreasing membrane fluidity. In contrast, PLs with cylinder shapes do not pack tightly in the membrane, resulting in increased membrane fluidity (Cullis & Kruijff, 1979; Figure 1.2).

Fatty acid characteristics

Fatty acyl chain length and degree of saturation modulate membrane fluidity. Long chain fatty acids have higher hydrophobic attractions compared to short chain fatty acids, resulting in more rigid membranes (Nikolaidis & Mougios, 2004). Unsaturated FAs increase fluidity of the membrane. Specifically, within MUFAs, membrane fluidity is promoted when the double bond resides in the middle of an acyl chain, indicating that membrane order is minimized under this condition (Marsh, 1999). Similarly, PUFAs with multiple double bonds are less able to pack closely to each other increasing fluidity with increasing numbers of double bonds (Yang *et al.*, 2011). Additionally, unsaturated fatty acids can adopt *cis* or *trans* conformation. FAs with *trans* configuration pack closely

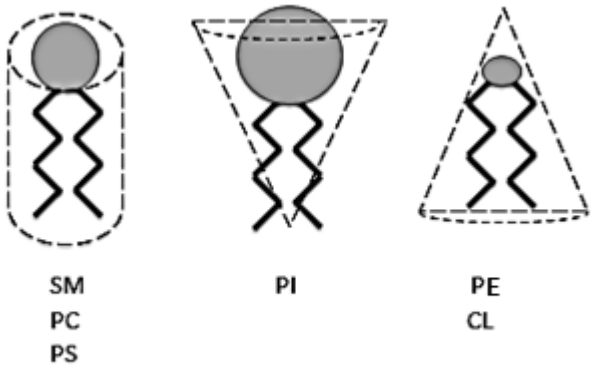

Figure 1.2. Molecular shapes of phospholipids incorporated in the membrane.

together and decrease membrane fluidity (Keogh at al., 1987; Stubbs *et al.*, 19981).

Cholesterol

Cholesterol can impact fluidity according to its concentrations. Cholesterol has attached steroid rings which are able to pack tightly with PL FA chains, restrict motion and decrease membrane fluidity (Voet & Voet, 2004). However, at high concentrations within a membrane, cholesterol decreases acyl chain hydrocarbons from interacting, restricting tight packing and increasing fluidity (Voet & Voet, 2004). However, the concentration of cholesterol in the membrane is largely dependent on the degree of unsaturation and length of the FA chains (Ramstedt & Slotte, 2002). With increased unsaturated FAs, as a result of cholesterol desorption, the concentration decreases (Ramstedt & Slotte, 2002). In contrast, with increase in SFA, cholesterol concentration increases due to attraction between SFA chains and the rigid steroid ring backbone of cholesterol (Ramstedt & Slotte, 2002).

Membrane structure protein function relationship

Protein function can be, in part, controlled and regulated by the local lipid environment, mediated partially through membrane fluidity. Some proteins require a fluid lipid environment for optimum function while some proteins prefer a more rigid environment (Edidin, 2003). For example, band 3 anion transporter activity decreases after increasing membrane cholesterol and increases with depletion (Bataglia & Schimmel, 1997; Schubert & Boss, 1982).

Impact of lipid composition on protein function

Specific lipids within membranes modulate biological function of the cell by their influence on membrane-associated proteins. The influence of lipids on membrane bound proteins is dependent on the asymmetrical distribution of lipids on each side of the bilayer. PS, PI and PE are mainly located on the cytoplasmic surface of the bilayer, whereas PC and SM comprise the external mono layer. PI in the inner leaflet of the bilayer has shown to be an important mediator in membrane-cytoskeletal association by regulating actin filament assembly, polymerization, and promoting activity of proteins that are essential in regulation of actin assembly (Hilpela *et al.*, 2004). External location of PS contributes to cell recognition for apoptosis and initiation of coagulation pathways (Hasegawa *et al.*, 2006). Similarly, CL exclusive localization in the inner layer of mitochondria is related to its modulating and stabilizing activity of the mitochondrial electron transport chain (Ritov *et al.*, 2006). Moreover, segregation of cholesterol and SM in lipid rafts provides an environment for proteins to partition into ordered raft domains to modulate their activity. Typical example includes the glycosylphosphatidylinositol (GPI) proteins, which are attached to the outer leaflet of the membrane via the GPI anchor in a lipid raft (Chatterjee & Mayor, 2001). Previous research has demonstrated that Na^{+}-K^{+}-ATPase activity can be influenced by the concentration of cholesterol in the area of the membrane where it is found (Yeagle, 1990).

While lipids can impact regulatory processes within the cell by their influence on proteins associated with the membrane, proteins are capable of dictating the lipid composition of the membrane around said protein, also called the lipid annulus. An important characteristic of the lipid bilayer is its hydrophobic core thickness, which is

related to fatty acid chain length and saturation (Deborah *et al.*, 1993; Killian, 1998). The hydrophobic thickness of the lipid bilayer is arranged to match the hydrophobic thickness of an integral membrane protein because of the high cost of exposing either fatty acyl chains or hydrophobic amino acids to an aqueous environment (Killian, 1993). Any mismatch between the hydrophobic thickness of embedded proteins and of the membrane cause lipids to bend, tilt and stretch to satisfy the hydrophobic matching at the interface (Figure 1.3; Webb *et al.*, 1993; Fattal & Shaul, 1993). Alternatively, hydrophobic mismatching can be minimized by substituting mismatched annular phospholipids with better matching neighbouring phospholipids. This phospholipid movement is mediated by flippase enzymes to flip the phospholipids to the opposite leaflet, or by translocase enzymes to displace phospholipids laterally along the membrane (Martinak & Hamilton, 2003; Hamilton, 2003; Jensen & Moritsen, 2004). Together, membrane lipid content influences cell regulatory process performed by proteins, where membrane proteins are able to assign or distribute specific phospholipids to areas along the membrane.

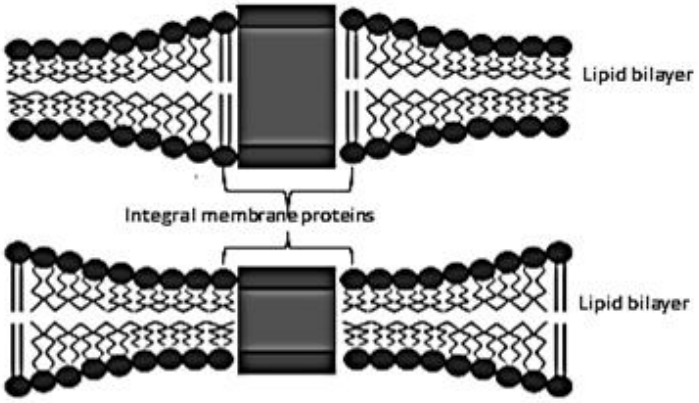

Figure 1.3. Schematic depiction of influence of proteins on physical properties of fatty acids. Shrinkage and bending of fatty acids corresponding to alterations in hydrophobic length of integral proteins.

Skeletal muscle

Skeletal muscle comprises 40% of body weight in normal weight individuals and is responsible for body movements (Owen *et al.*, 1978). Skeletal muscle is made up of myofibres that run throughout the muscle length. Each myofibre contains bundles of myofibrils comprised of smaller units of actin and myosin filaments. Actin and myosin are arranged in repeating units of sarcomeres, and their patterned arrangement gives striated muscle its characteristic banded appearance. Myofibre populations have different characteristic that also varies among different muscle types.

Skeletal muscle cell structure

Skeletal muscle cells house a variety of subcellular organelles with specialized proteins taking part to provide essential functions. To initiate contraction, impulses are transmitted from nerve endings to motor end plates of muscle fibres causing the depolarization of the cell membrane when Na^+ voltage-gated channels allow an influx of Na^+. Re-establishing resting membrane potential is the responsibility of the Na^+/K^+ ATPase, where it pumps 3 Na^+ and 2 K^+.

The skeletal muscle cell membrane or sarcolemma (SL) propagates the action potential across the membrane. SL is a three layer surface membrane including a lipid bilayer sandwiched between basal lamina and sub-membranous cytoskeletal network (Ozawa, 2001). The basal lamina is mainly composed of non-fibrillar collagen, non-collagenous glycoproteins, and laminin covering the cell (Timpl & Rohrbach; 1972). The sub-membranous cytoskeletal network is a lattice of costamere proteins anchored to the bilayer (Ozawa *et al.*, 2001; Campbell & Stull, 2003). The basal lamina and cytoskeletal network are known as mechanically tough layers and their structural coupling with the bilayer reinforces the fragile bilayer from any damage and maintains its function.

The SL extends into the cell, creating t-tubule invaginations to propagate the action potential to the sarcoplasmic reticulum (SR) via dihydropyridine receptors (DHPR) located on t-tubules that are in tight association with ryanodine receptors on the terminal cisternae of the SR (Lee *et al.*, 2002, Al-Qusairi & Laporte, 2011). The action potential transmitted to the SR results in Ca^{+2} release from the SR, which is essential for muscle contraction (Katz *et al.*, 1986; Kadambi *et al.*, 1997).

Tropomyosin and troponin C (TnC) are two other proteins integral to contraction. TnC is attached to tropomyosin and lies within the groove between actin filaments. In a relaxed state, tropomyosin blocks the attachment site for the myosin cross bridge, thus preventing contraction (Morphy *et al.*, 1983). With the release of Ca^{+2} from SR, it binds to TnC, which promotes a change in the spatial configuration of the troponin-tropomyosin complex (Zhao & Kawai, 1994). Tropomyosin slides over, exposing the binding sites on actin.

With the binding of myosin to actin, actomyosin is primarily in a weakly bound low-force state. With the release of inorganic phosphate (Pi), the cross bridge subsequently transforms into a strongly bound high-force state. The myosin head hydrolyzes ATP, through myosin ATPase, and the energy is used to create the power stroke. Cross bridges return to a rigor complex state following the release of ADP. After this power stroke, ATP re-binds to myosin, causing it to be released from actin and forms the detached high-energy state. Once myosin is loaded with that potential energy, it binds to actin again, reforming the high-energy/attached state of the cross bridge (Figure 1.4). Cytoplasmic Ca^{+2} is pumped back into the SR through sarco(endo)plasmic reticulum Ca^{+2} ATPase (SERCA) transporters on the SR.

The source of ATP to supply the main ATP consuming processes (SERCA, myosin ATPase, and Na^{+}/K^{+} ATPase) is the mitochondria. There are two distinct mitochondrial subpopulations identified in skeletal muscles. Subsarcolemmal (SS) mitochondria are located underneath the sarcolemma whereas intermyofibrillar (IMF) mitochondria are interspersed between myofibrils (Ferriera *et al.*, 2010).

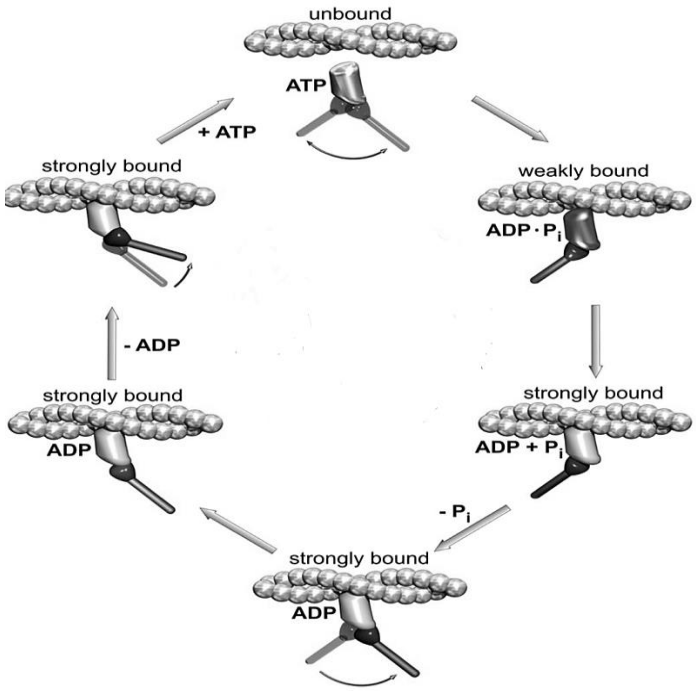

Figure 1.4. Actinomyosin ATPase cycle, binding of ATP, power stroke and Pi release. (Modified from Fitts, 2008)

Skeletal muscle fibre types

Skeletal muscles are classified into 4 main fibre types, slow oxidative (SO; type I), fast oxidative glycolytic (FOG; type IIa), fast glycolytic (FG; type IIb) (Pette & Staron, 2011) and a hybrid of IIa and IIb fibres identified as IId/x (Burkholder, 2005).

Type I, or SO, fibres have high levels of aerobic oxidative enzymes and rely on oxidative phosphorylation to produce ATP. These fibres have a high content of mitochondria and myoglobin. Moreover, it is observed that type I fibres have higher transport rate for glucose, free fatty acids, and amino acids (Rose *et al.*, 2005). As a consequence, type I fibres have a higher ability to generate more ATP through higher substrate entry into the cell. Due to ATP supply, these fibres show stability and fatigue resistance during prolonged submaximal activity, which makes them well adjusted for prolonged repetitive activities. Additionally, type I fibres have more and smaller motor units per muscle (Bottinelli *et al.*, 1999). Therefore, they have high sensitivity and rate of recruitment making them suitable for involvement in postural activity (e.g. joint stability). However, in terms of contractile properties, type I fibres have long twitch contraction times related to their low myosin ATPase kinetic activity and slow axonal conduction velocity that determines the slow contraction velocity of this fibre type (Moss *et al.*, 1995; Schiaffino *et al.*, 2007; Schiaffino and Reggiani, 2011, Wasterblad *et al*, 2010). Additionally, type I fibres have longer relaxation times explained by the lower rate and capacity for Ca^{+2} uptakes (Moss *et al.*, 1995). Given that the peak rate of tension development is limited by the time required for actinomyosin transition in bridge cycles, type I fibres produce lower peak tension but due to the simplicity of their neuromuscular

junctions, they elicit power at low stimulus frequencies (Ariano *et al.*, 1973; Scott *et al.*, 2001; Moss *et al*, 1995) (Table 1.2).

Type IIa, or FOG, fibres have aerobic oxidative and glycolytic enzymes making them suitable for long term (minutes- hours) anaerobic activities (Scott, 2001). Type IIa fibres have a very high capacity to generate ATP through oxidative metabolic processes, and hydrolyze ATP at a very rapid rate, resulting in higher contraction velocity compared to type I fibres (Schiaffino *et al.*, 2007). They have a high content of mitochondria and myoglobin and are fatigue resistant, making them suitable for sustained contraction (Schiaffino *et al.*, 2007) (Table 1.2). These fibres have short twitch contraction times with high myosin ATPase activity and short relaxation times related to more Ca^{+2} uptake by their SR. Compared to type I, type IIa fibres have higher rates of axonal conduction velocity and myosin ATPase activity creating shorter twitch contraction times (Ariano *et al.*, 1973; Adams *et al.*, 1993) (Table 1.2).

Type IIb fibres have the fastest twitch contraction time and have high content of anaerobic glycolytic enzymes to provide a rapid source of ATP that does not rely on mitochondria. However this pathway rapidly depletes glycogen storage and fatigue develops after brief usage (Hughes *et al.*, 1999). Additionally, type IIb fibres are characterized by the short time course of twitch and relaxation time with larger peak power output (Moss *et al.*, 1995; Scot *et al.*, 2001; Schiaffino *et al.*, 2007; Schiaffino and Reggiani, 2011, Wasterblad *et al*, 2010). Moreover, their neuromuscular junction creates low sensitivity to their recruitment saving them for activities requiring high force in short duration (Moss *et al.*, 1995; Schiaffino *et al.*, 2007; Schiaffino and Reggiani, 2011,

Wasterblad *et al*, 2010). Thus, type IIb fibres are involved in short burst activities requiring high power output.

Type IId/x fibres are a hybrid of type IIb and IIa fibres. They have a low content of mitochondria and ATP synthesis rates and rely on glycolysis to produce ATP. However, their glycolysis rates are lower than type IIb (Ariano *et al.*, 1973; Delp & Duan, 1996; Schiaffino & Reggiani, 2011). Motor units composed of type IId/x fibres have twitch properties including contraction and half-relaxation time similar to those of IIa and IIb units, and their resistance to fatigue is intermediate between that of IIa and IIb units but similar to type IIb, IId/x fibres are involved in short duration, high force activities (Schiaffino & Reggiani, 2011).

Skeletal muscle mechanics

Fast and slow twitch fibre compositions are potential determinants for muscle biomechanical function. Excitation contraction coupling leads to a twitch response from muscle units. Accordingly, contraction of large muscle groups is derived from temporal and spatial summation of single twitches. Repeated and rapid stimuli to muscle fibres create an amplified, sustained contraction called tetanus (Figure 1.5). Interaction between the force generated by the muscle, result of power strokes from cross bridges, and the load on the muscle results in shortening (concentric), no length change (isometric), or lengthening (eccentric) contraction of the muscle. Twitch force (P_t) is determined by intracellular Ca^{+2} transients and Ca^{+2} sensitivity, whereas tetanus force (P_0) is determined by peak of intra-cytoplasmic Ca^{+2} and the fraction of cross bridges that create force.

Table 1.2. Physical, contractile, and metabolic characteristics of mammalian muscle fibres.

Characteristics	Type I	Type IIa	Type IId/x	Type IId
Diameter	Small[1]	Intermediate[1]	Large[1]	Larger[1]
Motor unit size	Small[2]	Intermediate[2]	Large[2]	Larger[2]
Recruitment	Early[2]	Intermediate[2]	Late[2]	Later[2]
Contraction	Slow[1]	Fast[1]	Faster[1]	Fastest[1]
Twitch	Long[1]	Short[1]	Shorter[1]	Shortest[1]
Capillaries	Abundant[3]	Intermediate[3]	Sparse[3]	Rare[3]
Glycolytic capacity	Low[1]	Intermediate[1]	High[1]	Highest[1]
Oxidative capacity	High[1]	High[1]	Intermediate[1]	Low[1]
Myoglobin	High[1]	Intermediate[1]	Low[1]	Lower[1]
Glycogen	Low[1]	Intermediate[1]	High[1]	Higher[1]
Myosin ATPase	Slow[1]	Fast[1]	Fast[1]	Faster[1]
Resting [Ca^{2+}]	High	Intermediate	Low	Lowest
Peak [Ca^{2+}]	Low[1]	Intermediate[1]	High[1]	Highest[1]
Ca^{2+} release	Low[1]	Intermediate[1]	High[1]	Highest[1]
RyR:DHPR	Low[1]	Intermediate[1]	High[1]	Highest[1]
Ca^{2+} uptake	Low[1]	Intermediate[1]	High[1]	Highest[1]
SERCA density	Low[1]	Intermediate[1]	High[1]	Highest[1]
Ca^{2+}	Low[1]	Intermediate[1]	High[1]	Highest[1]

[1](Scott *et al.*, 2001), [2](Ariano *et al.*, 1973), [3](Billeter *et al.*, 1980)

Intracellular Ca^{+2} transients, peak of cytoplasmic Ca^{+2} and Ca^{+2} sensitivity are higher in fast fibre types. Comparing slow and fast twitch fibres, P_t to P_o ratio is higher in fast (0.25) than slow (0.20).

Isometric contractions

Isometric contractions are characterized by having a constant muscle length during activation. The force generated during an isometric contraction is dependent on the length of the muscle while contracting. Maximal isometric force (P_o) is produced at the muscle's optimum length, where the length of the muscle is at normal resting length. During isometric contractions, greater force is obtained when the number of available cross bridges is reduced by an increase in muscle length (Figure 1.6). The greater force capacity in longer muscle lengths is the collective results of active and passive tension of contractile protein and titin, respectively.

Concentric contractions

When the force produced by the muscle exceeds the force applied to the muscle, the muscle shortens. This is known as a shortening or concentric contraction. In concentric contractions, the force generated by the muscle is less than P_o. Inter sarcomere dynamics can be responsible for shortening-induced depression of isometric force (Edman *et al.*, 1992; Morgan, 1990). There are two conceptual possibilities explaining lower force of concentric contractions. The first possibility emphasizes an increased lateral spacing between actin and myosin filaments at short lengths reducing the probability of cross bridge interactions (Godt & Maughan, 1981). Interference of cross

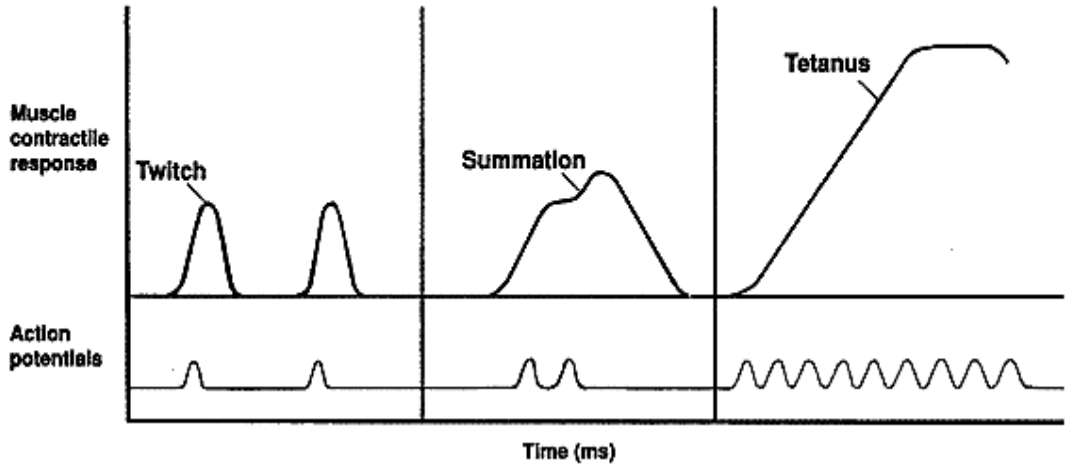

Figure 1.5. Pattern of muscle twitch, summations and tetanus.

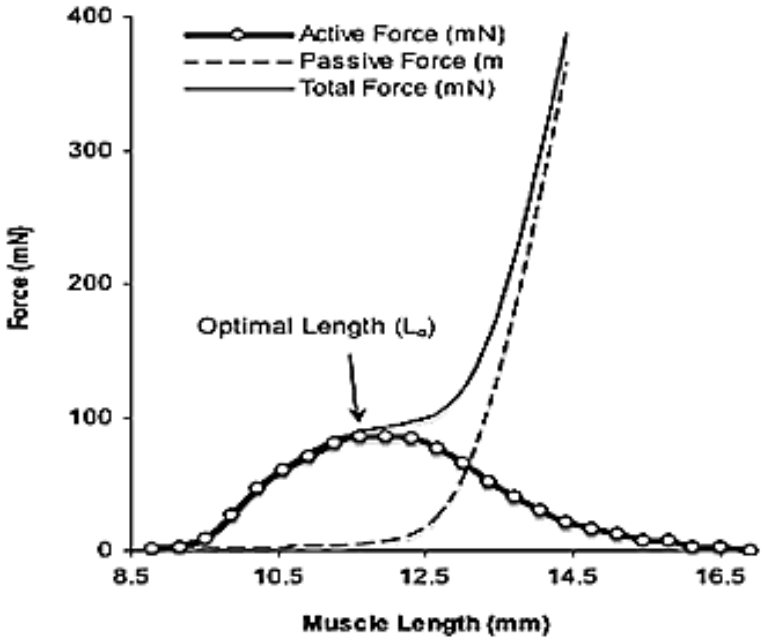

Figure 1.6. Length tension curve of a muscle. (Obtained from Gittings, 2009)

bridge interactions may occur with double overlap of thin filaments (Gordon *et al.*, 1966). The second possibility suggests that in extremely shortened muscle lengths, proper cross bridge attachments may be limited because of deformed myosin filaments. The deformed myosin heads create internal forces that may improperly position myosin in association with actin (Faulkner, 2003). However, deformation of myosin head occur only at extremely shortened lengths of sarcomere indicating that myosin deformity does not occur at typical physiological ranges of sarcomere lengths.

Eccentric contractions

When the force applied to a muscle exceeds the force produced by the muscle, the muscle lengthens. This is known as a lengthening or eccentric contraction. In eccentric contractions, the absolute muscle tensions are very high relative to P_o (Lieber *et al.*, 1991). Additionally, unlike concentric contractions, the absolute tension is relatively independent of lengthening velocity (Herzog & Leonard, 2000).

$$P_{\text{Eccentric contraction}} > P_o > P_{\text{Concentric contractions}}$$

Increased force in eccentric contractions could be related to decreased rate of cross bridge detachments, generating greater steady state force. Additionally, repeated eccentric contractions are known to cause substantial damage in myofibres that is mediated by injury to the elements of EC coupling machinery, including t-tubule rupture. When a muscle is stretched eccentrically, the t-tubules anchored to the contractile apparatus suffer a lateral stretch and get pulled out of position. This has an immediate

inhibitory impact on ECC as the voltage gated calcium channels within the t-tubule network must precisely align and physically couple with the ryanodine receptor gating the calcium vaults of the sarcoplasmic reticulum. Thus repeated eccentric contractions and failure in EC coupling leads to reduced Ca^{+2} release and fall in tension (Warren *et al.* 1993).

Membrane lipid composition in mammalian skeletal muscles

Membrane lipid composition can influence integral and peripheral membrane proteins, suggesting the composition of the membrane may be an important determinant of cellular function. Since fast and slow twitch fibres represent different contractile, metabolic and physical characteristics, it is suggested that membrane PL FA profiles may differ with muscle fibre type composition. Previous research suggests that membrane PL from fast and slow muscle types have similar amounts of PC and PE, which account for 70-75% of the total membrane PLs (Fiehn & Peters, 1971; Fiehn & Peter, 1973; Blackard *et al.*, 1997; Stefanyk *et al.*, 2010). In addition, slow muscle types have a higher content of PUFA, particularly the long chain n-3 PUFA, related to a high proportion of type I fibre in humans (Kriketos *et al.*, 1996). However, in rats, examinations of slow twitch oxidative SOL mitochondria revealed more SFA and less PUFA compared to fast twitch oxidative glycolytic red gastrocnemius and mixed plantaris mitochondrial membranes (Stefanyk *et al.*, 2010), suggesting unique membrane PL FA composition of mitochondria in different muscle types with variable fibre type composition. Together, these observations reveal the importance of membrane composition as a difference in function and energy production in muscles with different fibre type composition.

Sarcolemma Functions

The significance of the sarcolemma is attributed to its contributions to cellular functions such as synaptic transmission, action potential propagation, and excitation contraction coupling (Engel & Franzini-Armstrong, 1994). Besides the well-established physiological functions, the sarcolemma plays an essential structural role in skeletal muscle. During contractions it is of most importance for the myofibres to maintain their organization, which is provided, in part, through structural stability mediated by the sarcolemma (Ozawa *et al.*, 2001; Campbell & Stull, 2003).

Structural role

During muscle contraction, longitudinal and radial forces are generated by cross-bridges in the network of myofilaments. The generated force compresses the myofilament lattice, resulting in a radial force (Ozawa *et al.*, 2001). Since the myofilaments are ultimately anchored to the surface membrane, such radial forces are transferred to the sarcolemma and thereby exert tension upon the membrane (Roy *et al.*, 1999; Pardo *et al.*, 1983; Bloch & Gonzalez-Serratos, 2003; Shkryl *et al.*, 2009). To counter this force, muscle fibre membranes have structural elements that make them capable of withstanding both longitudinally and radially-directed mechanical stresses. One of these structures is the costameric linkage (Figure 1.7) in the subsarcolemmal region that aligns with the Z-disk and is physically coupled to the sarcolemma (Danowski *et al.*, 1992; Ozawa *et al.*, 1995). The major costamere protein complex is the dystrophin glycoprotein complex (DGC) (Figure 1.8; Pardo *et al.*, 1983). DGC is a large oligomeric complex with core components of dystrophin, along with α and β glycoproteins (Ervasti *et al.*, 2001; Ozawa

et al., 2001). The α-glycoprotein subunit is a peripheral protein that binds to laminin localized in the basal lamina. The β-glycoprotein unit is a transmembrane protein which links to dystrophin (Ervasti *et al.*, 2001; Sciandra *et al.*, 2003), and provides a physical linkage across the muscle membrane connecting the extracellular collagen matrix to the F-actin of the sarcomere unit (Figure 1.9; Crosbie *et al.*, 2000; Ervasti & Campbell, 1998). The DGC is associated with other mediator proteins that strengthen the non-covalent bonds from dystrophin to dystroglycan β-subunits (e.g. sarcospans and syntrophins sarcoglycans) (Ervasti *et al.*, 2001; Sciandra *et al.*, 2003). Taken together, the DGC helps to anchor the muscle cytoskeleton to the cell membrane via dystrophin and its binding partners. Importantly, DGC generates a rib like lattice to provide support for the sarcolemma (Ervasti, 2000; Ozawa *et al*, 1995; Ozawa *et al.*, 2001; Campbell & Stull, 2003; Peter *et al.*, 2011). Previous studies have revealed that there are at least two mechanisms whereby the DGC provides a flexible and elastic link between the actin cytoskeleton and the extracellular matrix to help stabilize the sarcolemma during muscle contraction. First, the DGC helps to distribute the mechanical forces associated with contraction over a broader membrane area by interacting with other structural elements exerting tension upon the sarcolemma. Second, the DGC transmits force across and beyond the membrane to the extracellular matrix to minimize increased force on the sarcolemma (Crossbie *et al.*, 1972; Durbeej & Campbell, 2002). This link helps to dissipate muscle contractile force from the intracellular cytoskeleton to the extracellular matrix. As a result, DGC aids to stabilize and preserve sarcolemma during contraction and prevent contraction-induced injury.

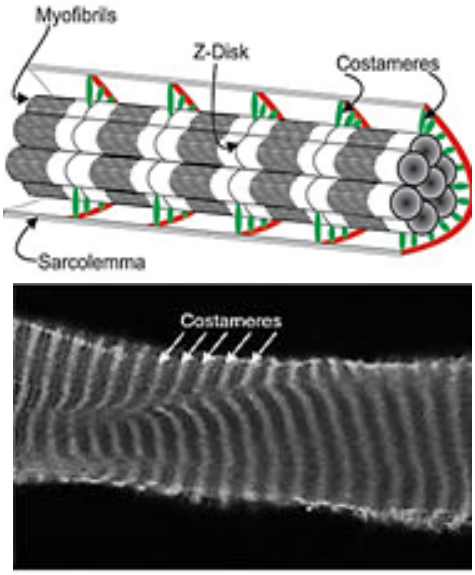

Figure 1.7. Demonstration of cellular location of costameres in skeletal muscle fibres. (Modified from Ervasti, 2003)

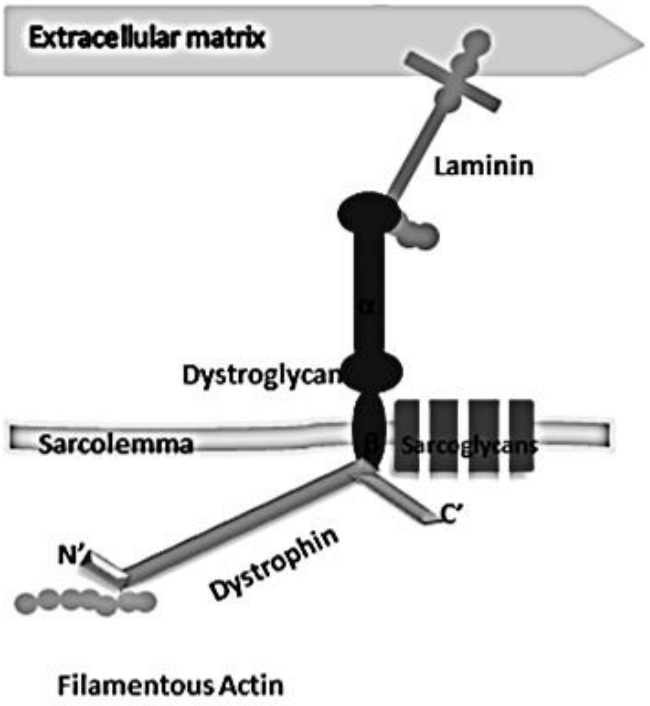

Figure 1.8. Schematic view of sarcolemma three layer structure (basal lamina, lipid bilayer and cytoskeletal network; modified from Roberts, 2001)

Cell signal transduction role

In addition to a structural role, SL regulates cellular signalling and muscle excitability. This regulation is possible through essential proteins embedded or anchored to the sarcolemma. One of the proteins involved in signaling pathways is the DGC. DGC and its associated protein networks are interconnected to signal regulatory proteins controlling calcium dependent activation of lytic enzymes. The most important signalling pathway associated with DGC is related to calcium and nitric oxide (NO). NO is produced by the Ca^{2+-} dependent enzyme neuronal nitric oxide synthase (nNOS), connected to DGC through the adaptor proteins syntrophins. The localization of nNOS at the SL regulates depolarization and subsequent calcium entry through voltage dependent calcium channels (Kim *et al.*, 2009). The regulation in calcium contributes to control for vasomodulation known to be important in contractile skeletal muscle. Additionally plasma membrane calcium/calmodulin ATPase pump (PMCA) localized to the SL is a known modulator of signal transduction pathways. There are many physical interactions between PMCA and other mediators to regulate and organize signaling transduction pathways.

All together, the primary focus for regulator complexes (nNOS, PMCA and etc.) is SL, and the detail introduction of mediators involved in signalling is beyond the scope of this thesis. Together, the signal transduction cascades associated with the DGC play important roles in cell survival signaling, cellular defense mechanisms, and regulation of the balance between cell survival and cell death (Rando, 2001). As such, presence of the DGC and its pivotal components not only physically stabilizes the sarcolemma, but helps

to anchor signalling molecules and regulate survival signalling pathways essential for cell function.

Mutations of different components of DGC or its associated protein network leads to skeletal muscle damage and impairment in muscle function. These impairments, in turn, lead to muscular dystrophies which vary in severity, age of onset and involvement of different muscle groups.

Muscular dystrophy

Muscular dystrophies are a group of X- linked recessive inherited neuromuscular diseases involving the mammalian muscular system. This group of diseases are characterized by progressive weakness and degeneration of skeletal muscles, with smooth and cardiac muscle manifestations later over the course of the disease. The most common and severe form of muscular dystrophy in children is Duchenne muscular dystrophy (DMD) produced by a point mutation in the dystrophin gene affecting 1 in 3600 infant males (Emery, 2002).

The symptoms usually appear before the age of 6 and may present as early as infancy. The first accompanying symptom is associated with motor muscular milestones causing a delay in the mean age of walking to 18 months. Progression of symptoms results in 90% of affected individuals to be wheelchair bound by 19-24 year of age (Emery, 2002; Worton, 1995; Darras *et al.*, 2008). The life expectancy for DMD is 20-24 years due to cardiac and respiratory muscle failure (Emery, 2002; Fauci, 2004).

The dystrophin gene has been identified as the largest gene in the human genome with 79 exons (Ahn & Kunkel, 1993). The large size of the dystrophin gene is known to

be the primary reason for the high incidence of DMD as mutations that occur at multiple locations (Coffey et a., 1999; Ahn & Kunkel, 1993). Mutations in the dystrophin gene leading to DMD result from duplications and deletions, with deletions being the most common (Koeing *et al.*, 1989).

As highlighted above, cytoskeletal proteins contribute to lateral transmission of force, and thereby they diminish the extent of force upon membrane during contraction. The absence of dystophin, and resulting impact on the DGC, compromises its ability to transfer force beyond the membrane. As such, contractile force will be directed toward the membrane causing muscle damage characterized by an immediate weakness and mechanical tearing of the membrane (Ervasti & Campbell, 1999).

Rodent model of muscular dystrophy, mdx mice

The most frequently used model for characterization of structural and functional properties of dystrophin deficiency is the *mdx* mouse. The *mdx* mouse has an X-linked point mutation in the dystrophin gene that results in a defective truncated protein (Bulfield *et al.*, 1984; Sicinski *et al.*, 1989). The point mutation occurs in exon 23 where thymine is replaced by cytosine making a defective protein that is shortened to 27% of its normal length (Bulfield *et al.*, 1984). The truncated protein is not able to bind to cytoskeletal elements, therefore, loses its role in providing stability for the membrane (Sicinski *et al.*, 1989).

Muscular dystrophy etiology

To explain the etiology for force reduction in muscular dystrophy, several hypotheses have been suggested. The first hypothesis is based on the anchoring role of the DGC in linking sarcolemma to intra and extracellular structures. The second hypothesis refers to the involvement of dystrophin and the DGC in signaling mechanisms that may include calcium and calcium-dependent activation of lytic enzymes. The third hypothesis is related to the appearance of bifurcations and branching in dystrophic fibres, which make them prone to split and tear.

Mechanical hypothesis

The mechanical hypothesis for DGC dysfunction is based on the DGC being a link between the subsarcolemmal cytoskeleton and the extracellular matrix. The disruption of the DGC, due to an absent or truncated dystrophin, may lead to sarcolemmal instability, membrane tears, and eventually muscle fibre necrosis (Mendell *et al.*, 1995, Campbell, 1995). The suggestion is that the DGC offers both structural and functional integrity to the sarcolemma by stabilizing it against stresses imposed during muscle contraction or stretch (Rybakova *et al.*, 2000; Blake *et al.*, 2002).

Evidence for structural support of the DGC arises from several studies comparing force deficits of *mdx* mice compared to wild type. Although *in vitro* experiments for inducing damage are not consistent in the literature, immediate force loss and contraction-induced sarcolemmal damage has been observed after eccentric contractions (Head *et al.*, 1992; Petrof *et al.*, 1993; Deconinck *et al.*, 1998; Raymackers, 2003; Consolino & Brooks, 2004; Chan *et al.*, 2007). Force loss in the mechanical hypothesis is

explained by segmental necrosis of muscle fibres, so the structural continuity required for effective force transmission along the longitudinal axis is lost and fibres are functionally impaired in transmitting force (Ohlendieck & Campbell, 1991). Additionally, it has been suggested that lateral transmission of force to the inter-fibre connective tissue space may provide a "tension bypass" around damaged areas and help to maintain some force-generating capacity in the presence of localized fibre injury (Huijing, 1999; Mass *et al.*, 2001). This compensatory mechanism might be defective in dystrophin deficiency given the predicted decrease in mechanical linkage between myofilaments and the extracellular matrix.

Other evidence in agreement with the mechanical hypothesis suggests that with development of membrane tears, the intracellular molecules leak out of the myocyte through the damaged membrane. One of the exclusive *ex vivo* surrogates of membrane damage are membrane impermeable low molecular weight dyes, specifically procion orange. Procion orange has a very lower molecular weight (630 g/mol), and infiltration into the myocyte is indicative of small tears in the membrane of damaged fibres (Petrof *et al.*, 1993; Whitehead *et al.*, 2006). Limitations of this method, however, are related to its potential toxicity and impact on peroxidation of membrane lipids producing additional membrane injury (Palacio *et al.*, 2002). This limitation has resulted in the use of alternative techniques for assessment of membrane damage, specifically, creatine kinase (CK) and fibronectin.

The muscle isoform of CK is an enzyme, ~81 kDa in size (or ~81,000 g/mol), which catalyzes the reversible conversion of creatine to phosphocreatine, consuming ATP. CK is normally found in the cytosol of skeletal muscle fibres and serum

concentrations are normally very low (~150 U/L) (Okinaka *et al.*, 1959). It is generally thought that if serum CK concentrations rise, it is due to sarcolemmal membrane damage, allowing muscle CK to leak out of the muscle fibre (Ozawa *et al.*, 1999). Limitation of CK in the evaluation of membrane damage is related to its measurement in *in vivo* conditions. Moreover, the serum CK activity level is highly variable between mice influenced by multiple variables including age and prior muscle activity (Sorichter *et al.*, 1998; Spurney *et al.*, 2009; Anderson *et al.*, 1996). As such, effluxes of CK may only represent the presence of membrane damage and do not necessarily reflect the location of damage within a given muscle (Sorichter *et al.*, 1998).

Another molecule indicative of membrane permeability is intracellular accumulation of fibronectin. Fibronectin is predominantly secreted by fibroblasts and exists as a dimer composed of two identical monomers with a molecular weight of 450 kDa, or ~450,000 g/mol (Pater *et al.*, 1987). Fibronectin is a component of the extracellular matrix and its localization in the cell is indicative of membrane damage (Palacio *et al.*, 2007). Despite considerable difference in molecular weight of fibronectin and procion orange (630 vs. 450,000 g/mol), fibronectin detection has demonstrated comparable results to procion orange (Palacio *et al.*, 2002). Moreover, in contrast to CK, and further to its *ex vivo* measurement, the levels are not variable in mice, making it appear as an appropriate measure for evaluating fibre membrane damage (Palacio *et al.*, 2002).

Together, despite limitations in different measures, the proportion of damaged fibres exhibiting procion orange have a direct association with decline in function as an aspect of muscle damage after injury (Petrof *et al.*, 1993). Importantly, a decrease in

contractile function may be either a cause or consequence of muscle fibre damage as indicated with procion orange positive fibres. Increase in procion orange uptake has also been associated with increase in Ca^{+2} entry and disturbed Ca^{+2} homeostasis resulting in necrosis suggesting procion orange is reflective of membrane micro-lesions and muscle damage in *mdx* (Whitehead *et al.*, 2006). However, increased plasma CK has not shown an association with declined muscle functional and histological parameters of muscle damage, more reflective of the presence of membrane lesions (Anderson *et al.*, 1996). With application of electrical stimulation to induce membrane injury, fibronectin was similarly detected in fibres positive for procion orange (Palacio *et al.*, 2002). This suggest that although the techniques of procion orange and fibronectin identifications are based on markedly different molecular weights, they both result in detecting membrane lesions and muscle damage. As such, fibronectin can be used to examine membrane damage without impacting membrane lipids.

There is evidence, however, that the mechanical hypothesis may not be solely responsible for the onset of DMD. With application of eccentric induced damage protocols to extensor digitorum longus (EDL) muscle of 9-12 day old control and *mdx* mice, it was discovered that the *mdx* genotype at a young age is resilient to injury and does not show additional damage (Grange *et al.*, 2002). Therefore, evidence is not conclusive to support the mechanical hypothesis as a mechanism that initiates DMD during early maturation. This has prompted questioning about the role of dystrophin in the protection of cell membranes in response to mechanical injury (Grange *et al.*, 2002).

Calcium hypothesis

The calcium hypothesis states that, in the absence of dystrophin, there would be an influx of calcium through the sarcolemma due to either abnormally functioning stretch activated channels (SAC) or cation-leak channels (Tutdibi *et al.*, 1999). The increased calcium entry contributes to a rise in cytosolic free calcium, which, in turn, activates calcium dependent proteases and eventually leads to muscle necrosis (Mallouk *et al.*, 2000, Alderton & Steinhardt, 2000). Previous research demonstrated that prevention of a rise in intracellular calcium following eccentric contractions resulted in a significant reduction in *mdx* muscle damage (Yeung *et al.*, 2005). This demonstrates that the influx of calcium and a higher intracellular calcium concentration contributes to muscle fibre damage and ultimate necrosis. Of course, with development of muscle damage, more Ca^{2+} can enter the fibre and potentially activate more Ca^{2+} leak channels, thereby providing an additional route for Ca^{2+} entry (Mallouk *et al.*, 2000; Alderton & Steinhardt, 2000).

Within the calcium hypothesis, abnormal calcium homeostasis may not be a direct effect of the absence of dystrophin. The cause of abnormal calcium homeostasis may be either a secondary result of muscle degeneration or be related to transient sarcolemmal wounds as a result of contraction-induced injury. Calcium was used to measure the muscle membrane permeability of EDL in 14 and 40 day old *mdx* and control mice. Calcium accumulation in muscle from the extracellular fluid was normal in 14 day old *mdx* mice, but by age 40, calcium levels were 3 times higher than control (Whitehead *et al.*, 2006). Assessment of membrane permeability with procion orange demonstrated that in 14 day old *mdx* mice, there was no evidence of abnormal muscle membrane

permeability, supporting the hypothesis that the alteration of membrane permeability was a secondary effect (McArdle *et al.*, 1994, Grange *et al.*, 2002). Additional support for the secondary effect of abnormal permeability is that, in *mdx* muscle, total calcium content rose acutely in muscle at an age that correlated with a period of necrosis and then returned to normal values during an ensuing regenerative phase (Reeve *et al.*, 1997).

In another study with the removal of calcium in the muscle-bath media or with the addition of streptomycin to block stretch activated channels, force declined to only 69–76% of its control value compared to ~ 56% in the presence of calcium (Zhang *et al.*, 2008). This demonstrated that although force deficit was greater in the presence of calcium, the removal of calcium and prevention of calcium-mediated cytoskeletal damage, force didn't completely recover to its normal value. This may suggests that calcium-mediated damage is not the only involved mechanism to explain why the absence of dystrophin causes muscles to be particularly susceptible to damage and degeneration.

The increased frequency of transient sarcolemmal wounds sustained during contraction in dystrophic muscle may be exacerbated by abnormal calcium homeostasis (Alderton *et al.*, 2000). When muscle contraction and activity in *mdx* muscle was inhibited through paralysis for 5-7 days, the abnormal rise in resting intracellular free calcium levels was mostly prevented. From this study, it was concluded that the damage from long-term contractile activity and increased calcium leak channel activity are the likely causes of differences in calcium homeostasis, but not the primary reason for the calcium influx from individual contractions (Alderton *et al.*, 2000). Increased levels of intracellular calcium have been reported by several investigators in *mdx* mice as early as

3 weeks of age. More specifically, increased calcium has been shown to localize at the sarcolemma, which may be due to calcium leak channels (Rolland *et al.*, 2006; Vandebrouck *et al.*, 2002; Yeung *et al.*, 2005). It is not yet clear if the increase in intracellular calcium is a primary or secondary outcome of the absence of dystrophin. The increased intracellular calcium associated with the onset of contraction in myofibres around 3 weeks of age, and lack of rise of calcium at 14 days with no change in membrane permeability, may suggest that calcium mediated damage may not be the initial event of the dystrophic pathology (Alderton *et al.*, 2000).

Branching hypothesis

The etiology of muscle degeneration in *mdx* mice is complicated by the fact that, as *mdx* muscle ages, the architecture of the dystrophic muscle fibres becomes abnormal. The abnormal fibres have branched and split appearance, which are more prone to damage during contractions. This is explained by the high shear stress upon branching points during intense contractile activity, leading to fibre rupture at these points (Chan *et al.*, 2007). With progression of disease, skeletal muscle fibres display more abnormal, branched and split appearance that is prominently seen in regenerated fibres (Figure 1.9; Head *et al.*, 1992; Chan *et al.*, 2007; Head, 2010; Chan & Head 2011; Head, 2011). In contrast to dystrophic fibres, branched fibres are hardly ever found in the muscles of dystrophin-positive control mice (Head *et al.* 1992; Chan *et al.* 2007; Lovering *et al.* 2009). Additionally, branched fibres are highly variable in their individual diameter size, leading to differing propagation velocities of action potentials with asynchronized contractile activity and extra stresses imposed on branching points (Isaacs

et al. 1973). Therefore, the change in morphology of dystrophic fibres contributes to fibre rupture after contractile activity and decline in force production during each contraction. Fibre branching and changes in morphology of dystrophic fibres increase with age (Isaacs *et al.* 1973; Schmalbruch, 1984; Head *et al.* 1992; Blake *et al.* 2002; Chan *et al.* 2007). One study on young *mdx* mice at the age of 6-8 weeks showed no significant force deficit compared to control. This age coincides with a period where fibre branching is minimally present so although the 6-8 week old muscles were identified as dystrophic, their force deficit was not significantly decreased (Chan *et al.*, 2007). Thus, the branching hypothesis suggest that the lack of dystrophin itself does not make muscle more prone to contractile damage, because the muscles from the young *mdx* mice were not more damaged than control muscles (Head *et al.* 1992; Chan *et al.* 2007). However, with the presence of branching in older ~28 weeks old *mdx* mice, eccentric contractions resulted in a force deficit of 58%, compared with only 25% for control animals (Chan *et al.*, 2007; Chan & Head, 2011). In another study using mouse pups aged 9–12 days old, EDL muscles from *mdx* mice showed no more damage than non-stretched muscles following eccentric contractions, as assessed by force deficit and dye uptake (Grange *et al.*, 2002). Taken together, it can be postulated that the large increase in susceptibility to damage from lengthening contractions that occurs with advancing age in *mdx* mice could be related to the development of branched fibres.

Chronology of mdx phenotype

Dysfunction in dystrophin is associated with a spectrum of pathologies including change in myofibre histology, abnormal biomechanical function, alterations in fibre type

and membrane lipid composition, and abnormal leaky membranes. This dystrophic phenotype is not similar through the lifespan and displays variable stages from mild to severe.

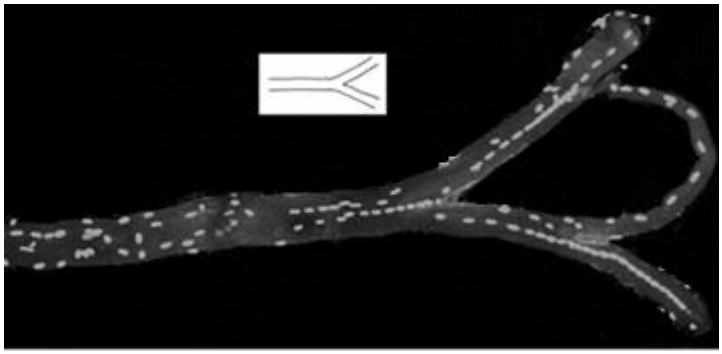

Figure 1.9. Demonstration of fibre branching in 28 wks old *mdx* mice. (Modified from Chan *et al.*, 2007)

Skeletal muscle histology

Dystrophic mice have a near normal life span (Blake *et al.*, 2002). From birth to 5 days of age, muscle fibres appear to be immature and there is no evidence of histological lesions (Durbeej *et al.*, 2002). With increased activity and weaning at 10-15 days, muscle fibres began to differentiate into type 1 and 2 fibres with no difference in fibre type distribution than wild types (Durbeej *et al.*, 2002).

At 3 weeks, muscles demonstrate excessive atrophy with variation in fibre size and degeneration of type II fibres (Bulfield *et al.*, 1984). In addition, plasma measurements demonstrate elevated levels of creatine kinase and pyruvate kinase. Moreover, phagocytic cells begin to appear in place of lost fibres, but there is no replacement of lost muscle by connective tissue and adipose cells (Bulfield *et al.*, 1984). The timing of muscular degeneration is highly variable within the literature, although it is generally agreed upon that maximum degeneration is seen between the 3rd and 10th week of age before decreasing to negligible levels after 10 weeks (DiMario *et al.*, 1989, Karpati *et al.*, 1990, Nagel *et al.*, 1990). The precise reason for the acute onset of the pathology at 3 weeks of age in fast twitch muscles is currently unknown. This may be related to adult-type muscle activity or to developmental changes in expression of various genes. These genes include the components of the glycoprotein complex, specifically utrophin, which are anchored to one another to form stable lattice structures. Utrophin is a homologue of dystrophin that is exclusively located at the neuromuscular junction. Similar to dystrophin, it has domains that bind to actin and the glycoprotein complex. In the absence of dystrophin, utrophin is up-regulated, localizes throughout the entire sarcolemma, and is able to partially compensate for dystrophin, thus conferring a degree of stability to

attenuate muscle pathology (Tanabe *et al.*, 1991; Gramolini *et al.*, 2001). Dysfunction in any of these network components is accompanied by adaptive up regulated responses in utrophin, masking the expression of the phenotype. However, with down regulation in the expression of these compensatory proteins around 3 weeks of age, dysfunction of DGC components becomes apparent (Khurana *et al.*, 1991).

After 5 weeks of age there is a vigorous regeneration response with the appearance of many central nucleated fibres that originate from their precursors, satellite cells (Carnwath and Shotton, 1987). After 5 weeks of age, there are cycles of degeneration and regeneration occurring in *mdx* muscle until approximately 10-11 weeks, when muscle fibre degeneration and necrosis decrease significantly and are delayed until approximately 18 months of age (Stedman *et al.*, 1991). In fact, after the initial wave of degeneration, *mdx* muscle only demonstrates low levels of damage with the disease following a more benign progression, maintaining a chronic but low grade of damage after 10 weeks of age (Grounds *et al.*, 2008). Eventually the regenerative process becomes exhausted and muscle begins to show signs of atrophy, weakness and fibrosis similar to that of DMD (Hakim *et al.*, 2011). Fibrosis is an excessive accumulation of extracellular matrix that is the end result of tissue damage and degeneration, resulting in permanent loss of fibres and replacement with connective tissue. Previous research has shown that *mdx* muscle at 8 weeks and 6 months display no apparent fibrosis. However, after 18 months fibrosis becomes evident (Hakim *et al.*, 2011; Desguerre *et al.*, 2012). Demonstration of fibrosis at late stages of the *mdx* phenotype indicates that the accumulation of collagen is cumulative and not apparent until late stages of disease progression.

Biomechanical functions

Isometric force development has been extensively studied in the *mdx* mouse, at various age groups reporting differences in force production relative to age match controls. Specifically, force production and power output of dystrophic EDL muscle are reported to be normal at 9-12 days of age and only reduce significantly after 12 days (Grange *et al.*, 2002). In support of early contractile dysfunction, EDL of 28 days old *mdx* mice displayed 15% less twitch force than control (Lowe *et al.*, 2006), which supports previous research from several other groups (Petrof *et al.*, 1993, Deconinck *et al.*, 1998, Raymackers, 2003). However, later on, at 4-8 weeks of age, there was no difference in force development of dystrophic muscles compared to controls (McArdle *et al.*, 1991; Deconinck *et al.*, 1998; Chan *et al.*, 2007). From 8-12 weeks of age, there is a more dramatic functional deficit of 15-25% in *mdx* muscle (Head *et al.*, 1992; Chan *et al.*, 2007; Harcourt *et al.*, 2007; Dellorosso *et al.*, 2001; Deconinck *et al.*, 1993) (Table 1.3). The force output continues to decline to 20% of control muscles at 12 weeks age, 30% at 20 weeks, 15% at 24-28 weeks and ~30% at 45 weeks of age (Table 1.3) (Lynch *et al.*, 2001; Consolino & Brooks, 2004; Head *et al.*, 1992). The variation in measured force deficits with age and the absence of a functional decline during 4- 8 weeks of age may be due to the variable nature of the contractile protocols. With regard to absolute tetanic force (P_0), skeletal muscles of *mdx* mice demonstrate forces that are comparable to, or even exceed that produced by control animals (Lynch *et al.*, 2001). This is especially common when animals are experimented on between 6-12 months of age, where hypertrophy of limb musculature occurs in *mdx* mice (De la Porte *et al.*, 1999, Hayes and

Williams, 1998). However, when normalised to cross sectional area to give specific force, peak tetanic force is consistently lower in *mdx* muscle relative to wild type mice.

Twitch kinetics, in general, are reported to be similar to that of control animals although some groups have reported a slowing of the twitch peak tension (TTP) and half relaxation times (HRT). Specifically, at 9-12 days the HRT and TPT of dystrophic muscle remained unchanged (Grange *et al.*, 2002). However, at 4-6 weeks, both the TPT and HRT were prolonged (Kometani *et al.*, 1989). Subsequently, at 10 weeks of age, the twitch kinetics showed to be similar to that of control (Deconinck *et al.*, 1998; Harcourt *et al.*, 2007). At 15 weeks a slowing of TTP and HRT has been reported (Watchko *et al.*, 2002). In contrast, at 13-52 weeks, faster TTP and HRT responses were obtained from *mdx* muscles (Pastoret & Sebille, 1993). Another study demonstrated that dystrophic muscle at 24 weeks reached peak tension significantly faster than controls (Hakim & Duan, 2012). However, HRT was prolonged at this age. The same pattern of decrease in TPT and increase in HRT was observed for dystrophic muscles at 20 months (Hakim & Duan, 2012). Again, the differences for changes in TPT and HRT may be related to differences in experimental methods of dystrophic muscles.

The impairment in the capacity of limb muscles in *mdx* mice to develop force early in life suggests that transient impairment in regenerated fibres may account for the decline in force development (Pastoret & Sebille, 1997). Embryonic and neonatal muscle fibres are known to have low capacities for the generation of force and the continued presence of embryonic and neonatal isoforms of myosin in regenerating muscle fibres in *mdx* mice may contribute to the functional impairments (Reisser *et al.*, 1985; DiMario *et al.*, 1991). Throughout later stages of the dystrophic phenotype, the hypertrophied state of

Table 1.3. Summary of studies demonstrating force deficits of normal and *mdx* fast-twitch muscles following eccentric contractions.

Study	**Age of the mice (wks)**	**Muscle**	**Significant force deficit**
Grange *et al.*, 2002	1-2	EDL	No
Lowe *et al.*, 2006	4	EDL	Yes
Chan *et al.*, 2007	4-8	EDL	No
McArdle *et al.*, 1991	5-6	EDL	No
Deconinck *et al.*, 1998	6-8	Diaphragm	Yes
Deconinck *et al.*, 1998	6-8	SOL	Yes
Deconinck *et al.*, 1998	6-8	EDL	No
Dellorosso *et al.*, 2001	8-12	TA	Yes
Harcourt *et al.*, 2007	10	EDL	Yes
Deconinck *et al.*, 1998	10	EDL	Yes
Raymackers, 2003	12	EDL	Yes
Petrof *et al.*, 1993	12-15	EDL	Yes
Consolino & Brooks, 2004	20	EDL	Yes
Lynch *et al.*, 2001	24-152	EDL	Yes
Head *et al.*, 1992	>45	EDL	Yes
Chan *et al.*, 2007	24- 28	EDL	Yes

EDL, extensor digitorum longus; SOL, soleus; TA, tibialis anterior.

fast and slow muscles with no concomitant increase in force reflects an increase in non-contractile tissue, likely due to the presence of degenerating and necrotic fibres. The presence of non-contractile tissue results in lower values for normalized force in fast and slow twitch muscle types in older *mdx* mice (Faulkner *et al.*, 1993).

Fibre type composition

Due to variations in fibre type composition of different muscles and frequency of their usage, the effect of the absence of dystrophin on overall muscle function and vulnerability to damage may not be uniform across different muscle types. Fast twitch fibres are known to be involved early in the progression of the dystrophic phenotype due to their size (smaller surface area to volume ratio) and lipid composition (less PUFAs) (Macpherson *et al.*, 1996; Lieber & Friden, 1988). Soleus (predominantly type I fibres) has a higher resistance to exercise induce injury compared to EDL (majority type II fibres), possibly due to its involvement in activities such as maintenance of posture and balance (Passaquin *et al.*, 2002). Experiments that relied on contractile damage similar to EDL *in vitro* demonstrated no difference in the susceptibility of soleus from both *mdx* and control mice to contraction-induced injury, suggesting the need for a more intense stretch injury protocol (Moens *et al.*, 1993; Consolino & Brooks, 2007, Chamberlain *et al.*, 2007). This resistance of soleus to damage may be explained by the high content of type I fibres (Table 1.4) (Augusto *et al.*, 2004; Smith *et al.*, 2013), and possible utrophin compensation. Type I fibres have a greater surface area to volume ratio that enables them to withstand forces produced by intense contractions. Moreover, type I fibres in *mdx* muscle demonstrate 3-4 times more up regulation of utrophin than type II fibres, providing compensation for stability of sarcolemma to damage (Selsby *et al.*, 2012).

Table 1.4. Fibre type composition of wild type adult mouse extensor digitorum longus and soleus.

	Type I	Type IIA	Type IID/X	Type IIB
EDL	Less than 1%	~1%	~19%	~71%
SOL	~32%	~42%	~15%	~1%

Data from Smith *et al.*, 2013; EDL, extensor digitorum longus; SOL, soleus.

In *mdx* with increased age and moving from immature to more mature and older mice, the proportion of type I and II fibres undergo changes. In EDL, which is type II dominant, there was no difference in the proportion of type I fibres at 4 weeks compared to wild-type. However, at 16 weeks, the proportion of type I fibres mildly increased as a result of changes in the activity of the original motor neurons, possibly as a compensatory response to muscle weakness (Carnwath & Shotton, 1986). At 24-32 weeks, type II fibres show a further decrease in number. In soleus, which is type I dominant, at the age of 6 weeks there is no apparent fibre type alteration. However, at 18 weeks, a decrease of type II fibres in *mdx* soleus was reported (Pastoret & Sebille, 1993). At 26 weeks there is a more pronounced shift from type II to type I fibres, with a rise of type I from 28% at 3 weeks, to 58% at 26 weeks (Pastoret & sebille, 1993; Massa *et al.*, 1997). A change in fibre type population in soleus is believed to attenuate muscle weakness as a result of dystrophic damage and helps to compensate the developed myopathy in *mdx* muscle.

Membrane lipid composition

Membrane lipid composition can influence integral and peripheral membrane proteins indicating the importance of membrane lipid composition as an essential modulator of cellular function. Analysis of *mdx* muscle membrane lipid composition with time-of-flight secondary ion mass spectrometry (TOF-SIMS) showed an increase in the ratio of 16:0 and 18:0 saturated fatty acids at 3 weeks of age in degenerated areas (Touboul *et al.*, 2004). Although this age coincides with the onset of acute degeneration in *mdx* skeletal muscles, membrane phospholipid composition at earlier ages hasn't been examined. Whole tissue analysis of phospholipid composition in *mdx* muscle demonstrated less PC and more PE and SM content during 8-10 weeks (Owens &

Hughes; 1970). Additionally, at 11-12 weeks, matrix-assisted laser desorption/ionization (MALDI) TOF mass spectrometry and tandem mass spectrometry analysis of phospholipid composition in skeletal muscle of *mdx* mice indicated a reduced 34:2 to 34:1 FA ratio in PC between highly diseased versus less impacted regions (Benabdellah *et al.*, 2009). It was inferred that the reduced 34:2 to 34:1 FA ratio in PC was due to a decrease in 18:2n6 to 18:1 FA ratio (assuming 16:0 being the other FA of PC). Subsequently, at 12 weeks, study on isolated mouse quadriceps demonstrated lower abundance of 22:6n3 and higher amount of 18:2n6 and 18:1, consistent with findings at 16-20 weeks (Tuazon & Henderson, 2012). Lower contents of 22:6n3 are consistent with similar finding in fore and hind limb dystrophic *mdx* mouse, suggesting loss due to oxidative damage (Owens & Hughes, 1970). However, elevation in 18:2n6 of *mdx* quadriceps demonstrates a discrepancy, given most literature show a decrease in *mdx* mice (Kunze *et al.*, 1975; Pearce *et al.*, 1981; Parce & Kakulus, 1980). Such alterations suggest that with an increase in age, the dystrophic membrane demonstrates increased saturation, underscoring the potential role of membrane lipid composition in the progression of the disease.

Taken together, throughout the available literature on PL FA content of *mdx*, there appears to be a consistent increase in the levels of PC and SM. Among fatty acids, increases in 18:1 have been reported most consistently. In addition, either decreases or increases in18:2n6 levels have also been observed. Furthermore, given the different fibre type composition of slow and fast muscle, it is plausible that reported alterations of PL FAs in literature are dissimilar as a consequence of the muscle examined. Moreover, there are limitations in literature related to gaps in information about membrane

composition of *mdx* isolated skeletal muscle at different ages. As such, to evaluate PL FA composition in dystrophic muscle, it is important to consider the plausible associations between PL FAs alterations and muscle fibre types with age.

Membrane PL FA composition is closely associated with cellular function. Type I and II fibres demonstrate unique contractile, physical and metabolic characteristics. Differences in fibre type distribution should therefore be considered as a determining factor when looking at the fatty acid profile in skeletal muscle membrane PL FAs. Fast twitch muscle in rats demonstrate more elongated and saturated FAs than slow twitch muscle. Additionally, type I fibres have been linked with increased proportion of longer and more highly unsaturated, particularly n-3 fatty acids, in muscle membrane PLs (Storlein *et al.*, 1991; Lie *et al.*, 1994). The correlation of fibre types to membrane lipid composition in mice has not been studied in detail. Moreover, the fibre type composition has a significant impact on metabolic and contractile function of skeletal muscle. Membrane lipid composition, however, is determined by fibre type composition. As such, the phenotype of muscular dystrophy is primarily explained by the fibre type composition. Indeed, the differences within PL FA composition of different fibre types may determine variations of metabolism and contractile functions within each muscle type.

Membrane permeability

Disruption to membrane integrity is another characteristic of the dystrophic phenotype. Literature that demonstrates changes in membrane permeability is dependent on the age of the mouse and surrogate of membrane damage (Table 1.6). These surrogates used in the literature can be classified in two different sizes; small (Ca^{+2}

sensitive markers, 40 g/mol; procion orange, 630 g/mol) and large (fibronectin, 450,000 g/mol; CK, 80,000 g/mol). Examination of *mdx* EDL at 2 weeks of age with small Ca^{+2} sensitive dyes revealed no change in permeability (Whitehead *et al.*, 2006). Similarly,

Table 1.5. Summary of studies identifying alterations in membrane lipid profile of skeletal muscles in muscular dystrophy in humans and *mdx* mice.

mdx mice	Age	Muscle
↑18:0/18:1 in PC of destructured areas; ↑16:0/16:1 in PC of destructured areas[4]	3 wks	Hind limbs
↓ PC, ↑PE, ↑SM of 8-16 wks [2]	8- 12 wks	Hind and fore limbs
↑PC34:2 and ↑PC34:1; ↓PC34:2/34:1 [3]	11-12 wks	Hind limbs
↓n-3 FA, ↑n-6 FA [5]	12 wks	Quadriceps
↓16:0 and↑18:1 for both PC and PE; ↑18:2 in PC, ↓22:6 in PE[1]	16-20 wks	Hind limb

PC, phosphatidylcholine; PE, phosphatidyl ethanolamine; FA, fatty acid; (Pearce & Kakulus, 1980)[1], (Owens & Hughes, 1970)[2], (Benabdellah *et al.*, 2009)[3], (Touboul, 2004)[4], **(**Tuazon & Henderson, 2012)[5]

with application of membrane impermeable procion orange at ~ 2 weeks (9-12 days), membrane permeability was still unaltered (Grange *et al.*, 2002). However, at 5 weeks of age, by use of Ca^{+2} sensitive markers, membrane permeability was shown to be increased (Whitehead *et al.*, 2006). Later on, at 10-14 weeks, *mdx* EDL demonstrated increased permeability to procion orange (Petrof *et al.*, 1993; Deconinck *et al.*, 1998). Detection of membrane disruptions with high molecular weight CK demonstrated elevated levels of this enzyme in serum at 3-7 weeks of age (McArdle *et al.*, 1994). The evidence in the literature suggest that during the first 2 weeks, *mdx* myofibres are not showing any increase in membrane permeability to even small markers of damage (Whitehad *et al.*, 2006; Grange *et al.*, 2002). However, due to a rise in serum CK at 3 weeks, it is assumed that at this age membrane disruption membranes appears, allowing passage of even larger markers of damage (Whitehead *et al.*, 2006). Increased membrane permeability with small size markers hasn't been studied between 2 and 5 weeks (Ca^{+2} markers increased at 5 weeks; Whitehead *et al.*, 2006). However, due to increased CK levels at 3 weeks, it is assumed that the lesions in membrane were large enough to allowing the passage of both small and large surrogates of damage. With increased age, at 7-15 weeks, the membrane remains permeable to both procion orange and CK (McArdle, 1994; Deconinck *et al.*, 1998; Petrof *et al.*, 1993). Together, measurements with small markers of damage indicate no change in the membrane permeability during the first 2 weeks but after 3 weeks, membrane lesions accommodate the passage of both small and large damage markers.

Lack of evidence of abnormal muscle membrane permeability at earlier ages may suggest that changes in membrane permeability are a secondary effect of absence of

dystropin (McArdle *et al.*, 1994, Grange *et al.*, 2002). Support for a secondary effect of abnormal permeability was that, in *mdx* muscle, total calcium content rose acutely at an age that correlated with a period of necrosis and then returned to normal values during the regenerative phase (Reeve *et al.*, 1997). It may be possible that altered membrane permeability until 3 weeks of age may not be evident because mice at this age are not actively moving around the cage and, therefore, contraction of muscles may be limited. This is consistent with the abnormal calcium homeostasis and correlates with the onset of contraction in *mdx* myotubes, suggesting that contraction is necessary before changes in intracellular Ca^{+2} occur (Alderton *et al.*, 2002).

Table 1.6. In vivo and ex vivo surrogates of muscle damage in evaluation of membrane damage

Surrogate	Molecular weight	Muscle	Age (wk)	Membrane leak
PO	630	EDL	1-2	Neg [1]
Calcium	40	EDL	2	Neg [2]
CK	82.000	*In vivo*	3-7	Pos [3]
Calcium	40	EDL	6	Pos [2]
PO	630	EDL	10	Pos[4]
PO	630	EDL	14	Pos[5]
Fibronectin	450.000	EDL	unknown	Pos[6]

PO, procion orange; CK, creatine kinase; EDL, extensor digitorum longus; (Grange *et al.*, 2002)[1], (Whitehead *et al.*, 2006)[2], (McArdle, 1994)[3], (Deconinck *et al.*, 1998)[4], (Petrof *et al.*, 1993)[5], (Palacio *et al.*, 2002)[6].

Statement of the problem

The membrane structure-protein function relationship indicates that an association exists between membranes and their associated proteins, because a protein can modulate the membrane and vice versa. Evidence suggests that the absence of dystrophin mediates an alteration in the lipid composition of the sarcolemma membrane. Additionally, it has been revealed that the underlying factor that leads to muscle pathology early in life is independent from dystrophin dysfunction (Lowe *et al.*, 2006). Potential influences of dystrophin dysfunction on skeletal muscle membrane composition have been suggested including increased SFA and MUFA and deceased PUFA (Pearce & Kakulus, 1980, Benabdellah *et al.*, 2009). However, these findings, for the most part, have been based on dystrophic changes in lipid content in mixed hind limb muscle without examining muscles with predominant fibre type composition. Observed changes in membrane damage of *mdx* muscle, along with changes in membrane lipid composition, raises a plausible association between muscle damage and membrane composition. Moreover, the membrane lipid composition and susceptibility of *mdx* fast and slow twitch muscles to damage is not similar across ages. As the pathological features of muscular dystrophy are cumulative over time, examination of the phenotype at one age group with no consideration of its progression may be insufficient and mask or falsely suggest the associated damage. To the author's knowledge, there have been no studies that have addressed muscle-type specific responses to eccentric induced damage and fibrosis in dystrophic skeletal muscle and the relationship to membrane phospholipid fatty acid composition in different age groups. Thus the purpose of this thesis was to examine the

association of membrane PL FA composition and the susceptibility of fast and slow twitch skeletal muscle to eccentric induced damage and fibrosis.

Objectives

The primary objective of the current research was to examine the association between skeletal muscle membrane PL composition and the role of absence of dystrophin in the muscle's susceptibility to eccentric induced damaged and fibrosis. This objective was accomplished by examining the FA profile of each PL species in skeletal muscles of varying fibre-type composition (soleus which is predominantly type I and less susceptible to damage and EDL which is predominantly type II and more susceptible to damage) in a rodent model of muscular dystrophy, the *mdx* mouse. Specifically, the PL FA composition in each muscle type will be correlated against eccentric induced measure of membrane damage (identification of inter-fibre fibronectin after *in vitro* eccentric contraction damage), and fibrosis in dystrophic muscle compared to wild type. Moreover, since the dystrophic pathology increases with age, a group of young (10 weeks) and older (20 weeks) *mdx* mice were selected to examine the strength of association between alterations in membrane PL FA compositions and muscle damage with age.

Hypotheses

It was hypothesised that alterations in membrane composition (increased SFA and MUFA, decreased PUFA) in the absence of dystrophin protein will be positively (SFA and MUFA) or negatively (PUFA) correlated to increased eccentric induced muscle damage and fibrosis. From this main hypothesis, it can also be hypothesized that:

i. The correlations of altered membrane lipid composition with eccentric induced muscle damage and fibrosis listed above will be stronger at 20 weeks, when the dystrophic phenotype is more severe, compared to 10 weeks.

ii. EDL, which has more type II fibres, will be more susceptible to damage and have more significant and stronger correlations listed above compared to soleus, which has more type I fibres.

CHAPTER 2: METHODS

Animals

Ten control (*C57BL/10*) and dystrophin-deficient (*C57BL/10ScSn-Dmd^{mdx}/J*) mice at age 8 weeks were obtained from Jackson's Laboratory (Bar Harbour, Maine, USA). All mice were housed in the Brock University Comparative Biosciences Facility in an environment maintained at 22±1°C with a 12:12 hour light (6:00am to 6:00pm)-dark (6:00pm to 6:00am) cycle. Animals had access to rodent chow (14.3% protein, 4% fat, 48% carbohydrate; 2014 Teklad Global 14% Protein Rodent Maintenance Diet, Harlan Laboratories, Mississauga, Ontario) and water *ad libitum*. All experimental procedures and protocols were approved by the Brock University Research Subcommittee on Animal Care and conformed to the Canadian Council of Animal Care guidelines.

Experimental design

For the purpose of this study, two groups of 10 (n_{WT}: 5; n_{mdx}: 5) and 20 (n_{WT}: 5; n_{mdx}: 5) week old mice were selected. Both extensor digitorum longus (EDL) and soleus (SOL) were isolated from hind limbs. One EDL and SOL was maintained as a control, while the muscles of the contralateral limb were used for stretch injury. After the stretch protocol, both stretched and control muscles were dissected into three equal parts, with the middle 1/3 used for histochemistry and the two proximal and distal 1/3 of muscle were snap frozen for lipid analysis (Fig. 2.1).

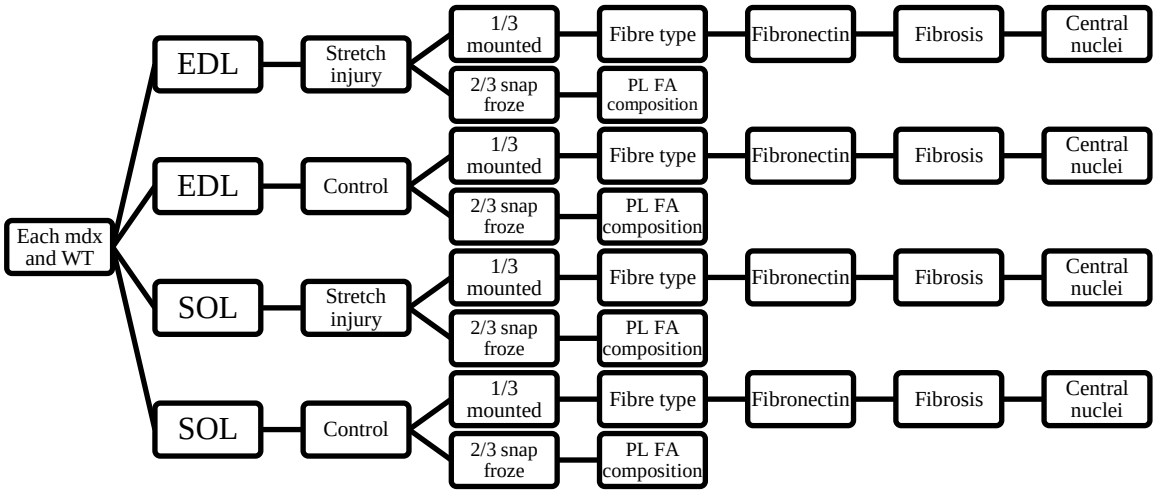

Figure 2.1. Over view of experimental design. WT, wild type; EDL, extensor digitorum longus; SOL, soleus.

In vitro muscle preparation

Muscle isolation

Each mouse was anesthetised through an intraperitoneal injection of sodium pentobarbital (60 mg/kg body weight). EDL and SOL from both hind limbs were removed. Specifically, the EDL proximal tendon was located lateral to the knee under the distal end of the rectus femoris, looped with 6-0 silk suture and cut at this point to maximize the length of the tendon stump. Tendon sutures were tied as close to the myotendinous junction as possible, but not in contact with the muscle fibres. Optimum placement of the sutures ensured less contribution of the tendon to compliance, and minimized failure of this attachment during stimulation. The distal tendon was located under the tibialis anterior (TA) tendon, loop sutured and all tendons leading to the toes were cut before removing the muscle. For dissection of SOL, first the distal achilles tendon (which includes the distal soleus tendon) was cut from tuber calcanei. This was followed by peeling all posterior compartment muscles away from the rest of the limb. The distal tendon of SOL was localized at the most posterior tendon of the peeled compartment and sutured. The proximal SOL tendon was identified on the interior surface of the muscles close to the knee, loop sutured and cut as close as possible to the back of the knee to maximize the length of the tendon stump. All the dissected muscles were placed into oxygenated Ringer solution (137mM NaCl; 24 mM $NaHCO_3$; 11 mM d-glucose; 5 mM KCl; 2 mM $CaCl_2$; 1 mM NaH2PO4H2O; 1 mM MgSO4; 0.025 mM d-tubocurarine chloride) at 25 ºC to equilibrate for 20 min.

Muscle attachment to apparatus

After equilibration, EDL and SOL were maintained at resting length in bathing solution by using the silk sutures of proximal and distal end as anchors to maintain resting length. Resting length was achieved at a length in which the muscle was not stretched or compressed. The contralateral muscle was mounted to the servomotor controlled by a dual-mode lever system (305B acquired through a 604C analog to digital interface) with one end of the muscle tied to the immovable pin, and the other end attached to the lever arm of the position feedback servomotor. Muscle stimulation was applied using flanking platinum electrodes driven by a Model 701B biphase stimulator (Aurora Scientific, Inc.). All aspects of muscle isolation, stimulation, servomotor control, force assessments and software control were performed by W. Gittings.

Eccentric induced muscle damage

Establishment of optimum length

Muscles were adjusted to the optimum length (L_o) for the development of isometric twitch force. The muscles were stimulated with a single electrical pulse to produce a twitch response. Stimulation voltage was that which produced a maximal twitch response. Muscle length was adjusted very carefully and in small increments (or decrements) to longer (or shorter) lengths with 30 seconds of rest between twitch responses. L_o was achieved when twitch force was maximal. To measure L_o, the length between the myotendinous junctions was recorded using a graded magnifier and monitored prior to and after muscle stimulation to ensure L_o was maintained.

Establishment of frequency-force relationship

Once L_o was achieved, the frequency force relationship was established. The muscle was stimulated at increasing frequencies, typically 10, 30, 50, 80, 100, 120, 150, 180, 200, and 250 Hz for a period of 500 msec with periods of 3 minutes rest between stimuli. Maximum absolute isometric tetanic force (P_o) was determined from the plateau of the frequency-force relationship. The plateau was achieved at 150 Hz for EDL and 100 Hz for SOL.

Maximum isometric twitch and tetanus force

To provide a baseline for comparison, muscles were stimulated at 150 Hz for EDL and 100 Hz for SOL for 500 ms to obtain control maximum isometric tetanus. After 3 minutes of rest, muscles were stimulated at 80 Hz for 0.2 ms to obtain the maximum isometric twitch force. The control maximum twitch and tetanic isometric force were measured and normalized for muscle cross section by dividing the mass of the muscle (g) by the product of its length (L_o, cm) and density (1.06 g/cm^3) and expressed in square millimetre.

EDL stretch injury

In vitro eccentric damage for EDL was conducted as per Petrof *et al.* (1993). Briefly, muscles were left quiescent for 10 min. After establishment of L_o, maximum isometric twitch and tetani, muscles were stimulated at 80 Hz for 700 ms. During the initial 500 ms of stimulus, muscles were maintained at their L_o (isometric contraction) and the last 200 ms, stretched at rate of 0.5 L_o/sec) to yield a total displacement of 0.1 L_o creating an eccentric contraction. With 4 minutes of rests in between each contraction,

muscle stretch injury was repeated five times. Post twitch and tetanic responses was obtained immediately and 15 minutes after the last stretch injury contraction.

SOL stretch injury

SOL damage was completed following Warren *et al.* (1994). Briefly, muscles were left quiescent for 10 min and L_o was determined. Initial measurements included isometric twitch force with a 0.5 ms pulse at 80 Hz and tetanic force at 500 ms trains of 0.5 ms pulses at 100 Hz spaced 3 minutes apart. For stretch injury, muscle length was initially shortened from L_o to $0.9L_o$ followed by immediate lengthening from 0.9 L_o to 1.1 L_o (V: 1.5 L_0/S). During lengthening, SOL was stimulated at 125 Hz for 133 ms. Eccentric contractions was repeated 10 times with 4 minute of rest in between each series of stretch injury. Post injury measurements were obtained immediately and 15 minutes after last stretch injury contraction.

Specific force calculation

To obtain normalized forces from EDL and SOL and control for existing hypertrophy in *mdx* myofibres, the cross sectional area for each muscle was determined by dividing the mass of muscle (g) by the product of its optimum fibre length (L_f) and density of mammalian muscle (1.06 mg/mm^3), and presented as specific force (sP; equation below). L_f was determined by multiplying L_o by the previously determined muscle length to fibre length ratio, 0.44 for the EDL and 0.71 for the SOL (Brooks & Faulkner, 1988).

sP (g/mm^2) = Tetanic or twitch force / (muscle mass/ L_f * 1.06)

Histochemistry and Immunohistochemistry

Muscle Embedding

After stretch injury, the mid 1/3 of both damaged and control muscles from EDL and SOL were mounted on a small mound of cryomatrix on cork plates and cooled in methylbutane as per Steinbrecht & Zierold (1984).

Fibronectin

Immunohistochemistry was completed on 5 µm sections obtained from a cryostat (HM 560 MV, Thermo Fischer Scientific) at -20 ^{o}C to identify intracellular accumulation of fibronectin as a marker of eccentric induced injury. This was achieved through the use of an avidin biotin complex method (Wilchek, 1935). To ensure proper tissue adhesion, superfrost colorfrost (VWR, PA) micro slides were used. Briefly, to further increase the adherence of tissue to the slides, tissue sections were initially fixed in cooled acetone (-20 $^{\circ}$C) for 15 minutes. After washing (3 times for 5 minute in Tris-buffered saline (TBS)), slides were incubated for 10 minutes at room temperature in 3% H_2O_2 diluted in methanol to block endogenous peroxidase activity. After another wash in TBS, non-specific binding was blocked with 250 µl of blocking buffer (5% bovine serum albumin, 0.3% triton X100 in TBS) for 30 min. Without washing, 250 µl of primary anti-mouse fibronectin monoclonal antibody produced in rabbit (Sigma) previously diluted to 1/100 in blocking buffer was applied to the slide sections for 2 hours at room temperature. After washing with TBS (3 times for 5 min), 250 µl of anti-rabbit secondary biotinylated

antibody (Sigma) diluted to 1/150 in blocking buffer was applied to each tissue section for 30 min at room temperature. After another session of washing with TBS (3 times for 5 min), 150 µl of strepavidin peroxidase was added to each slide for 30 min at room temperature and washed after in TBS (3 times for 5 min). Avidin peroxidase was previously prepared by mixing 10 µL of avidin and 10 µL of biotin-peroxidase in 1 mL of TBS. To prepare the slides for visualization, slides were incubated for 1-2 min in 250 µl of 3, 3'diaminobenzidine (DAB) diluted to 1% in double distilled water (DDW). DAB is oxidized in the presence of peroxidase resulting in the deposition of a golden brown precipitate at the site of enzymatic activity. DAB development was closely monitored followed by immediate immersion in DDW after precipitation. Finally, slides were washed in DDW 2 times for 3 min. Negative controls (no application of primary antibody) were used to determine non-specific binding of secondary antibody. Four regions (each 0.07 mm^2, accounting for 20% of total cross section area) of each slide were randomly selected and all the immune reactions were identified. The selected regions were scored to quantify the magnitude of fibronectin entry as a percentage of fibronectin-positive fibres on each muscle section (mean ± SE).

Masson's trichrome staining

Masson's trichrome staining was used to quantify fibrosis (collagen accumulation) and regeneration (centralized nuclei) in muscle sections as per Ruegg and Meinen (2014). Briefly, 12 µm sections on superfrost slides (VWR) were incubated in 10% formalin and Bouin solution for 1 and 12 hours, respectively followed by 2 minutes of washing under running tap water followed by 1 min of wash with DDW. Slides were

treated with hematoxylin achieved by mixing equal parts of Weigert iron hematoxylin A (1% hematoxylin in ethanol) & B (30% ferric chloride and 7.5% HCL in DDW) (Trichrome staining kit, Sigma) for 5 minutes and washed in DDW for 3 minutes. Scarlet acid fuchsin/ Biebrich scarlet acid fuchsin (0.9 % Biebrich scarlet, 0.9% fuchsin, 1% acetic acid) was used for cytoplasm staining for 5 minutes, and washed for 3 minutes in DDW. To prepare the uptake of aniline blue that stains the collagen fibres dark blue, slides were incubated with phosphotungstic and phosphomolybdic acid (1 volume of phosphotungstic, 1 volume of phosphomolybdic and 2 volumes of DDW) for 10 minutes. Each section was incubated with aniline blue (2.5% in 2% acetic acid) and washed in DDW after 5 minutes. Slides were dehydrated in ascending concentration of ethanol at 70%, 80%, 90%, 100% and xylene (98.5% xylenes in ethylbenzene basis) each for 3 min. Finally, slides were mounted with 1 drop of xylene based mounting media (Depex, Fisher Scientific) and stored at room temperature. High magnification photographs of each muscle cross section were taken using a computer based image processing software (NIS elements; series 4, Nikon & Image-Pro 7.0.1). Muscle cross-sectional area was measured manually by drawing around the outer border of the fibre. Fibrotic areas stained in blue were quantified in the whole cross section by drawing around each area, divided by the muscle cross-sectional area and reported as percentage of fibrosis across the muscle. Total fibres and fibres with centralized nuclei were identified manually in 4 region of muscle (each 0.07 mm^2 for ~20% of cross section), and reported as percentage of regenerated fibres.

Myosin ATPase staining

Myosin ATPase was quantified as per Brooke & Kaiser (1970). Briefly, sections of muscle (12 µm) were pre-incubated in alkaline solution (alkaline solution: 7.05% glycine, 18 mM calcium chloride, 0.1 N sodium hydroxide in DDW, pH 10.2) for 15 minutes. After rinsing, tissue sections were incubated in ATP solution (2.7 mM ATP dissolved in alkaline solution, pH 9.4) for 15 minutes. After 3 washes with 1% calcium chloride, slides were incubated with 2% cobalt chloride. Final step was completed by incubating the slides for a few seconds in 1% ammonium sulfide used to provide a black precipitate. Slides were then dehydrated by submersing in rising concentration of ethanol at 70%, 80%, 90%, 100% and xylene (Sigma, cat no. 247642) each for 3 min. Finally, slides were mounted with 1 drop of xylene based mounting media (Depex, Fisher Scientific) and stored at room temperature.

Lipid analysis

Lipid extraction

Frozen muscle samples were homogenized in 10 volumes of Tris HCL (pH 8.0). Lipids were extracted from the homogenate according to Bligh & Dyer (1959). Briefly, 70 µl of whole muscle homogenates were added to 3.75 ml of chloroform: methanol (1:2) supplemented with 0.1% butylated hydroxytoluene and vortex for 2 minutes. Samples were vortexed briefly after the addition of 1.25 ml of chloroform. DDW was added (1.25 ml), samples were vortexed and spun at 720g for 6 minutes. Lipids were then isolated by collecting the bottom chloroform phase, and stored at –20°C until further analysis.

Thin layer chromatography

Thin layer chromatography (TLC) was used to separate individual PL species as per Mahadevappa and Holub (1987). Briefly, pre-coated silica gel 60 plates (EMD, Mississauga, ON, CA) were heated at 110°C for 20 minutes and kept in a desiccating chamber to cool before use. Samples were dried down under nitrogen and re-suspended in chloroform: methanol (2:1) and spotted onto the plate. The plates were then placed in a chamber containing a solvent system (chloroform: methanol: acetic acid: water; 50:37.5:3.5:2) for approximately 2 hours. The plate was removed and set to dry before being sprayed with dichloroflouroscene (DCF) solution (1:1 methanol: water and 2',7'-DCF filtered and washed with petroleum ether) and set in a chamber containing 25% ammonium hydroxide in DDW for 5 minutes to develop. The plate was viewed under ultraviolet light and the bands marked (from origin: sphingomyelin, phosphatidylcholine, phosphatidylserine, phosphatidylinositol, phosphatidylethanolamine, cardiolipin) and scraped into individual 15mL kimex tubes.

Methylation

The scrapings were methylated as per Mahadevappa & Holub (1987). In brief, 6% H_2SO_4 in methanol was added to each tube with 10 µg of internal standard (tridecanoic acid; 13:0) and incubated at 80°C for 2 hours. Samples were allowed to cool, 1 mL of water and 2 mL of petroleum ether were added, and the solution was vortexed before being centrifuged for 6 minutes at 720g. The top phase was extracted and put into a microvial (Fisher Scientific, CA, USA), dried down under nitrogen and resuspended in 10 µL of dichloromethane for analysis by gas chromatography.

Gas chromatography

The FA composition of each PL was analyzed by gas chromatography (GC; Bradley, *et al.*, 2007). A 1 µl sample of fatty acid methyl esters (FAME) from each sample was injected into a GC (Trace GC Ultra, Thermo Electron Corp, Milan, Italy) supplied with a split/splitless injector, a fast flame ionization detector (FFID), and Triplus AS auto sampler (Trace GC Ultra, Thermo Electron Corp, Milan, Italy). With helium as a carrier gas, FAMEs were separated on a UFM RTXWAX analytical column (Trace GC Ultra, Thermo Electron Corp, Milan, Italy) and identified by comparison of their retention times with those of a known standard solution (Supelco 37 component FAME mix, Supelco, Bellefonte, PA, USA). The areas of each individual peak were converted to concentrations with the aid of tridecanoic acid (13:0) as the internal standard.

Statistical analysis

Values are expressed as mean ± standard error (SE). To assess differences between groups (WT vs. *mdx*) and age (10 wks and 20 wks), a two way analysis of variance (ANOVA) was used (R core team, Austria, Vienna, 2013). Post hoc Tukey's test was used to determine differences within groups and ages for variables of interest (fibre type composition, PL FA composition, intracellular fibronectin, fibrosis, and twitch characteristics). Linear correlations between variables (PLFA composition, intracellular fibronectin and fibrosis) were determined with Pearson correlation coefficients. Statistical significance was defined as $P < 0.05$ for all analysis.

CHAPTER 3: RESULTS

Morphometric

At 10 weeks of age, body mass was similar between *mdx* (29.2 ± 3.9g) and WT (25.2 ± 1.0g), however at 20 weeks of age, *mdx* mice were significantly heavier (35.5 ± 1.5g) compared to 20 week old WT (28.9 ± 3.3g) and 10 week old *mdx*. Both EDL and SOL muscle masses were greater in *mdx* compared to WT for both age groups (Table 3.1). Cross sectional areas and percent fibre types were similar between genotypes and ages for each muscle, with the exception that type I fibres were higher and type II fibres were lower in EDL of 20 week old *mdx* compared to 10 week olds.

Contractile properties before and after the stretch injury

A series of 5 eccentric contractions at the rate of 0.5 L_o/S in dystrophic EDL at 10 weeks resulted in ~30% decline in maximum isometric twitch after 15 min of fatigue recovery, which was ~2.5 times greater than the WT (Table 3.2). At 20 weeks, there was an ~55% depression in force output in *mdx* EDL, compared to ~4.5 % in WT. Moreover, the lengthening contractions resulted in 25% tetanic force depression in *mdx* EDL at 10 weeks, which was ~2 times greater than in WT. At 20 weeks, force declined to 65% after 15 min of rest, which was ~3 times more than that of WT. The half relaxation time (HRT) and time to peak tension (TPT) of dystrophic and WT EDL remained unaltered across both 10 and 20 weeks.

In SOL, after 10 eccentric contractions at 1.5 L_o/S and 15 minutes of fatigue recovery, the isometric twitch and tetanic responses remained unchanged across WT and *mdx* at 10 and 20 weeks (Table 3.3). After recovery from fatigue, the HRT and TPT were unaltered across dystrophic and WT SOL at 10 and 20 weeks.

Table 3.1. Body mass, muscle mass, muscle cross sectional area and percent fibre type of extensor digitorum longus and soleus muscles for 10 and 20 week old wild type and *mdx* mice.

	Body mass (g)	EDL					SOL				
		Mass (g)	XSA (mm^2)	L_0 (mm)	Type I Fibres (%)	Type II Fibres (%)	Mass (g)	XSA (mm^2)	L_0 (mm)	Type I Fibres (%)	Type II Fibres (%)
WT-10	27.7 ± 0.5	12.7 ± 1.6	2.2 ± 0.2	11.8 ± 0.1	5.0 ± 2.0	95.7 ± 5.5	14.1 ± 2.7	1.3 ± 0.2	12.2 ± 0.1	36.3 ± 7.1	64.7 ± 2.2
mdx-10	27.8 ± 0.2	18.2 ± 6.1	3.0 ± 1.4	11.9 ±0.3	5.1 ± 2.4	96.0 ± 2.4	18.7 ± 4.8*	2.2 ± 0.7	11.9 ± 0.2	40.7 ± 8.5	60.0 ± 5.5
WT-20	31.7 ± 0.2	12.9 ± 2.8	1.1 ± 0.3	12.2 ± 0.3	7.2 ± 1.3	93.8 ± 4.3	15.6 ± 2.0	1.0 ± 0.2	12.7 ± 0.2	38.4 ± 4.1	63.6 ± 4.1
mdx-20	35.4 ± 0.2	18.8 ± 3.6*	1.4 ± 0.2	12.4 ± 0.2	18.5 ± 1.3*†	82.9 ± 6.0*†	19.4 ± 2.2*	1.1 ± 0.3	13.1 ± 0.2	43.2 ± 2.8	57.3 ± 4.4

Values are mean ± SEM; n=5; EDL, extensor digitorum longus; SOL, soleus; WT-10, wild type 10 weeks old; WT-20, wild type 20 weeks old; *mdx*-10, *mdx* 10 weeks old; *mdx*-20, *mdx* 20 weeks old; XSA, cross sectional area; * denotes significantly different from WT of the same age; † denotes significantly different from 10 wks.

Table 3.2. Contractile parameters obtained from EDL of WT and *mdx* at 10 and 20 weeks of age.

EDL	WT						*mdx*					
	10 wks			20 wks			10 wks			20 wks		
	Control	Post	15min Post	Control	Post	15min Post	Control	Post	15min Post	Control	Post	15min Post
Twitch (g/mm^2)	1.93 ± 0.3	1.19 ± 0.4	1.20 ± 0.34	2.25 ± 0.34	1.58 ± 0.34	1.46 ± 0.33	1.59 ± 0.40	0.95 ± 0.31 *	0.97 ± 0.26 *	1.6 ± 0.26	0.54 ± 0.09 *†¥	0.72 ± 0.06 *†¥
Tetanus (g/mm^2)	9.5 ± 1.3	6.98 ± 1.57	7.74 ± 1.69	10.4 ± 1.45	7.86 ± 1.26	8.68 ± 1.45	6.7 ± 1.6	3.79 ± 1.02 *	4.74 ± 1.15 *	6.59 ± 0.95	1.96 ± 0.58 *†¥	3.36 ± 0.65 *†¥
Twitch HRT (ms)	27.1 ± 7.4	9.8 ± 1.3	22.8 ± 5.9	21.4 ± 2.1	12.1 ± 0.9	19.2 ± 3.1	23.1 ± 2.6	16.5 ± 2.8	23.1 ± 4.2	22.5 ± 4.7	15.2 ± 1.1	24.6 ± 2.2
Twitch TPT (ms)	19.2 ± 2.8	16.0 ± 0.4	17.3 ± 0.8	21.4 ± 1.5	16.4 ± 1.2	17.1 ± 0.6	18.3 ± 0.8	17 ± 0.4	16.5 ± 1.3	20.9 ± 3.5	17.7 ± 1.9	17.3 ± 1.4

Values are expressed as mean ± SEM; EDL, Extensor digitorum longus; WT, Wild type; HRT, half relaxation time; TPT, time to peak tension * denotes significant from controls. † denotes significance from WTs within same age. ¥ denotes significance from 10 wks within same genotype.

Table 3.3. Contractile parameters obtained from SOL of WT and *mdx* at 10 and 20 weeks of age.

SOL	WT						*mdx*					
	Control	10 wks Post	15min Post	Control	20 wks Post	15min Post	Control	10 wks Post	15min Post	Control	20 wks Post	15min Post
Twitch (g/mm^2)	1.51 ± 0.21	1.10 ± 0.17	1.19 ± 0.19	1.61 ± 0.10	1.16 ± 0.08 ¥	1.21 ± 0.08	0.95 ± 0.2	0.60 ± 0.15	0.67 ± 0.16	1.44 ± 0.18	0.8 ± 0.11	0.94 ± 0.12
Tetanus (g/mm^2)	9.49 ± 0.88	8.63 ± 0.76	8.80 ± 0.76	10.03 ± 0.64	8.9 ± 0.6	9.11 ± 0.71	6.3 ± 1.17	5.66 ± 0.99 *	5.75 ± 1.02	10.00 ± 1.21	8.52 ± 0.99 *	8.53 ± 0.99
Twitch HRT (ms)	38.7 ± 2.1	32.5 ± 4.7	32.4 ± 1.3	51.9 ± 2.1	48.3 ± 4.1	43.4 ± 1.7	61.3 ± 4.2	60.2 ± 3.9	58.4 ± 2.1	58.9 ± 5.2	51.7 ± 3.6	55 ± 4.6
Twitch TPT (ms)	37.2 ± 2.1	35.2 ± 3.8	34.8 ± 2.7	38.7 ± 2.0	36.2 ± 6.1	36.1 ± 3.1	32.5 ± 2.1	31.1 ± 3.6	31.3 ± 2.7	33.9 ± 1.8	31.7 ± 1.5	30.5 ± 2.4

Values are expressed as mean ± SEM; SOL, Soleus; WT, Wild type; HRT, half relaxation time; TPT, time to peak tension. * denotes significant from control.

Membrane composition

Membrane lipid analysis demonstrated decreased PC and increased SM in dystrophic EDL at 10 and 20 weeks compared to WTs (Fig. A.4). In general, among the four major FA classes, MUFA were increased and n6 PUFA were decreased in *mdx* EDL at 10 and 20 weeks compared to WTs. Specifically, among PL species, 18:0 and MUFA (mainly 18:1) were increased and PUFA (mainly 18:2n6) was decreased in *mdx* EDL compared to WT at 10 and 20 weeks in PC and PS (Table A.1, Table A.4). Moreover, MUFA (mainly 18:1) was increased and n6 PUFA were decreased in *mdx* EDL at 20 weeks in SM and PE compared to WT (Table A.2, Table A.3). In PI and CL FAs, there was an increase in MUFA and a decrease in PUFA in *mdx* at both age groups compared to WTs (Table A.5, Table A.6).

In SOL, among PL classes, CL was increased in *mdx* at 10 and 20 weeks compared to WTs. In general, MUFA remained unchanged at 10 weeks in dystrophic phenotype compared to WTs but increased at 20 weeks. Moreover, n6 PUFA was decreased at 10 and 20 weeks in *mdx* compared to WTs (Fig. A.7). Specifically in CL, SM, and PE, there was increased MUFA with decreased n6 PUFA in *mdx* SOL in 20 weeks compared to WT (Table A.7-A.9). In PC, only MUFA were increased in *mdx* at 10 and 20 week (Table A.10). Finally, in PI and PS, MUFA was increased and PUFA (mainly 18:2n6) was decreased (Table A.11, Table A.12).

Eccentric induced muscle damage

Intracellular fibronectin

In general, the percentage of total fibres that were fibronectin positive did not differ between stretched and non-stretched EDL (Fig 3.1). The only exception was that the percentage of fibronectin-positive fibres was higher in stretched 20 week old *mdx* compared to non-stretched 20 week old *mdx*, 20 week old WT, and 10 week old *mdx*.

The percentage of total fibres that were fibronectin positive did not differ between stretched vs. non-stretched SOL (Fig 3.2). However, the percent fibronectin-positive fibres were higher in both non-stretched and stretched 20 week old *mdx* SOL compared to 10 week old *mdx* and 20 week old WT.

Overall, type II fibres in both EDL and SOL muscles of WT and *mdx* in both age groups were the majority of fibres with intracellular fibronectin (Fig 3.1 and Fig. 3.2). In EDL, the ratio of fibronectin positive type I to type II fibres was increased in 20 wks old *mdx* compared to their WTs, but the ratio remained unchanged in 10 wks old *mdx* mice. In SOL, the ratio was unaltered in *mdx* at both 10 and 20 week. Moreover, in SOL independent of membrane damage, the proportion of type I and II fibres positive forfibronectin remained unchanged across WTs and *mdx* at both age groups.

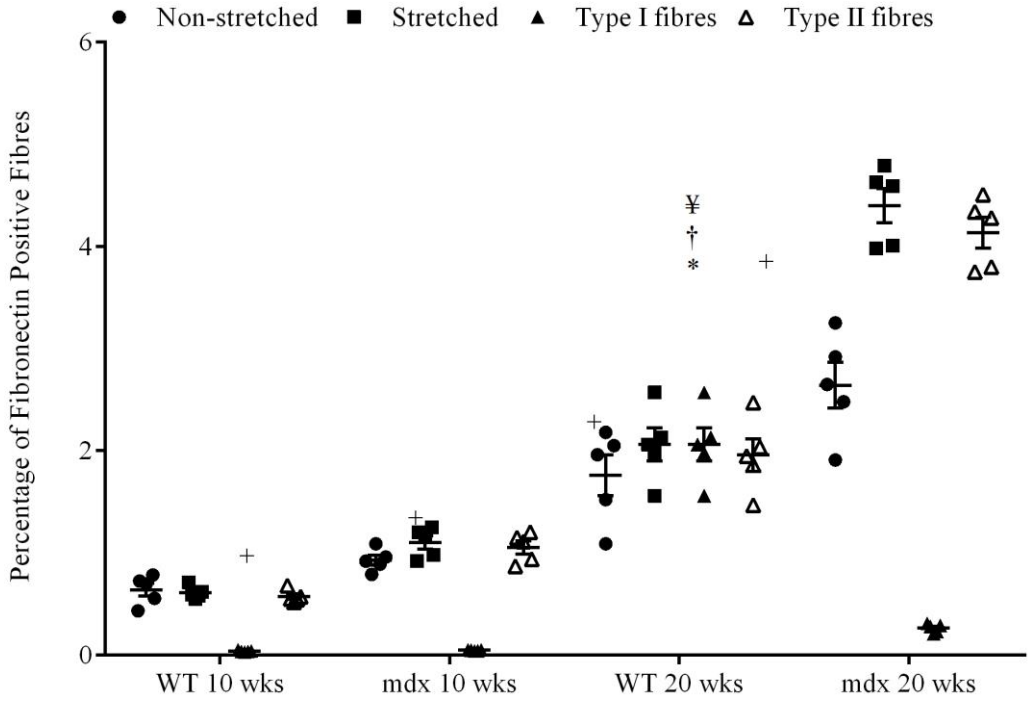

Figure 3.1. Percent fibronectin-positive fibres in wild type and mdx stretched and non-stretched extensor digitorum longus muscle at 10 and 20 weeks of age. Percentage of fibronectin positive fibres represents the fibres with intracellular fibronectin divided by the total number of fibres. Type I and II fibres represent the fibres with intracellular fibronectin from stretched muscle. Values are mean ± SEM; WT, wildtype; * denotes significance from non-stretched; † denotes significance from WT within the same age group; ¥ denotes significance from 10 weeks of age within the same genotype; + denotes significance from type I fibres.

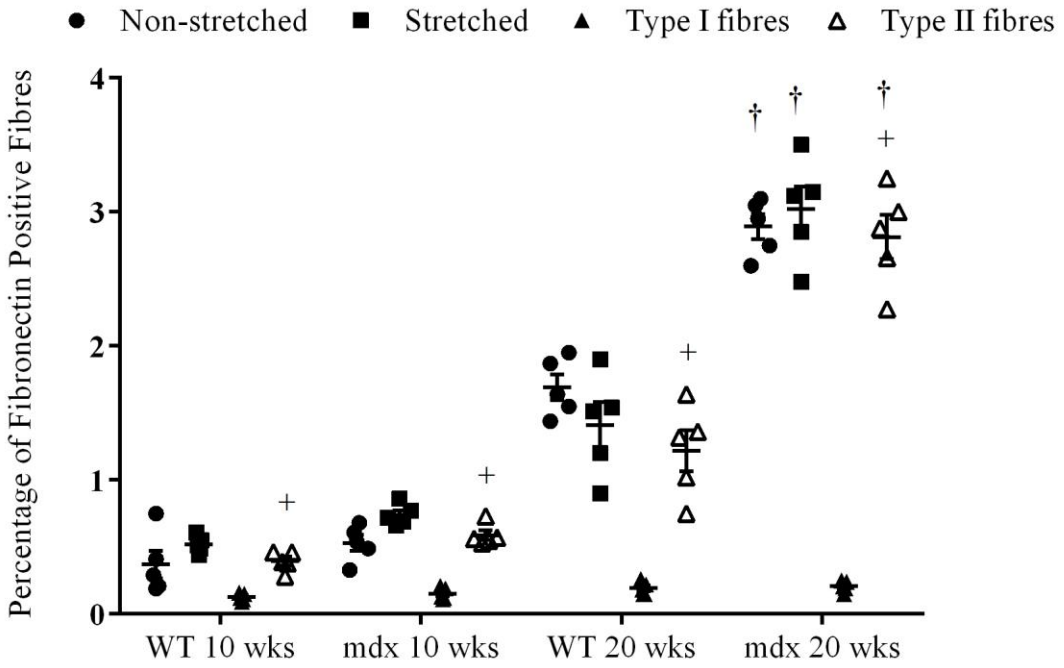

Figure 3.2. Percent fibronectin-positive fibres in wild type and *mdx* stretched and non-stretched soleus muscle at 10 and 20 weeks of age. Percentage of fibronectin positive fibres represents the fibres with intracellular fibronectin divided by the total number of fibres. Type I and II fibres represent the fibres with intracellular fibronectin from stretched muscle. Values are mean ± SEM; WT, wildtype; † denotes significance from WT within the same age group; + denotes significance from type I fibres.

Influence of membrane lipid composition on eccentric induced muscle damage

To assess the correlation of membrane lipid composition on eccentric induced muscle damage, only the PL and FAs that significantly changed in EDL or soleus were selected.

For SM FA, the general trend was that saturated and monounsaturated fatty acids demonstrated a positive correlation with percent fibronectin-positive fibres whereas polyunsaturated fatty acids were negatively correlated (Fig 3.3). Specifically, SM 16:0 (10 wks; r: 0.73, p: 0.04, 20 wks; r:0.12, p:0.05), 18:0 (10 wks; r: 0.97, p:0.02, 20 wks; r:0.42, p: 0.04), and 18:1 (10 wks; r:0.67, p:0.03, 20 wks; r: 0.59, p: 0.03) were significantly positively correlated with percent fibronectin- positive fibres in both 10 and 20 week old *mdx* EDL. In contrast, only 20 week old WT SM 16:0 (r=0.89, p=0.03), 18:0 (r=0.39, p=0.04), and 18:1 (r=0.31, p=0.05) were significantly positively correlated to percent fibronectin-positive fibres. SM 18:2n6 was significantly negatively correlated in 10 week old *mdx* (r=-0.73, p=0.03) and WT (r=-0.77, p=0.03) and approached significance (p=0.07) in 20 week old *mdx*.

For PC FA, the general trend was 16:0 and 18:2n6 demonstrated a negative correlation with percent fibronectin-positive fibres whereas 18:0 and 18:1 demonstrated a positive correlation (Fig 3.4). Specifically, these correlations were significant in *mdx* for all PC FA in both age groups (16:0 at 10 wks *mdx*; r=-0.63, p=0.02, 16:0 at 20 wks *mdx*, r=-0.81, p=0.07, 18:0 at 10 wks *mdx*; r:=0.93, p=0.01, 18:0 at 20 wks *mdx*; r=0.59, p=0.04, 18:1 at 10 wks *mdx*, r=0.83, p=0.04; 18:1 at 20 wks *mdx*, r=0.89, p=0.01; 18:2n6 at 20 weeks *mdx*, r=-0.74, p=0.04), with the exception of 18:2n6 at 10 weeks of age. In contrast, significance was only found with 18:0 (r=0.79, p=0.01), 18:1 (r=0.88, p=0.04),

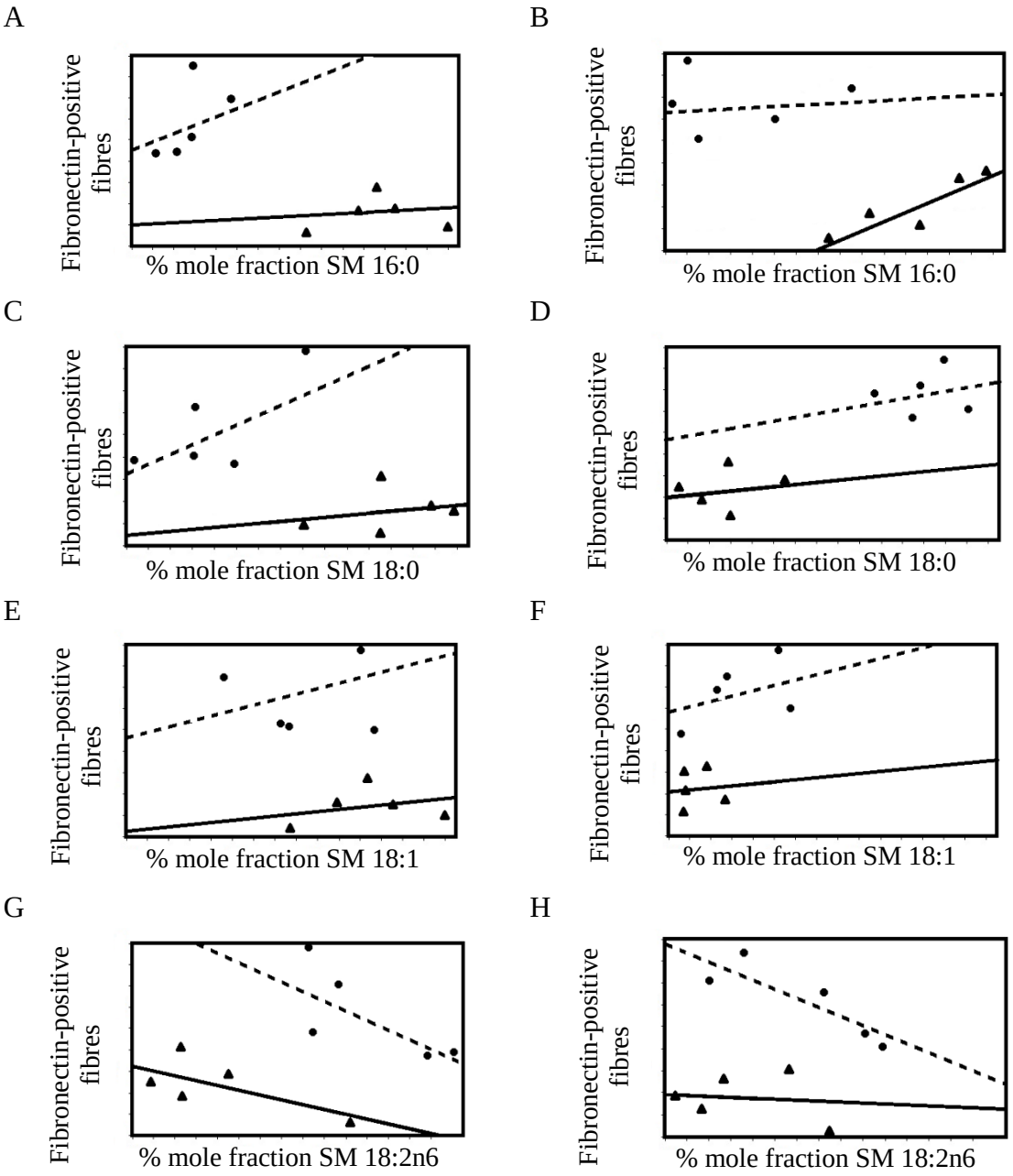

Figure 3.3. Linear fitted regression model of eccentric induced damage correlated with membrane sphingomyelin (SM) A) 16:0 at 10 weeks (WT, r=0.11, p=0.25; *mdx*, r=0.73, p=0.04), B) 16:0 at 20 weeks (WT, r=0.89, p=0.03; *mdx*, r=0.12, p=0.05), C) 18:0 at 10 weeks (WT, r=0.17, p=0.07; *mdx*, r=0.97, p=0.02), D) 18:0 at 20 weeks (WT, r=0.39, p=0.04; *mdx*, r=0.42, p=0.04), E) 18:1 at 10 weeks (WT, r=0.21, p=0.07; *mdx*, r=0.67, p=0.03), F) 18:1 at 20 weeks (WT, r=0.31, p=0.05; *mdx*, r=0.59, p=0.03), G) 18:2n6 at 10 weeks (WT, r=-0.77, p=0.03; *mdx*, r=-0.73, p=0.03), and H) 18:2n6 at 20 weeks (WT, r=-0.14, p=0.81; *mdx*, r=-0.87, p=0.07) in wild type (WT; solid lines) and *mdx* (dashed lines) extensor digitorum longus muscle.

and 18:2n6 (r=-0.91, p=0.02) at 10 weeks of age and 16:0 (r=-0.94, p=0.01) and 18:1 (r=0.91, p=0.02) at 20 weeks of age in WT.

In contrast to EDL, SOL membrane damage was not significantly correlated to any CL FA (Fig. 3.5).

Fibrosis

Fibre regeneration and fibrosis

Percentage of fibres with central nuclei was higher in *mdx* compared to WT in both fibre types at 10 weeks and 20 weeks of age for EDL (Fig 3.6) and SOL (Fig 3.7). Fibrosis was highest in 20 week old *mdx* compared to 10 week old *mdx* and 20 week old WT for EDL and soleus (Figure 3.8).

Influence of membrane lipid composition on fibrosis

Similar to correlations to eccentric induced muscle damage, only the PL and FAs that significantly changed in EDL (SM 16:0, 18:0, 18:1, 18:2n6 and PC 16:0, 18:0, 18:1, 18:2n6) and soleus (CL) were selected (Appendix A Table A.2, A.3, A.8).

For SM FA in EDL, most of the correlations were not significant. The exceptions were 16:0 in 10 week old *mdx* (r=0.70, p=0.01), 18:1 in 20 week old *mdx* (r=0.42, p=0.04), and 18:2n6 in 10 week old WT (r=0.37, p=0.05) were significantly positively correlated with percent fibrosis, whereas 18:2n6 in 10 week old *mdx* (r=-0.49, p=0.03)

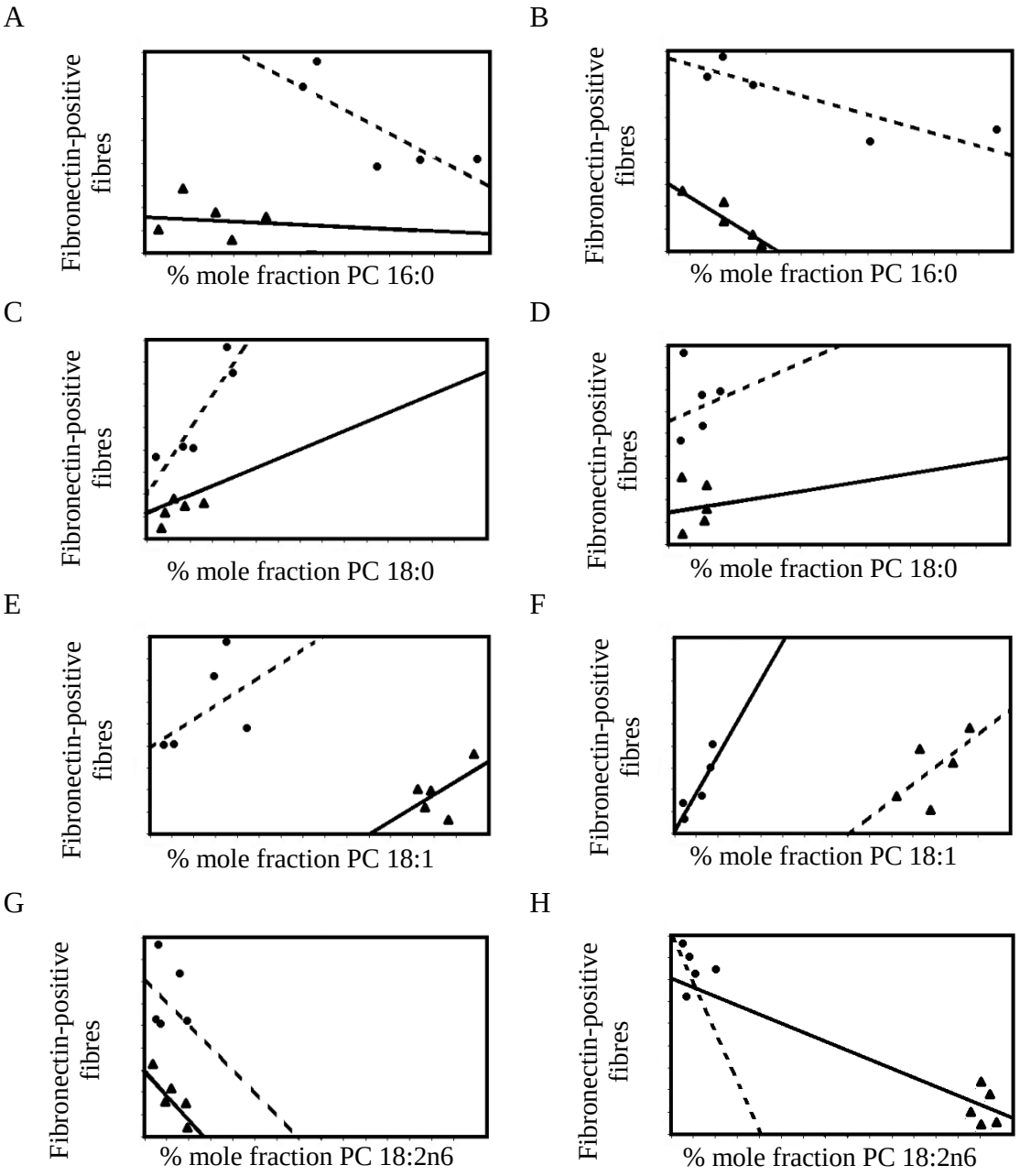

Figure 3.4. Linear fitted regression model of eccentric induced damage correlated with membrane phosphatidylcholine (PC) A) 16:0 at 10 weeks (WT, r=-0.14, p=0.82; *mdx*, r=-0.63, p=0.02), B) 16:0 at 20 weeks (WT, r=-0.94, p=0.01; *mdx*, r=-0.81, p=0.07), C) 18:0 at 10 weeks (WT, r=0.79, p=0.01; *mdx*, r=0.93, p=0.01), D) 18:0 at 20 weeks (WT, r=0.45, p=0.08; *mdx*, r=0.59, p=0.04), E) 18:1 at 10 weeks (WT, r=0.88, p=0.04; *mdx*, r=0.83, p=0.04), F) 18:1 at 20 weeks (WT, r=0.91, p=0.02; *mdx*, r=0.89, p=0.01), G) 18:2n6 at 10 weeks (WT, r=-0.91, p=0.02; *mdx*, r=-0.09, p=0.87), and H) 18:2n6 at 20 weeks (WT, r=-0.20, p=0.73; *mdx*, r=-0.74, p=0.04) in wild type (WT; solid lines) and *mdx* (dashed lines) extensor digitorum longus muscle.

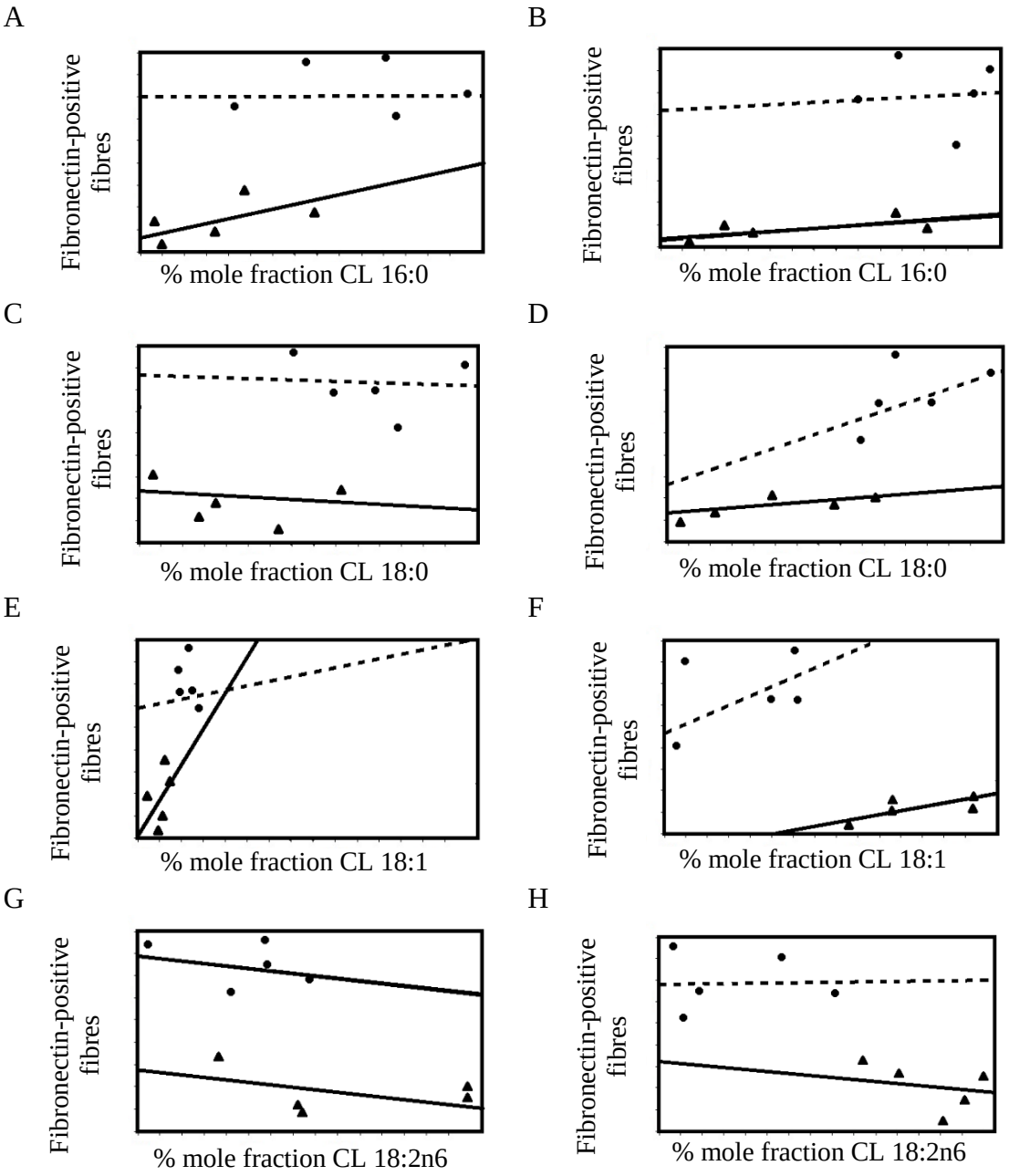

Figure 3.5. Linear fitted regression model of eccentric induced damage correlated with membrane cardiolipin (CL) A) 16:0 at 10 weeks (WT, *r*=0.34, *p*=0.56; *mdx*, *r*=-0.001, *p*=0.99), B) 16:0 at 20 weeks (WT, *r*=0.65, *p*=0.23; *mdx*, *r*=0.08, *p*=0.89), C) 18:0 at 10 weeks (WT, *r*=-0.32, *p*=0.58; *mdx*, *r*=-0.14, *p*=0.81), D) 18:0 at 20 weeks (WT, *r*=0.84, *p*=0.06; *mdx*, *r*=0.42, *p*=0.47), E) 18:1 at 10 weeks (WT, *r*=0.45, *p*=0.43; *mdx*, *r*=0.53, *p*=0.34), F) 18:1 at 20 weeks (WT, *r*=0.53, *p*=0.34; *mdx*, *r*=0.52, *p*=0.36), G) 18:2n6 at 10 weeks (WT, *r*=-0.41, *p*=0.49; *mdx*, *r*=-0.45, *p*=0.43), and H) 18:2n6 at 20 weeks (WT, *r*=-0.12, *p*=0.84; *mdx*, *r*=-0.02, *p*=0.9) in wild type (WT; solid lines) and *mdx* (dashed lines) soleus muscle.

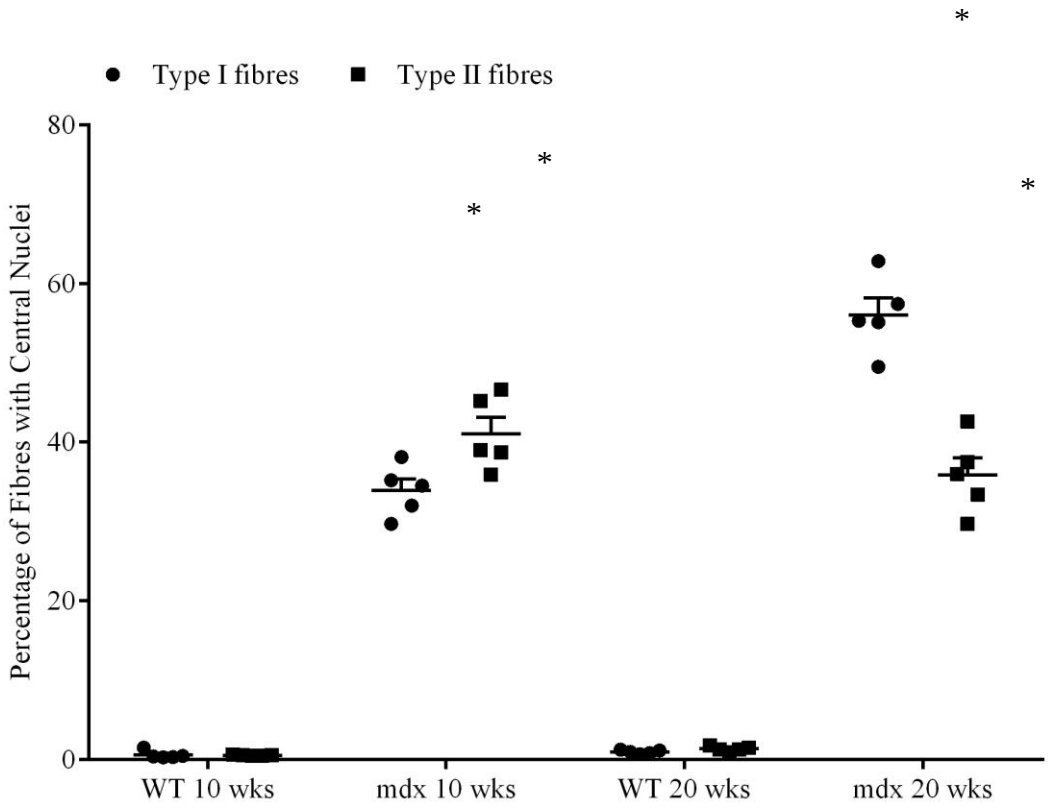

Figure 3.6. Percentage of type I and II fibres with central nuclei in wild type and *mdx* extensor digitorum longus at 10 and 20 weeks of age. Values are mean ± SEM; WT, wild type; * denotes significance from WT within the same age group.

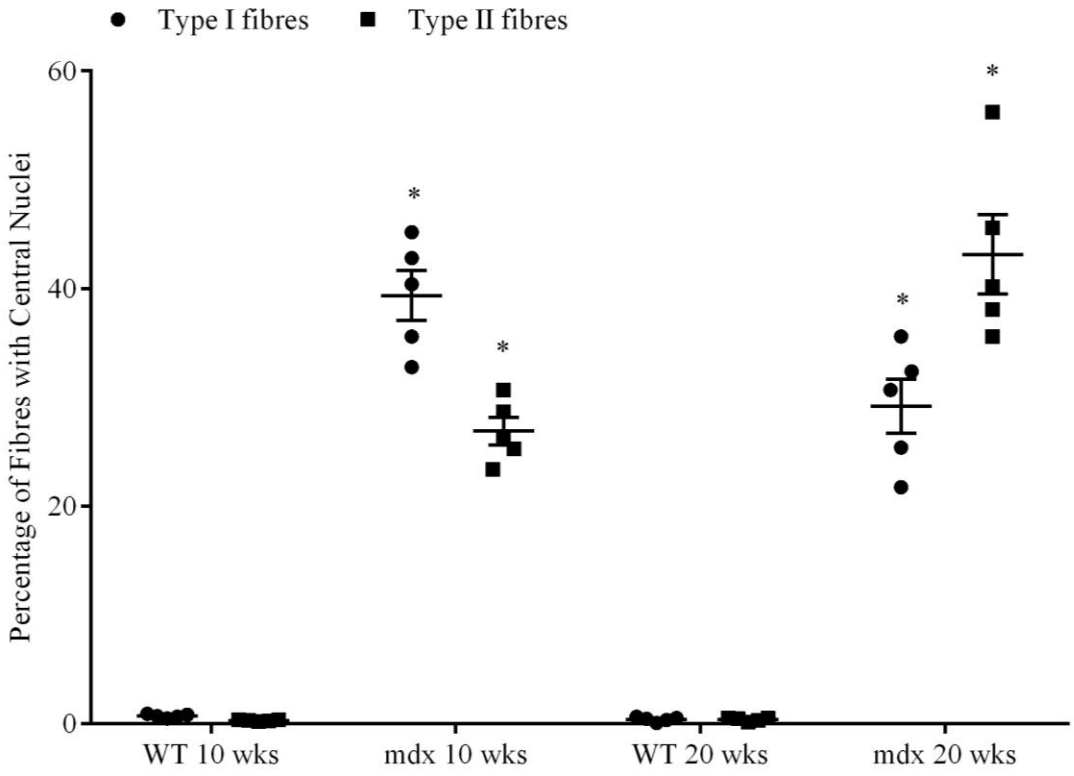

Figure 3.7. Percentage of type I and II fibres with central nuclei in wild type and *mdx* soleus at 10 and 20 weeks of age. Values are means ± SEM; WT, wild type; * denotes significance from WT within the same age group.

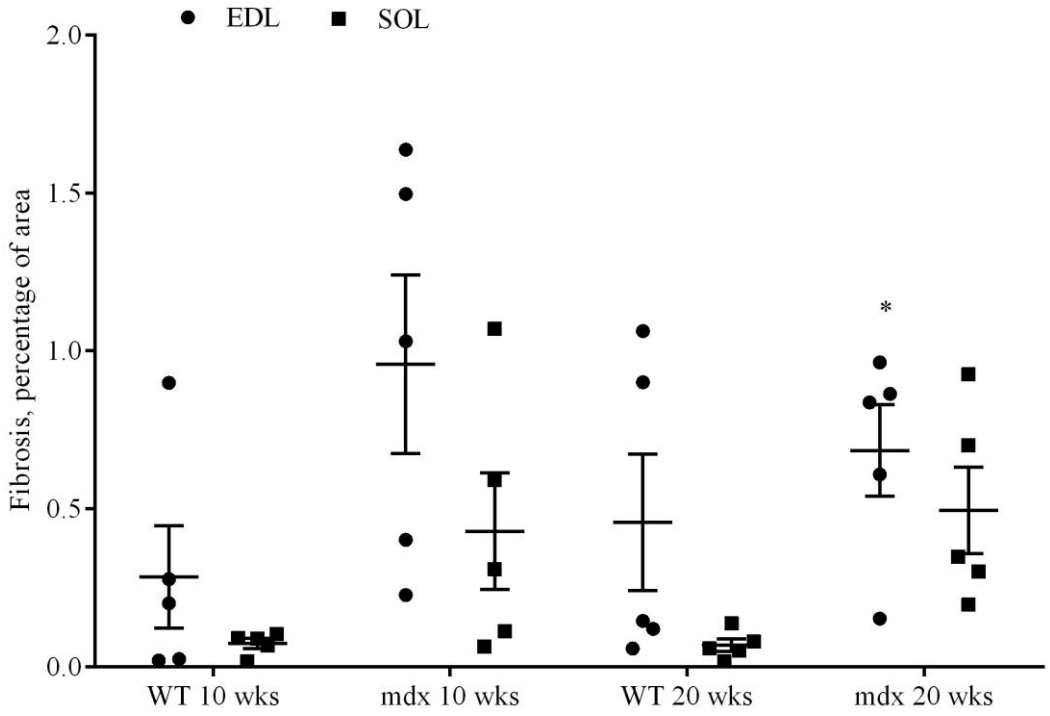

Figure 3.8. Percentage of fibrosis in extensor digitorum longus and soleus. Values are means ± SEM; WT, wild type; * denotes significance from WT at 20 weeks.

and 20 week old WT (r=-0.39, p=0.03) were significantly negatively correlated (Fig 2.9).

Similar to SM, most of the PC FA correlations in EDL were not significant. The only exceptions were that in 10 week old mice, 16:0 in *mdx* (r=0.85, p=0.05) and 18:0 in WT (r=0.73, p=0.05) were significantly positively correlated with fibrosis (Fig 3.10).

There were no clear trends in soleus CL FA when correlated against fibrosis (Fig 3.11). At 10 weeks of age, 16:0 was significantly positively correlated with fibrosis in both *mdx* (r=0.76, p=0.03) and WT (r=0.29, p=0.05) whereas 18:0 was significantly negatively correlated (WT, r=-0.22, p=0.04; *mdx*, r=-0.97, p=0.03). At 20 weeks of age, 16:0 for *mdx* (r=-0.90, p=0.03) and WT (r=-0.73, p=0.05), 18:0 for WT (r=-0.89, p=0.04), and 18:2n6 for *mdx* (*mdx*, r=-0.87, p=0.04) were significantly negatively correlated with fibrosis, whereas 18:1 in *mdx* was significantly positively correlated.

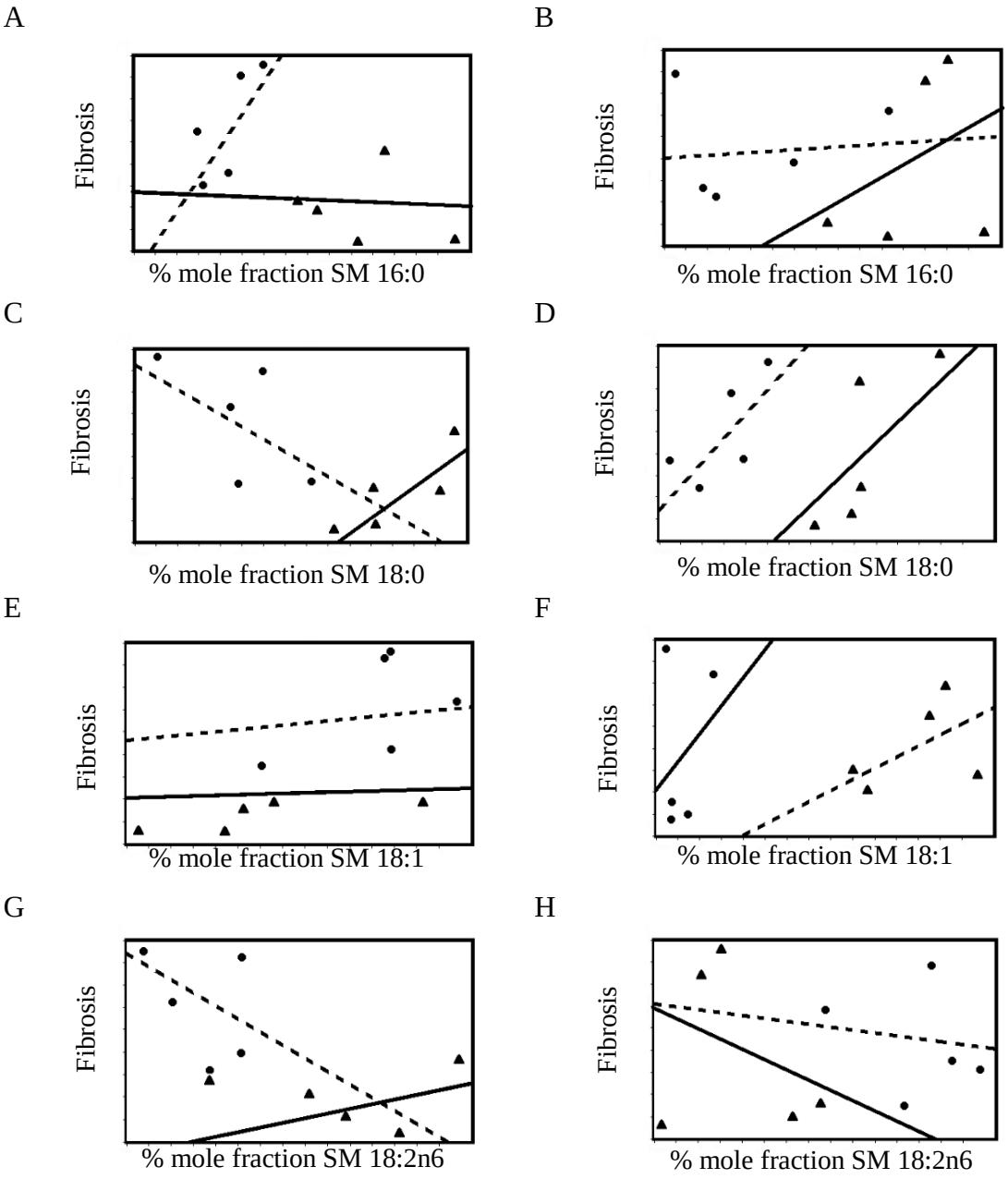

Figure 3.9. Linear fitted regression model of fibrosis correlated with membrane sphingomyelin (SM) A) 16:0 at 10 weeks (WT, r=-0.06, p=0.12; *mdx*, r=0.70, p=0.01), B) 16:0 at 20 weeks (WT, r=0.36, p=0.21; *mdx*, r=0.13, p=0.38), C) 18:0 at 10 weeks (WT, r=0.77, p=0.12; *mdx*, r=-0.46, p=0.42), D) 18:0 at 20 weeks (WT, r=0.39, p=0.51; *mdx*, r=0.64, p=0.23), E) 18:1 at 10 weeks (WT, r=0.01, p=0.97; *mdx*, r=0.10, p=0.86), F) 18:1 at 20 weeks (WT, r=0.60, p=0.28; *mdx*, r=0.42, p=0.04), G) 18:2n6 at 10 weeks (WT, r=0.37, p=0.05; *mdx*, r=-0.49, p=0.03), and H) 18:2n6 at 20 weeks (WT, r=-0.39, p=0.03; *mdx*, r=-0.18, p=0.07) in wild type (WT; solid lines) and *mdx* (dashed lines) extensor digitorum longus muscle.

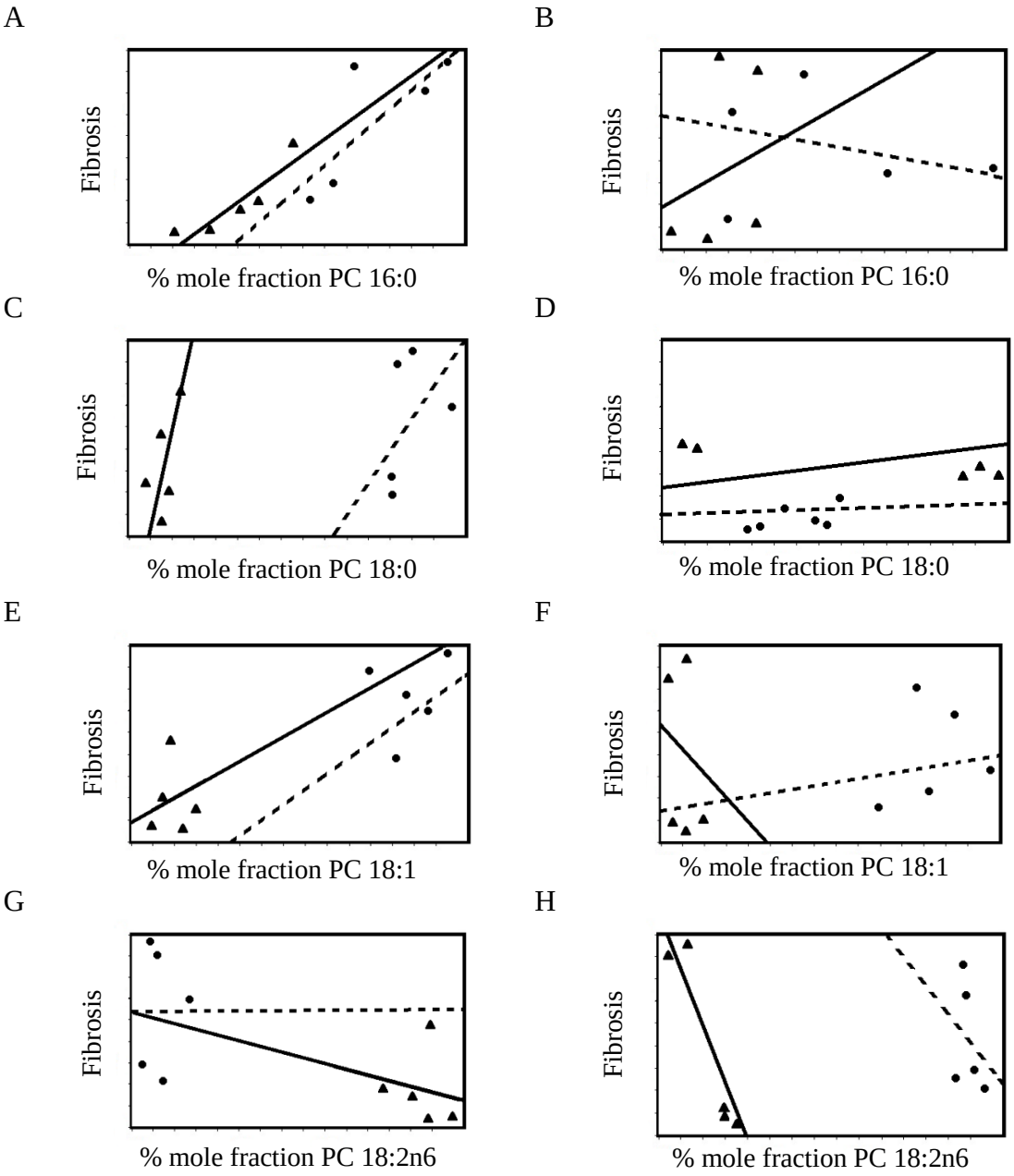

Figure 3.10. Linear fitted regression model of fibrosis correlated with membrane phosphatidylcholine (PC) A) 16:0 at 10 weeks (WT, r=0.71, p=0.06; *mdx*, r=0.85, p=0.05), B) 16:0 at 20 weeks (WT, r=0.22, p=0.71; *mdx*, r=-0.33, p=0.57), C) 18:0 at 10 weeks (WT, r=0.73, p=0.05; *mdx*, r=0.60, p=0.07), D) 18:0 at 20 weeks (WT, r=0.36, p=0.11; *mdx*, r=0.10, p=0.47), E) 18:1 at 10 weeks (WT, r=0.21, p=0.13; *mdx*, r=0.25, p=0.14), F) 18:1 at 20 weeks (WT, r=-0.21, p=0.15; *mdx*, r=0.10, p=0.47), G) 18:2n6 at 10 weeks (WT, r=-0.77, p=0.12; *mdx*, r=-0.04, p=0.42), and H) 18:2n6 at 20 weeks (WT, r=-0.39, p=0.51; *mdx*, r=-0.64, p=0.23) in wild type (WT; solid lines) and *mdx* (dashed lines) extensor digitorum longus muscle.

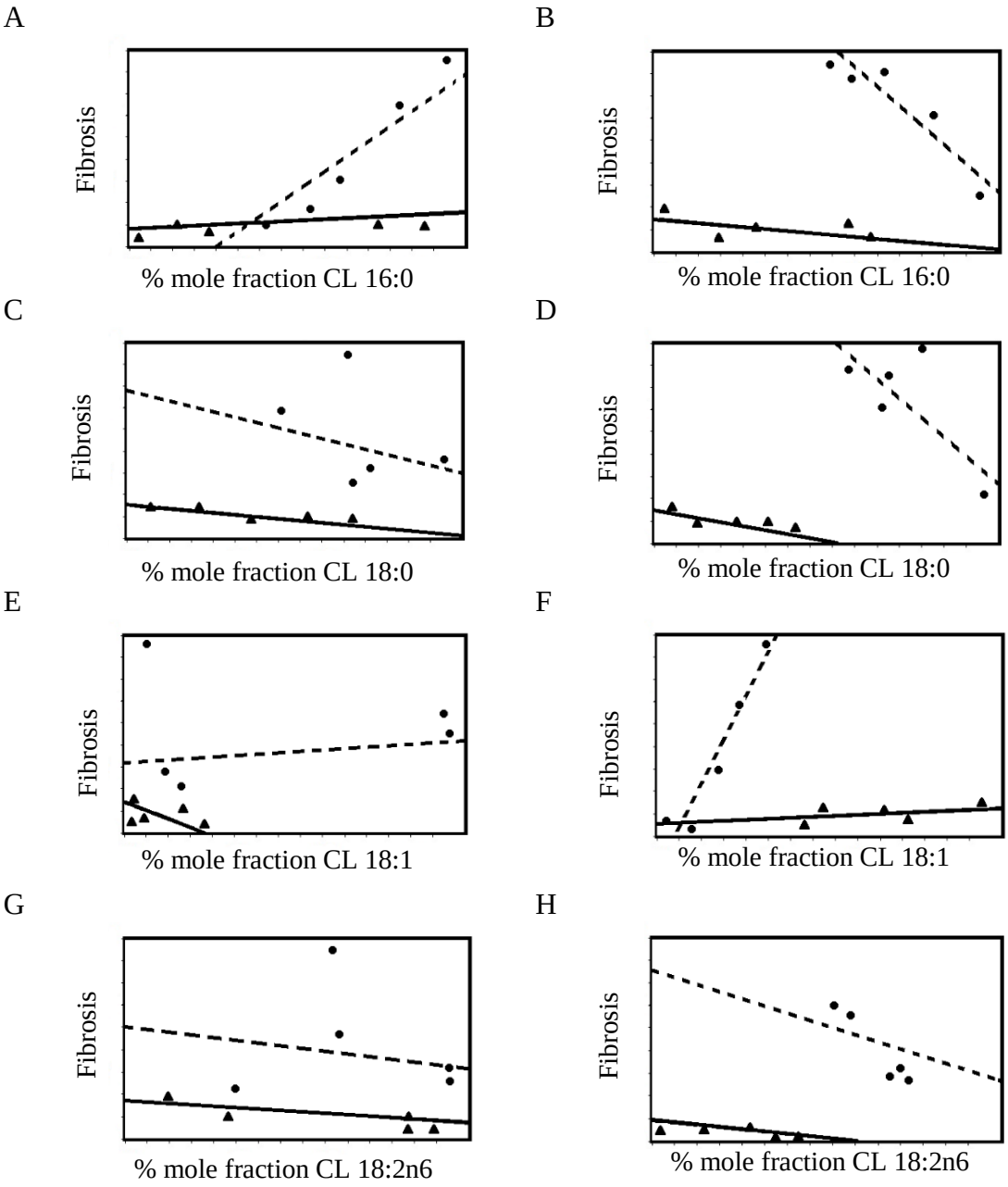

Figure 3.11. Linear fitted regression model of fibrosis correlated with membrane cardiolipin (CL) A) 16:0 at 10 weeks (WT, r=0.29, p=0.05; *mdx*, r=0.76, p=0.03), B) 16:0 at 20 weeks (WT, r=-0.73, p=0.05; *mdx*, r=-0.90, p=0.03), C) 18:0 at 10 weeks (WT, r=-0.22, p=0.04; *mdx*, r=-0.97, p=0.03), D) 18:0 at 20 weeks (WT, r=-0.89, p=0.04; *mdx*, r=-0.67, p=0.20), E) 18:1 at 10 weeks (WT, r=-0.42, p=0.09; *mdx*, r=0.19, p=0.35), F) 18:1 at 20 weeks (WT, r=0.14, p=0.43; *mdx*, r=0.76, p=0.04), G) 18:2n6 at 10 weeks (WT, r=-0.12, p=0.83; *mdx*, r=-0.31, p=0.27), and H) 18:2n6 at 20 weeks (WT, r=-0.45, p=0.12; *mdx*, r=-0.87, p=0.04) in wild type (WT; solid lines) and *mdx* (dashed lines) soleus muscle.

CHAPTER 4: DISCUSSION

The present study examined the association of membrane phospholipid fatty acids of muscles with varying fibre-type composition with eccentric induced damage and fibrosis in 10 and 20 week old *mdx* and WT mice. To our knowledge this is the first study that has assessed the severity of the dystrophic phenotype in relation to alterations in membrane PL FA composition in fast and slow muscle types.

The major novel finding from the present study is that membrane PL FA composition is associated with skeletal muscle markers of eccentric induced damage. Specifically, membrane SFA and MUFA are positively correlated to eccentric induced muscle damage, while PUFA are negatively correlated. Membrane PL FA composition, however, was not associated with skeletal muscle markers of fibrosis. It was also demonstrated that; 1) EDL was more susceptible to eccentric induced damage, with more significant and stronger correlations to membrane PL FA compositions compared to SOL, and 2) membrane PL FA composition was correlated to eccentric induced damage in *mdx*, and less so for WT, at both 10 and 20 weeks.

Model of muscular dystrophy*, mdx*

The *mdx* mouse has been studied extensively to better understand muscle pathology in the dysfunction of the DGC. The current research has attempted to further build our understanding of the contractile properties, alterations in membrane permeability with *in vit*ro eccentric induced damage,, fatty acids composition, histopathology and fibre type populations of two muscle types (predominant type I and II) at two ages (10 and 20 weeks) in *mdx* mice.

Fibre type involvement in mdx

Type II fibres are believed to be more susceptible to damage within a dystrophic phenotype, whereas type I fibres are more resistant. Moreover, with increased age, as a potential compensatory mechanism, type I:II ratio increases (Pastoret & Sebille, 1993). In the present study, type II fibres were the majority of fibres displaying damage in EDL. Additionally in dystrophic EDL, the percentage of type II fibres decreased from 97% to 70% from 10 to 20 weeks of age. Consistent with the present findings, type II fibres in dystrophic EDL were reported to gradually decrease with age going from ~93% at 6 weeks to ~90% at 16 weeks and finally to ~78% at 32 weeks (Carnwath & Shotton, 1987). Since type II fibres have been previously reported to be more susceptible to dystrophic damage (Lieber & Friden, 1988), increase of type I fibre types population possibly represent a compensatory response to the disease.

In SOL, despite demonstrating that type II fibres in *mdx* were most susceptible to damage, fibre type percentages were unaltered at 10 and 20 weeks. A decrease in type II fibres in *mdx* SOL was previously reported to occur at 26 week (Carnwath & Shotton, 1987). This later involvement might be related to the resistant nature of type I fibres in SOL to a dystrophic phenotype due to their wider Z lines and larger isoforms of sarcomeric proteins creating a more stable sarcomere assembly (Agarkova *et al.*, 2004; Prado *et al.*, 2005). Therefore, because of resistance of SOL to the dystrophic phenotype, examination of fibre types at 20 weeks may not reflect the fibre type alterations.

Histopathological changes in mdx myofibres

Findings of the present study demonstrated increased centrally located nuclei in myofibres, indicative of regeneration in both EDL and SOL at 10 and 20 weeks of age compared to WT. Additionally, dystrophic EDL at 20 weeks showed an increase in the rate of regeneration compared to 10 weeks as before. Increased regeneration in *mdx* is in agreement with previous literature reporting that the dystrophic myofibres undergo regeneration starting at 7 weeks and the process continues until 52 weeks in both EDL and SOL (Bullfield *et al.*, 1983; Tanabe *et al.*, 1986; Pastoret & Sebille, 1994). Specifically, in agreement with the current study, examination of EDL in weekly intervals after birth showed an increase in the rate of regeneration with age (8 to 26 weeks, Carnwath & Shotton, 1987). Together, both *mdx* EDL and SOL at 10 and 20 weeks demonstrated regeneration to compensate for dystrophic degeneration respectively.

Fibrosis and collagen accumulation are pathological hallmarks of muscular dystrophy in *mdx* muscle in which myofibres are replaced by progressive deposition of collagen when degradation outpaces regeneration. Absence of significant differences in fibrosis at 10 weeks between WT and dystrophic EDL in the present study (0-1%) is likely due to adequate regeneration at this age, as was previously reported (Bulfield *et al.*, 1984). However, at 20 weeks of age there was ~2.5% fibrosis of *mdx* EDL compared to WT. The 2.5% fibrosis at 20 weeks is also in agreement with a previous study reporting no apparent perimysial or endomysial fibrosis at 18 weeks in *mdx* and 5% at 24 weeks (Tanabe *et al.*, 1986). Increased fibrosis in dystrophic EDL at 20 weeks compared to WT is assumed to be related to ongoing regeneration to compensate for muscle fibre

degeneration. Substantial increases of up to 30% in collagen area fraction have been reported only after 52 weeks of age, which coincides with a decrease in regeneration (Pastoret & Sebille, 1994, Smith & Barton, 2014). As such, *mdx* EDL and SOL from 10 and 20 weeks demonstrate degeneration of myofibres with some but not complete regeneration, with small increases in fibrosis, respectively.

Alterations in membrane phospholipid fatty acid composition

Dysfunction in dystrophin is associated with changes in membrane PL FA composition. Findings of the present study demonstrated increased MUFA and decreased PUFA, which is in agreement with previous studies demonstrating increased MUFA and decreased PUFA in degenerated regions of mixed muscle hind limb (Hughes, 1972; Kunze *et al.*, 1975; Pearce *et al.*, 1981; Taboul *et al.*, 2004). Moreover, findings revealed that changes in membrane MUFA and PUFA were similar for *mdx* EDL at both 10 and 20 weeks suggesting that a 10 week increase in age may not alter the phenotype of PL FA composition in dystrophic EDL.

In SOL, similar to EDL, membrane MUFA experienced an increase while PUFA were decreased in *mdx* compared to WTs, and this did not differ between 10 and 20 weeks. Although this is the first study to examine membrane PL FA composition in SOL, the general trend of increased MUFA and decreased PUFA is in agreement with previous examination of *mdx* hind limb or quadriceps muscles (Pearce & Kakulus, 1980; Owens & Hughes, 1970; Benabdellah *et al.*, 2009; Touboul, 2004; Tuazon & Henderson, 2012). Together, these findings indicate that dystrophic EDL and SOL demonstrate similar

change in membrane composition, which remains unaltered with an increase in age from 10 to 20 weeks.

Changes in lipid composition of membranes may be dictated by the membrane structure protein functional relationship. Dysfunctional dystrophin may result in changes to the membrane composition to allow for more saturated (increase in 18:0 and 18:1) and less unsaturated (decrease in 18:2n6) PL. The degree of saturation in membrane PLs plays an important role in membrane stability and its susceptibility to oxidative damage. Such oxidative damage has been proposed as a possible mediator of the dystrophic pathology, possibly through excessive intracellular calcium (Terrill, 2013). Role for oxidative stress is supported by a wealth of preclinical studies in *mdx* mice that report benefits such as improved muscle pathology and decreased necrosis with many antioxidant drugs (Dorchies *et al.*, 2006; Buetler *et al.*, 2002). Furthermore, PUFA are extremely sensitive to oxidation (Song *et al.*, 2000). Consequently, a high concentration of PUFAs in phospholipids makes them prime targets for reaction with oxidizing agents, such as free radicals. However, in dystrophic membranes, given the heightened oxidative stress, membrane PL FA may demonstrate an adaptive response to oxidative condition by decreasing the abundance of PUFAs and increasing MUFA or SFA. This adaptation enables the membranes to obtain a higher structural stability and a lower susceptibility to oxidative damage. This highlights the potential importance of membrane composition in vulnerability to dystrophic damage. Identification of such changes is important because it may help to better understand the role of membrane lipid composition in dystrophic damage and progression of the disease.

Muscle damage after stretch injury protocol

In the present study, the stretch injury protocol was successful in inducing significant force deficit after stretch injury in EDL. Findings indicate a decrease in maximal isometric tetanic properties in *mdx* myofibres of 25% and 65% in 10 and 20 weeks old *mdx* EDL after 15 minutes of fatigue recovery which was ~2 and ~3.5 times greater than wild types (Table 3.2). Force deficits at 10 weeks are in agreement with results obtained from EDL of 12-14 weeks old *mdx* showing 30-40 % decline in isometric force after similar stretch injury experiments (Petrof *et al.*, 1993). Importantly, although some research demonstrated a 20-30 % decrease in isometric force in *mdx* at 12-16 weeks, the observed discrepancies may be related to the experimental stretch injury protocols, including differences in the rate of passive stretches and number of repeated eccentric contractions (Moens *et al.*, 1993). Importantly, eccentric contractions with faster velocities are more likely to subject the muscle to injury due to the greater levels of produced tension above that compared to slower velocity of eccentric contractions (Armstrong *et al.*, 1983). This is the first study that has stretched dystrophic EDL at 0.5 L_o/sec at 10 and 20 weeks, with previous experiments being on different age groups and/or applying faster or slower velocities of eccentric contractions (Moens *et al.*, 1993; McArdle *et al.*, 1991; Deconinck *et al.*, 1998; Raymackers *et al.*, 2003; Consolino & Brooks, 2004).

EDLs of *mdx* at 20 weeks had ~1.5 times greater maximal isometric force depression compared to 10 weeks, which was ~60% of that produced in WT. Greater force depressions at 20 weeks was in agreement with earlier research in *mdx* EDL at the age of 16-24 weeks showing 20- 55% decrease in isometric force (McCully & Faulkner,

1985; Sacco *et al.*, 1992). However, it is difficult to compare the magnitudes of maximal isometric force deficits obtained from the current study with the ones reported in the literature because the protocols including the lengthening velocities were different or the force was measured on different ages other than 20 weeks.

Force decline of *mdx* EDL after damage suggests that in the absence of dystrophin, the threshold level for muscle damage is decreased, rendering the muscles more susceptible to damage induced by eccentric contractions. Specifically, in the absence of dystrophin, the structural continuity that is provided by dystrophin and its associated proteins for an effective force transmission along the longitudinal axis is lost, which in turn, results in fibres that are functionally impaired in transmitting force (Ohlendieck & Campbell, 1991). The precise underlying mechanism for decreased force output in *mdx* EDL may be related to failures in ECC. Eccentric contractions in the absence of dystrophin lead to structural changes in the sarcomere resulting in overstretched sarcomere with Z-line streaming throughout the fibre (Fridén *et al.*, 1981). This, in turn, results in changes to the structure of the sarcomere and a persistent opening of stretch-activated channels (Allen, 2004). Since these channels are permeable to Na^+, increased $[Na^+]_i$ is observed. Consequently, Na^+ pumps extrude the excess intracellular Na^+ with osmotically equivalent water putting hydraulic load onto the t-tubules causing dilation. The change in property of t-tubules, therefore, reduces effective action potential propagation down the t-tubules, which, in turn, reduce SR Ca^{2+} release and tension development (Yeung *et al.*, 2002; Yeung *et al.*, 2003; Franco *et al.*, 1990). Moreover, the present study showed that older *mdx* EDL had an increase in the proportion of type I fibres. As such, it can also be assumed that a deficit in isometric force generation at 20

weeks in *mdx* EDL may be a result of a shift from type II to I fibres (Table 3.1). Although increased non-contractile fibrotic tissue may further compromise contractile function of muscle, especially in older *mdx*, observed fibrosis in the current study is believed to be too small to account for a decline in contractile function (Bulfield et al, 1983; Leronimakis *et al.*, 2013). Thus the influence of fibre type alteration and defective regeneration are assumed to explain the severity of damage associated with age.

In SOL, force production after the stretch injury protocol with lengthening at the rate of 1.5 L_o/S, did not differ between *mdx* and WT. Previous literature examining mechanical damage with different stretch injury protocol in SOL showed a 20% drop in force in both *mdx* and WT strains at 4-6 weeks and 10 % in 12-20 weeks (Moens *et al.*, 1993, Warren *et al.*1992). In the current study the velocity of eccentric contraction was 1.5 L_o/S repeated 10 times, but literature protocols applied different rate of lengthening contractions ranging from 1.5 L_o/S at 4-6 weeks repeating for 15 times and 1.7 L_o/S at 12- 20 weeks repeated for 6 times (Moens *et al.*, 1993, Warren *et al.*1992). Overall, in *mdx* SOL muscle, eccentric contractions did not cause a large force drop that implies the threshold for damage is higher in these muscles, in agreement with the finding that fast muscle fibres are preferentially affected by the disease (Webster *et al.*, 1988). The underlying mechanism responsible for less vulnerability of type I fibres to eccentric damage is likely related to the ultrastructural differences between type I and type II fibres. Type I fibres have wider Z-lines compared to type II fibres, which reflect more attachments for thick and thin filaments inferring higher stability (Yamaguchi *et al.*, 1985). Moreover, type I fibres contain larger isoforms of the sarcomeric proteins, which play a role in sarcomere assembly (Agarkova *et al.*, 2004; Prado *et al.*, 2005). Also, these

fibres express a higher molecular weight, and more elastic, isoforms of non-contractile proteins (i.e. titin) than type II fibres. The higher compliance of non-contractile proteins (titin) in slow fibres may transmit less stress during eccentric contractions on these fibre types, which in turn, may result in type I fibres being more resistant eccentric damage (Prado *et al.*, 2005).

The force deficit after muscle damage is proportional to the force developed during stretch, which is produced at higher velocities of lengthening (McCully & Faulkner 1986, Warren *et al.* 1993). Moreover, there is widespread agreement that damage increases with the number of eccentric contractions and with the length of the stretch (McCully & Faulkner, 1985, Warren *et al.* 1993; Lieber & Friden, 1988, Brooks *et al.* 1995). As such, to ensue damage in type I dominant SOL, increases in length and rate of stretch parallel to increases in the number of eccentric contractions may lead to deficiency in the development of isometric force.

Taken together, the stretch injury protocol was successful in inducing 2-3.5 fold greater force depression in dystrophic EDL compared to WTs. In SOL, however, the stretch injury experiment did not contributed to force deficit. The force deficit in dystrophic EDL but not SOL may suggest that the stretch injury protocol resulted in contraction induced damage to EDL, which, due to absence of force decline after stretch injury, was not present for SOL.

Membrane damage after eccentric contraction

Eccentric stretch injury in *mdx* EDL did not show increased fibronectin entry at 10 weeks but resulted in a ~2 fold increase in fibronectin entry at 20 weeks. This is the

first study to assess membrane damage in dystrophic muscles at 10 and 20 weeks using a large molecular weight marker in fibronectin. Membrane damage has been detected in *mdx* EDL using procion orange, a much smaller molecular weight molecule which can infiltrate through disrupted cellular membranes allowing for the detection of microtears in the membrane. At 8-10 weeks, after 10 eccentric contractions at the rate of 1.5 L_o/S, procion orange uptake was increased to 10% in *mdx* EDL (Whitehead *et al.*, 2006). By the age of 12-14 weeks of age, after 5 eccentric injuries at the rate of 1.5 L_o/S, uptake was increased to 18% in dystrophic muscle (Petrof *et al.*, 1993). At 15-20 weeks, with application of 6 eccentric contractions at the velocity of 1.7 L_o/S, procion uptake was present in 15% of fibres (Moens *et al.*, 1993). Finally, at 20 weeks, after a single lengthening contraction at 30% of strain, 15% of fibres were procion positive (Consolino & Brooks, 2003). Altogether, identification of procion dye in dystrophic fibres in literature demonstrates higher damage than to the present study due to the size of the membrane damage marker. Fibronectin is ~750 times larger and may not have the ability to pass through microtears similar to the way smaller procion orange can. Detection of intracellular fibronectin is reported to be an effective alternative marker for identifying altered membrane permeability (Palacio *et al.*, 2000), indicating larger disruptions in the membrane. Specially, the microtears in dystrophic EDL at 20 weeks may be large enough to accommodate a greater uptake of fibronectin compared to 10 weeks, further suggesting that intracellular accumulating of fibronectin is indicative of larger membrane damage. Moreover, the association of fibronectin positive fibres with force deficit in dystrophic EDL suggests that fibronectin indeed its slow infiltration due to its larger molecular size may be an adequate marker for detection of membrane damage. However, irrespective of

the technique of quantifying damage, this study showed that following stretched contractions, membrane permeability of *mdx* muscles progressively increased with age.

The present study demonstrated decrease in force output of dystrophic EDL (~25% at 10 weeks and ~65% at 20 weeks) after eccentric contractions. However, fibronectin positive fibres indicating membrane damage was increased to 5 %. This finding firstly suggests that the extent of force loss exceeds the percentage of fibronectin containing fibres. Secondly, the correlation of membrane damage with force deficit in dystrophic EDL at 20 weeks demonstrated that membrane damage has significant contributions to force loss (Appendix A.3, r: 0.48, $p < 0.05$). Association of membrane damage with force loss has previously been reported in dystrophic EDL at 10-12 weeks with infiltration of procion orange (r: 0.6, p, 0.02) where 20% of fibres were infiltrated with procion orange (Petrof et al., 1993). Moreover, marked 60% force deficit in mdx EDL after stretch injury at 9-12 days was associated with 9% uptake in procion orange (Grange et al., 2002). Disproportional decrease in force output and membrane damage may indicate to involvement of additional mechanisms in muscle damage other than membrane damage. Loss of contractile strength is induced not only by damage observable by light microscopy (infiltration of markers) but also by breakdown of ECC (Balnave & Allen 1995; Warren et al. 2002). This EC uncoupling may occur as a result of damage to the mechanosensitive Ca^{+2} channels, Na^{+} channels and intracellular Na^{+} concentrations that were not indicated by infiltration of extracellular markers. Altogether, despite larger size of fibronectin for detection of membrane damage findings further support the role of membrane damage in force deficit of dystrophic muscles after

eccentric contractions. Further research may provide insight on the initial role of underlying factor in membrane damage after eccentric contractions.

In the present study, 10 eccentric contractions at the rate of 1.5 L_o/S did not result in fibronectin uptake by SOL at 10 and 20 weeks. This is in agreement with the literature as stretch injury (6 lengthening at 1.7 L_o/S) in 15 week old *mdx* SOL did not demonstrate differences in procion orange entry (Moens *et al.*, 1993). Absence of damage using procion orange as a marker was also observed in 20 week old *mdx* SOL (single 60 % stain at 2 Lo/S) (Consolino & Brooks, 2004). Despite the differences in the surrogates of damage used in the current study and the literature, SOL myofibres demonstrated greater resistance to stretch injury than before. This finding may be attributed to their higher proportion of type I fibres, with different biomechanical properties (i.e. wider Z- lines, larger sarcomeric proteins, more elastic titin) that infer higher resistance to membrane damage.

Correlation of membrane composition with eccentric induced damage muscle damage

The membrane structure-protein functional relationship may provide insight into the association of dystrophin dysfunction and membrane composition. Alterations in membrane lipid composition have been examined in current and previous research. Moreover, examination of *mdx* myofibres strongly supported the idea that one of the associated factors in a dystrophic phenotype is alterations in membrane permeability, implying an abnormally “leaky” membrane. As such, to better understand the role of alteration of membrane lipid composition in pathogenesis of the disease it is important to

examine how the changes in membrane lipid composition may be associated with membrane damage.

As previously highlighted, membrane PL FA composition demonstrated similar changes in increased SFA and MUFA with decrease in PUFA in dystrophic muscles with progression from 10 to 20 weeks. However, parallel to increase in *mdx* age, the fibronectin positive fibres suggestive of eccentric induced damage were increased from 10 to 20 weeks. In addition, fibrosis was elevated from 10 to 20 weeks in dystrophic muscle. Progression of eccentric induced damage and fibrosis from 10 to 20 weeks despite unaltered membrane PL FA composition may suggest different trajectory between changes in membrane PL FA composition and eccentric induced damage and fibrosis. Despite no differences between 10 and 20 weeks in membrane lipids, the correlations to eccentric induced damage and fibrosis might still be present. Examination of such correlations is important as it may provide insights about the role of altered PL FA composition in muscle damage.

EDL

In the present study, it was hypothesized that alterations in membrane composition in *mdx* EDL may be associated with eccentric induced damage. Indeed, findings indicated significant correlation between an increase in membrane saturation with fibronectin-positive myofibres compared to WT. Muscle damage was more evident in membranes with higher percent mole fraction of SM 18:1, PC 18:0 and lower SM 18:2n6 and PC 18:2n6. It is important to note that since previous examination of isolated

sarcolemma by mechanical skinning demonstrated PC and SM as the major constituents of sarcolemma than to other PL species (Fajardo *et al.*, 2013), it is assumed that these PLs obtained from whole muscle membrane analysis are somewhat reflective of the sarcolemma.

It has previously been established that increases in eccentric induced muscle damage due to increases in saturation is of importance because eccentric induced damage to the muscle would be accompanied by an influx of calcium and disturbance of calcium homeostasis (Leijendekke, 1996). However, since a correlation of membrane PL FA with eccentric induced damage does not imply causality; two possible theories might explain the association of membrane PL FA with eccentric induced damage. (Fig.4.1). In both theories, it is implied that there would be a rise in $[Ca^{2+}]_i$, a subsequent impairment in Ca^{2+} homeostasis and activation of various degradation pathways, which would lead to muscle fibre necrosis (Whitehead *et al.*, 2006). Moreover, since dysfunctional dystrophin was not associated with increased membrane permeability during the first 2 weeks of age (Grange *et al.*, 2002; Head *et al.*, 2004), both models are only applicable to ages after 3 weeks, in which the membrane demonstrates contraction-induced damage. Alternatively, the absence of dystrophin is accompanied by altered membrane lipid composition that makes the membrane more susceptible to contraction-induced damage (Fig 4.1.B).

The first theory suggests increased susceptibility of dystrophic muscles to contractions lead to series of events driving increased membrane saturation. Firstly, dysfunctional dystrophin is associated with diminished support for the membrane during contraction, leading to contractile force directed into the membrane resulting in membrane damage (Fig 4.1 A). Muscle damage after eccentric contractions is supported

by a decrease in contractile performance of dystrophic muscle after mechanical damage (Head *et al.*, 1992; Petrof *et al.*, 1993; Deconinck *et al.*, 1998; Raymackers, 2003; Consolino & Brooks, 2004; Chan *et al.*, 2007). Increase in membrane damage is evidenced by the

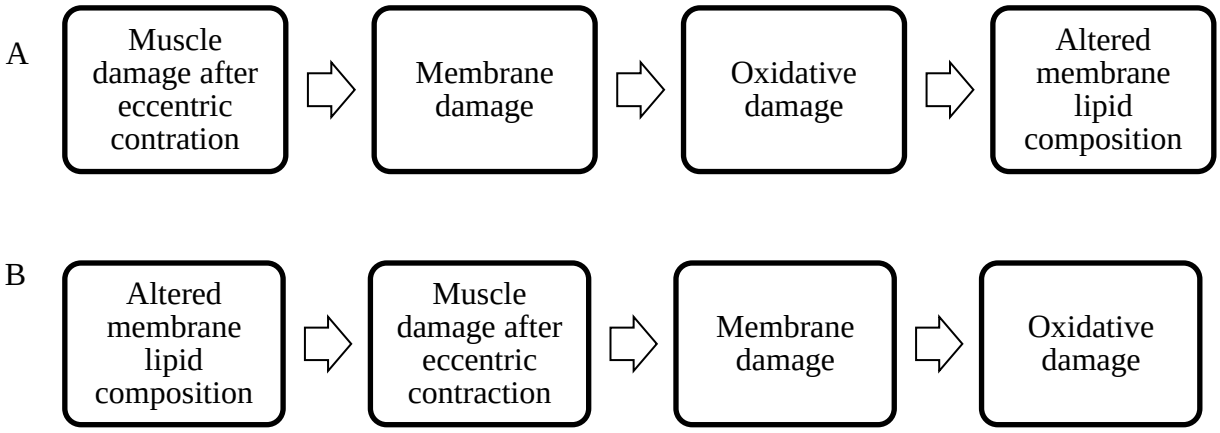

Figure. 4. 1. Presentation of two possible models in association of membrane phospholipid fatty acid composition with muscle damage with dysfunction in dystrophin. A; Muscle damage after eccentric contrations as associated with dysfunctional dystrophin is the leading event driving membrane damage, followed by oxidative damage to the membrane ultimately resulting change in membrane lipid composition. B; Change in PL FA composition as associated with dysfunctional dystrophin driving muscle damage after eccentric contraction, leading to membrane damage with subsequent oxidative damage to the membrane. PL, phospholipid; FA, fatty acid.

finding that dystrophin offers both structural and functional integrity to the sarcolemma by stabilizing it against stresses imposed during muscle contraction or stretch (Blake *et al.*, 2002). Secondly, damage to the membranes drives an increase in membrane permeability, mediating the influx of Ca^{+2} through the sarcolemma. Increased permeability of membranes has been shown with small and large surrogates of membrane damage in dystrophic muscles after contraction (Whitehead *et al.*, 2006; McArdle *et al.*, 1994; Petrof *et al.*, 1993). Thirdly, the increased calcium entry contributes to an approximately threefold rise in cytosolic free calcium as previously reported in *mdx* muscle (Mallouk *et al.*, 2000, Alderton & Steinhardt, 2000). This rise in cytosolic calcium activates proteases which promote the activation of phospholipase (especially phospholipase A_2 (PLA_2)), which in turn attacks mitochondrial and other membrane phospholipids, giving rise to lysophospholipids and free FAs. Lysophospholipids disrupt membrane lipid organization and free fatty acids may have a detergent action, causing membrane damage. This is derived from evidence that increased Ca^{+2} concentration activates PLA_2, based on the observation that enzyme efflux (e.g. CK) from experimentally damaged muscles suffering Ca^{+2} overloads can be blocked by PLA_2 inhibitors (Jackson *et al.*, 1984). Moreover, among the free fatty acids liberated is arachidonic acid, which may promote reactive oxygen species (ROS) production by the mitochondria (Gissel, 2005). Additionally, accumulation of Ca^{+2} in mitochondria linked to disturbances in Ca^{+2} homeostasis promote generation of ROS by the mitochondria that leads to peroxidation of membrane lipids (Gissel, 2005; Reppeto *et al.*, 2012). Finally, free oxygen radicals initiate further chain reactions resulting in conversion of PUFA to further fatty acid radicals (Reppeto *et al.*, 2012), stabilized by rearrangement into more

saturated forms (as seen with increased SFA, MUFA and decrease in PUFA; Owens & Hughes, 1970; Pearce & Kakulus, 1980). Noteworthy, free radical mediated damage in muscular dystrophy is attributed to the defect in neuronal nitric oxide synthase (nNOS) known as a member of dystrophin complex, which is lost in dystrophin deficiency (Brenman *et al.*, 1995). Nitric oxide (NO), a product of nNOS, has rapid and versatile reactions with free radicals preventing a redox environment in myofibres (Tidball & Wehling-Henricks, 2007). Therefore, with loss of the protective role of NO in scavenging free radicals, oxidative stress increases in dystrophic myofibres. Evidence demonstrating the importance of nNOS deficiency in the pathology of *mdx* is the prevention of histological pathology and sarcolemmal lesions in *mdx* by expression of transgene nNOS in dystrophic muscles (Wehling et al, 2001). It is also important to note that although the initial leading event for muscle damage is the contraction induced membrane micro-lesions, these processes ultimately lead to increased saturation of membranes, causing further influx of calcium, and activation of a continuous cycle that ultimately contributes to further membrane damage. As such, in the first theory muscle damage as a result of calcium entry may underlie the increased saturation of the PL FA compositions of the membrane.

The alternative theory suggests that increased contraction-induced membrane damage is a result of events from increased saturation in membranes (Fig 4.1.B). Firstly, due to the membrane structure-protein functional relationship, dysfunction in dystrophin may be associated with increased SFA and decreased PUFA in membranes (Owens & Hughes, 1970; Pearce & Kakulus, 1980). Secondly, the shift from unsaturated towards saturated FAs in membrane increases the van der Waals forces between the hydrocarbon

chains due to increased interaction between FA chains (Yang *et al.*, 2011). As a possible result of increased interaction, the sarcolemma folding (ratio of membrane surface to cell volume) may decrease (Hutter, 1991). Thus, during an eccentric contraction, a membrane with fewer sarcolemma folds may not accommodate the stretch, which subjects the membrane to stress and likely leads to membrane damage (Hutter, 1991, Grange *et al.*, 2002). Examination of the mechanical strength of the dystrophic myofibre membranes, which report a fourfold decrease in membrane stiffness of *mdx* myotubes than that of WT (Pasternak *et al.*, 1995), further supports decreased resistance of dystrophic fibres to stretch. Thirdly, decreased resistance of membranes to mechanical perturbations gives rise to the development of transient membrane tears, evidenced by increased membrane permeability (Whitehead *et al.*, 2006; McArdle *et al.*, 1994; Petrof *et al.*, 1993). Increased membrane permeability, in turn, allow extracellular Ca^{2+} to rapidly enter the fibre (Mallouk *et al.*, 2000) leading to activation of proteases as wells as peroxidases. This finally results in generating oxidative damage to the membrane (Gissel, 2005). This theory focuses on the governing role of the lipid bilayer in driving resistance to injury and membrane damage. Thus, in this theory, it is likely that the intrinsic strength of the sarcolemma is a property of lipid bilayer, not under the impact of membrane damage, which is affected in the absence of dystrophin, leading to membranes that are susceptible to dystrophic damage.

As highlighted previously, with increased age in *mdx*, the dystrophic phenotype including membrane susceptibility to damage become more severe from 9 weeks to 24 weeks of age (Head *et al.*, 1992; Deconinck *et al.*, 1998; Blake *et al.*, 2002; Consolino & Brooks, 2004; Chan *et al.*, 2007). Thus, in the present study, it was also hypothesized

that the extent of eccentric induced damage fibronectin positive fibres would have stronger associations with increased membrane saturation in older *mdx* at 20 weeks. This was not seen as the association of membrane lipid composition with eccentric induced damagemuscle damage at 10 week of age was stronger compared to 20 weeks. Specifically, despite an increase in the susceptibility of dystrophic EDL to damage at 20 weeks, membrane lipid composition remained unaltered. The weakening correlations at 20 weeks might be related to the shift in fibre type composition from 10 to 20 weeks. Specifically, at 20 weeks of age there is continued preferential loss of type II fibres with an increase in the proportion of type I fibres in dystrophic EDL, which in turn, may change the membrane composition. These type I fibres have more PUFA in their membranes and less SFA (Kriketos *et al.*, 1996; Stefanyk *et al.*, 2010). Moreover, the proportion of type II fibres decreased from 10 to 20 weeks with increased age. Type II fibres are composed of more saturated FAs (Kriketos *et al.*, 1996; Stefanyk *et al.*, 2010). As such, possibly due to reciprocal influences of both fibre type shifts and dystrophic phenotype on membrane composition, this may have contributed to weaker correlations at 20 weeks of age in *mdx* EDL.

SOL

Soleus is composed mostly of type I fibres. Type I fibres have different sarcomeric assembly resulting in more resistance to dystrophic damage than type II dominant muscle types (larger sarcomeric proteins, higher compliance in titin and wider Z-lines) (Agarkova *et al.*, 2004; Prado *et al.*, 2005). Additionally, type I fibres have more SFA and less PUFA (especially n6 PUFA) in their membranes (Stefanyk *et al.*, 2010).

Importantly, due to unsaturation, PUFA side chains have higher susceptibility to oxidative stress, and more easily attacked by free radicals than SFA (Song *et al.*, 2000). Thus lower abundance of PUFA in SOL may provide some stability against dystrophic injury.

Stretch injury in SOL at the velocity of 1.5 L_o/S repeated for 10 times did not result in increased fibronectin entry in either WT or dystrophic mice at 10 and 20 weeks. In terms of membrane PL FA, only CL demonstrated changes with phenotype, which is an exclusively mitochondrial PL (Bleijerveld, *et al.*, 2007). As a result, membrane composition in dystrophic SOL did not correlate strongly with eccentric induced damage . Future studies should examine stretch injury protocols that induce greater fibronectin entry post-injury.

Changes in mitochondrial membrane composition of SOL without increases in muscle damage may raise the possibility that muscle damage may be a preceding event to alterations in membrane composition (Fig.4.A). Dysfunctional dystrophin in SOL is associated with muscle damage after eccentric contractions and membrane damage (not detected due to insufficient stretch injury protocol or large size of damage marker). As a result of sarcolemma micro-lesions, Ca^{+2} loads on muscle increases, which in turn leads to elevated mitochondrial Ca^{+2} concentrations and activation of phospholipase (Gissel, 2005). This finally leads to increased ROS production in mitochondria, and with it, the risk of attacking mitochondrial membrane lipids (converting PUFA to MUFA or SFA). Since mitochondria act as a regulator in Ca^{+2} overloads, the changes in its membrane composition may be a prelude to changes in sarcolemma composition. Impact of mitochondria Ca^{+2} overloads on its membrane was demonstrated with increased activity

of the transition pore (Duchen, 2004). Thus increased saturation in mitochondria membrane composition without changes in SL may be indicative to the initial role of membrane damage in driving alterations in mitochondrial membrane composition with further involvement of SL due to failure in Ca^{+2} homeostasis. It is assumed that with the application of more severe stretch injury, more Ca^{+2} may accumulate in the fibres, resulting in changes to more than mitochondria PL, including SL.

Correlation of membrane composition with fibrosis

As highlighted previously, fibrosis is characterized by alterations in extracellular matrix deposition as a consequence of persistent muscle damage following eccentric induced tissue injury without sufficient regeneration (Antonio *et al.*, 2011). Fibrosis or chronic muscle damage in *mdx* mice is a late onset process with dramatic increases after 52 weeks of age (Pastoret & Sebille, 1994). In the present study, fibrosis was increased at 20 weeks in EDL (2.5% fibrosis compared to WT), which is consistent with 5% fibrosis of *mdx* EDL at 24 weeks (Tanabe *et al.*, 1986), and not in SOL.

EDL

It was hypothesised that membrane PL FA composition of dystrophic fibres would be correlated with fibrosis. Findings showed that fibrosis accumulation in EDL was not highly correlated to membrane PL FA composition. It is important to note that fibrosis is the end stage of muscle damage, and represents the loss of myofibres. In the present study, membrane composition, however, characterizes the altered membrane PL

FA of healthy, degenerated and regenerated myofibres. Increase in SFA and MUFA with decrease in PUFA might be attributed to a chain reaction that initiated only after eccentric induced damage and fibrosis might not further influence changes in FA composition of the membrane. Moreover, the present study demonstrated increased amounts of myofibre regeneration at 20 weeks compared to 10 weeks (Fig 3.6), indicating a compensation for damaged fibres. As such, due to only 2.5% fibrosis and increased regeneration at 20 weeks, association of fibrosis with membrane PL FA of remaining fibres was weak. Furthermore, type I and II fibres have different PL FA composition, especially type II being dominantly composed of less PUFA/more saturated FA than to type I fibres (Kriketos *et al.*, 1996; Stefanyk *et al.*, 2010). In parallel to increased age, the proportion of type I/II increases, which resulted in increased saturation in dystrophic membranes at 20 weeks. Thus increased age not only results in increased PUFA in membranes creating more stability for the membranes but shift of type II fibres, which are known to be more susceptible to fibrosis. The PL FA analysis, however, was completed on whole muscle tissue including membranes of both fibre type populations. Therefore, the changes in fibre type composition may mask some of the true changes in PL FA between fibres and the association with fibrosis.

SOL

Increased fibrosis is associated with elimination of susceptible fibres to damage, which tend to be type II fibres. Since SOL is a type I dominant muscle, it was hypothesized that the correlation of membrane composition in remaining fibres to fibrosis would be weaker compared to EDL, which is type II dominant muscle. Findings

of the present study indicate increased membrane MUFA and decreased PUFA through increases 18:1 and deceased 18:2n6, respectively. Despite these findings, there was no evidence of fibrosis in *mdx* soleus at 10 or 20 weeks of age. Previous research has identified fibrogenesis in soleus in late stages at 52 weeks (Tanabe, 1986), related to influence of lower susceptibility of type I fibres to damage, which suggest fibrosis would occur in SOL after 20 weeks.

Lack of association between increased saturation in membrane lipid composition and fibrosis in SOL is assumed to be related to two underlying factors. First, the high proportion of type I fibres in SOL, making up 37-40 % of the fibre types (Augusto *et al.*, 2004; Smith *et al.*, 2013), result in a higher mitochondrial density. Mitochondria act as Ca^{+2} buffer with rapid uptake of surplus Ca^{+2}, avoiding detrimental changes in Ca^{+2} concentrations within the muscle. Participation of mitochondria in Ca^{+2} handling may results in less Ca^{+2}-derived muscle damage, lower susceptibility of membrane lipid to peroxidation, and less changes to membrane composition (Gissel, 2006). Although membrane composition of dystrophic EDL and SOL demonstrated similar changes, this may be due to continuous involvement of SOL in maintenance of posture compared to the locomotory function of EDL. As such, SOL with higher ratio of type I fibres may be more resistant to repeated degeneration and necrosis with less evidence present of membrane damage.

Secondly, in addition to the influence of fibre types, regenerated myofibres might be an underlying factor in the lower susceptibility of *mdx* soleus to fibrosis. Examination of central nucleated myofibres in SOL suggests ongoing regenerative responses in *mdx* at both 10 and 20 weeks with a total of 65% and 72% regenerated fibres, respectively. Since

regenerated fibres restore muscle structure and function upon injury, *mdx* SOL myofibres do not show evidence of fibrosis. Moreover, since SOL is a type I dominant muscle type, respective regenerated myofibres are mainly type I, known to have lower susceptibility to fibrosis. Thus, as fibrosis was absent in dystrophic SOL, the analyzed PL FA represents the whole membranes of SOL myofibres, showing increased in PUFA/MUFA. Increased saturation may be a result of eccentric induced damage, which due to inadequate stretch injury and relatively high molecular weight marker of damage was not detected. As such, no link was detected between membrane PL FA and fibrosis in dystrophic SOL at 10 and 20 weeks.

Summary and conclusions

The present study demonstrated that absence of dystrophin in *mdx* is associated with various pathologies. These include switch in fibre type populations, histopathology (i.e. regeneration and fibrosis), change in the membrane PL FA composition, contractile properties and membrane permeability. Moreover, this research highlighted the underlying associations between membrane composition and dystrophic-derived injuries.

Examination of fibre type involvement in dystrophic muscles revealed the majority of involved fibres were type II, and with increased age, the percentage of dystrophic type II fibres decreased. Such an alteration in fibre types may highlight a compensatory response of dystrophin deficient muscle to contraction-mediated damage by shifting to type I fibres, which appear to be more resistant. Moreover, dystrophic muscle demonstrates abnormal histology compared to WT, including myofibre

regeneration (central nucleated fibre) and fibrosis. This research demonstrated increased regeneration in EDL and SOL at 10 and 20 weeks, suggesting compensation for dystrophic degeneration. Moreover, fibrosis was only minimally present in dystrophic muscle (especially EDL) at 20 weeks. The histopathology of *mdx* muscles indicate that regeneration of muscle has an important role in preventing fibrosis especially at 10 and 20 weeks. Furthermore, dysfunctional dystrophin is linked to an alteration in membrane PL FA composition. Examination of whole muscle membrane lipid composition demonstrated increased saturation in *mdx* EDL and SOL at 10 and 20 weeks. These changes support the idea that as a result of oxidative damage, lipids of membranes experience oxidative stress that is manifested as a possible conversion of PUFA to SFA. Additionally, the dystrophic phenotype is involved with altered membrane permeability. Identification of fibronectin after eccentric stretch demonstrated increase in membrane damage in dystrophic EDL at 20 weeks, suggesting disruption of cell membrane integrity in 5 % of fibres after eccentric contractions.

Increased saturation of membrane was correlated to susceptibility of the EDL, but not SOL, to eccentric induced damage. In dystrophic EDL, eccentric induced damage to the muscle may have been accompanied by an influx of Ca^{2+}, a subsequent loss of Ca^{2+} homeostasis and the activation of lipid oxidation pathways targeting membrane lipid composition, which in turn resulted in increased saturated forms of PL FA in the membrane. Alternatively, due to membrane structure-protein functional relationship, increased saturation in dystrophic membranes was possibly accompanied by decreased mechanical strength of sarcolemma, which after eccentric contractions mediated membrane damage, followed by Ca^{+2} entry, disturbed Ca^{+2} homeostasis and final

oxidative damage. In dystrophic SOL, alterations in membrane lipid composition were not linked with susceptibility to eccentric induced damage. This may be related to unsuccessful mechanical damage in SOL due to the relatively high proportion of type I fibres, which are more resistant to mechanical damage. Furthermore, despite a lack of evidence for membrane damage, mitochondrial membrane PL FA of dystrophic SOL was altered, suggesting eccentric induced muscle damage may proceed changes to membrane lipid composition in this muscle.

It is important to note that expression of a muscle-specific nNOS transgene in dystrophic muscle prevented the majority of histologically discernible pathology in *mdx* mice, including a reduction in sarcolemmal lesions (Wehling et al, 2001). However, a recent study showed that there is not a simple relationship between decreasing oxidative stress (increase nNOS) at the sarcolemma and the severity of dystrophic damage (Harper *et al.*, 2002). Moreover, this research suggested that increase in saturation accompanied by decrease susceptibility to oxidative damage was not linked to alleviation of damage. This might be in contrary to the speculations that by decreasing the susceptibility of membranes to oxidative stress (increase saturation, increase nNOS), the respective damage decreases. These evidences are consistent with a "two hit hypothesis" (Rando, 2001) because it might indicate that decreased susceptibility to oxidative damage may not be the only mechanism in pathology of dystrophic muscles. This interpretation is supported by the study showing nNOS null mutant mice, which have heightened susceptibility to oxidative stress does not demonstrate pathologies (Crosbie *et al.*, 1998). Therefore, it indicates that although increased saturation may be an adaptation to oxidative stress, it is not sufficient to prevent pathology in dystrophin deficient muscles.

It further indicates that in addition to oxidative stress to the membranes that results in increased saturation, other pathways may be involved in the expression of the pathology.

Alterations in membrane lipid composition, however, did not appear to be linked to the vulnerability of *mdx* myofibres to fibrosis. In both EDL and SOL, this may be due to very little to no fibrosis along with increased proportion of type I fibres that may have impacted the composition of the membrane of remaining fibres. Moreover, observed changes in membrane lipid composition of dystrophic muscle (increased saturation) may be a consequence of a cascade of events following eccentric induced muscle damage, and fibrosis may not influence the lipid composition of membranes.

Taken together, the results of this research demonstrated the *mdx* muscle pathology and its progression with age. It also suggests that membrane lipid composition is associated with dystrophic damage. In this association, altered membrane lipid composition or increased membrane damage may be the preceding event. Specifically an increase in saturated membrane maybe linked with greater contraction induced damage. This further implicates the significance of membrane composition in modification of damage in muscular dystrophy.

Limitations and future studies

Despite the association of muscular dystrophy phenotypes in muscle damage and membrane PLFA compositions, there are number of limitations to the study that require future research.

First, findings of the present study have assessed the association of phenotypes including eccentric induced damage and fibrosis with membrane PL FA composition. However, fibre type compositions and the supporting role of regeneration on susceptibility of *mdx* myofibres to damage, the relation of alteration in membrane PL FA composition and muscle damage was solely correlative and not causative. As such, we were not able to demonstrate alterations of membrane PL FA composition as an underlying initial etiology of muscle damage in muscular dystrophy. To address this limitation, it is suggested to examine the pathology of *mdx* before 5 weeks of age where regeneration is minimal. Assessment of isolated fast and slow twitch myofibres may also provide insight about the underlying role of membrane PL FA composition in the presentation of dystrophic process at different ages without the influence of fibre type shifts.

Second, the symptoms of the dystrophic pathology are cumulative and there are several different stages in the severity of the disorder between growth, maturation and aging (Keeling *et al.*, 2007). After 10 weeks of age, degeneration of dystrophic fibres subside, that results in chronic but low grade damage (Grounds *et al.*, 2008). However, from 20 weeks onward the cycles of regeneration gradually decrease. In the present study, we have utilized two groups of age at 10 and 20 weeks of age, that led to a narrow age range of 10 weeks that may not represent the temporal changes of the phenotype from early to later ages. To address this limitation, it is suggested to examine all aspects of phenotype before 3 weeks (degeneration is not present and myofibres are not susceptible to damage) and after 18 months of age (fibrosis prominently increases, regeneration highly decreases) to examine the trajectory of the association between

membrane PL FA and muscle susceptibility to damage (Grange *et al.*, 2002; Whitehead et al, 2005; Stedman *et al.*, 1991). Examination of dystrophic phenotypes before 3 weeks contributes to investigate the association between phenotypes with minimum influence of myogenesis. Moreover, evaluation of *mdx* muscle damage after 18 months may provide more concrete evidence of the cumulated fibrosis that may not be apparent at 20 weeks of age.

Practical advantages of investigating PL FA of skeletal muscle fibres

Emerging evidence from a wide variety of muscle models has established the importance of membrane lipid content in mammalian skeletal muscles. As these emerging studies become more conventional, the ability to detect, identify, and characterize lipid changes in various skeletal muscle disorders will promote the understanding of the important role of cell membrane in human disease. While the genetic defect for DMD was identified in 1987, there is still no effective treatment for DMD (Odom *et al.*, 2007; Radley *et al.*, 2007). The therapeutic research approach that has received most attention to present is replacement of functional dystrophin complex by genetic, cell transplantation or molecular interventions (Chakkalakal, 2005; Lovering, 2005). Thus the mechanism by which regenerated *mdx* fibres restore adequate function in the absence of dystrophin may help provide clues to effective non-genetic interventions for muscular dystrophy in humans.

This research has underscored the importance of certain PL FA compositions in mitigation of damage to dystrophic myofibres. In parallel, membranes and their lipid profile can be influenced by administration of exercise and exogenous nutritional or

pharmaceutical factors to possibly reduce the extent of myofibre pathology. Involvement of PUFA in membranes may be associated with change in membrane fluidity (Garzetti *et al.*, 1993). Through alteration in such membrane physical parameters, dystrophin deficient muscles may be more capable to endure the shearing force of contractions. Therefore, it would be of interest to examine dystrophic muscles phenotype after involvement with pharmaceutical, dietary and exercise interventions.

References

Agarkova, I., Schoenauer, R., Ehler, E., Carlsson, L., Carlsson, E., Thornell, L. E., & Perriard, J. C. (2004). The molecular composition of the sarcomeric M-band correlates with muscle fibre type. *European Journal of Cell Biology*, *83*(5), 193-204.

Ahn, A. H., & Kunkel, L. M. (1993). The structural and functional diversity of dystrophin. *Nature Genetics*, *3*(4), 283-291.

Alberts, B., Johnson, A., Lewis, J., Raff, M., Roberts, K., & Walter, P. (2002*).* Cell junctions, cell adhesion, and the extracellular matrix. *Molecular biology of the cell.* New York: Garland Science.

Alderton, J. M., & Steinhardt, R. A. (2000). Calcium influx through calcium leak channels is responsible for the elevated levels of calcium-dependent proteolysis in dystrophic myotubes. *Journal of Biological Chemistry*, *275*(13), 9452-9460.

Allen, D. G. (2004). Skeletal muscle function: role of ionic changes in fatigue, damage and disease. *Clinical and experimental pharmacology and physiology*, *31*(8), 485-493.

Anderson, J. E., McIntosh, L. M., & Poettcker, R. (1996). Deflazacort but not prednisone improves both muscle repair and fiber growth in diaphragm and limb muscle in vivo in the *mdx* dystrophic mouse. *Muscle & nerve*, *19*(12), 1576-1585.

Antonio L., S., Christopher J., M., Berta, V., Esther, A., Eusebio, P., & Pura, M. (2011). Chapter seven: Cellular and Molecular Mechanisms Regulating Fibrosis in Skeletal Muscle Repair and Disease. *Current Topics in Developmental Biology*, *96* (Myogenesis), 167-201.

Armstrong, R. B., Ogilvie, R. W., & Schwane, J. A. (1983). Eccentric exercise-induced injury to rat skeletal muscle. *Journal of Applied Physiology*, *54*(1), 80-93.

Asayama, K., Dettbarn, W. D., & Burr, I. M. (1986). Differential Effect of Denervation on Free-Radical Scavenging Enzymes in Slow and Fast Muscle of Rat. *Journal of Neurochemistry*, *46*(2), 604-609.

Balnave, C. D., & Allen, D. G. (1995). Intracellular calcium and force in single mouse muscle fibres following repeated contractions with stretch. *The Journal of Physiology*, *488*(1), 25-36.

Bell, G. H., Davidson, J. N., & Scarborough, H. (1976). Textbook of Physiology and Biochemistry. *Academic Medicine*, *34*(6), 621.

Benabdellah, F., Yu, H., Brunelle, A., Laprévote, O., & De La Porte, S. (2009). MALDI reveals membrane lipid profile reversion in *mdx* mice. *Neurobiology of Disease*, *36*(2), 252-258.

Blackard, W. G., Li, J., Clore, J. N., & Rizzo, W. B. (1997). Phospholipid fatty acid composition in type I and type II rat muscle. *Lipids*, *32*(2), 193-198.

Blake, D. J., Weir, A., Newey, S. E., & Davies, K. E. (2002). Function and genetics of dystrophin and dystrophin-related proteins in muscle. *Physiological Reviews*, *82*(2), 291-329.

Bleijerveld, O. B., Brouwers, J. F., Vaandrager, A. B., Helms, J. B., & Houweling, M. (2007). The CDP-ethanolamine pathway and phosphatidylserine decarboxylation generate different phosphatidylethanolamine molecular species. *Journal of Biological Chemistry*, *282*(39), 28362-28372.

Bligh, E. G., & Dyer, W. J. (1959). A rapid method of total lipid extraction and purification. *Canadian Journal of Biochemistry and Physiology*, *37*(8), 911-917.

Bottinelli, R., Pellegrino, M. A., Canepari, M., Rossi, R., & Reggiani, C. (1999). Specific contributions of various muscle fibre types to human muscle performance: an in vitro study. *Journal of Electromyography and Kinesiology*, *9*(2), 87-95.

Brenman, J. E., Chao, D. S., Xia, H., Aldape, K., & Bredt, D. S. (1995). Nitric oxide synthase complexed with dystrophin and absent from skeletal muscle sarcolemma in Duchenne muscular dystrophy. *Cell*, *82*(5), 743-752.

Brooke, M. H., & Kaiser, K. K. (1970). Muscle fibre types: how many and what kind? *Archives of Neurology, 23*(4), 369-379.

Brooks, S. V., Zerba, E., & Faulkner, J. A. (1995). Injury to muscle fibres after single stretches of passive and maximally stimulated muscles in mice. *The Journal of Physiology, 488*(2), 459-469.

Brown, R. E. (1998). Sphingolipid organization in biomembranes: what physical studies of model membranes reveal. *Journal of Cell Science, 111*(1), 1-9.

Buetler, T. M., Renard, M., Offord, E. A., Schneider, H., & Ruegg, U. T. (2002). Green tea extract decreases muscle necrosis in *mdx* mice and protects against reactive oxygen species. *The American Journal of Clinical Nutrition, 75*(4), 749-753.

Bulfield, G., Siller, W. G., Wight, P. A., & Moore, K. J. (1984). X chromosome-linked muscular dystrophy (*mdx*) in the mouse. *Proceedings of the National Academy of Sciences, 81*(4), 1189-1192.

Campbell, K. P., & Stull, J. T. (2003). Skeletal muscle basement membrane-sarcolemma-cytoskeleton interaction mini-review series. *Journal of Biological Chemistry, 278*(15), 12599-12600.

Carnwath, J. W., & Shotton, D. M. (1987). Muscular dystrophy in the *mdx* mouse: histopathology of the soleus and extensor digitorum longus muscles. *Journal of the Neurological Sciences*, *80*(1), 39-54.

Chamberlain, J. S., Metzger, J., Reyes, M., Townsend, D., & Faulkner, J. A. (2007). Dystrophin-deficient *mdx* mice display a reduced life span and are susceptible to spontaneous rhabdomyosarcoma. *The FASEB Journal*, *21*(9), 2195-2204.

Chan, S., Head, S. I., & Morley, J. W. (2007). Branched fibres in dystrophic *mdx* muscle are associated with a loss of force following lengthening contractions. *American Journal of Physiology*, *293*(3), 985-992.

Chatterjee, S., & Mayor, S. (2001). The GPI-anchor and protein sorting. *Cellular and Molecular Life Sciences*, *58*(14), 1969-1987.

Clore, J. N., Li, J., Gill, R., Gupta, S., Spencer, R., Azzam, A., & Blackard, W. G. (1998). Skeletal muscle phosphatidylcholine fatty acids and insulin sensitivity in normal humans. *American Journal of Physiology-Endocrinology and Metabolism*, *275*(4), 665-670.

Consolino, C., & Brooks, S. (2004). Susceptibility to sarcomere injury induced by single stretches of maximally activated muscles of *mdx* mice. *Journal of Applied Physiology*, *96*(2), 633-638.

Cooper, R. A., Durocher, J. R., & Leslie, M. H. (1977). Decreased fluidity of red cell membrane lipids in abetalipoproteinemia. *Journal of Clinical Investigation*, *60*(1), 115-121.

Crosbie, R. H., Lim, L. E., Moore, S. A., Hirano, M., Hays, A. P., Maybaum, S. W., & Campbell, K. P. (2000). Molecular and genetic characterization of sarcospan: insights into sarcoglycan–sarcospan interactions. *Human Molecular Genetics*, *9*(13), 2019-2027.

Crosbie, R. H., Straub, V., Yun, H. Y., Lee, J. C., Rafael, J. A., Chamberlain, J. S., & Campbell, K. P. (1998). *mdx* muscle pathology is independent of nNOS perturbation. *Human Molecular Genetics*, *7*(5), 823-829.

Cullis, P. R., & de Kruijff, B. (1979). Lipid polymorphism and the functional roles of lipids in biological membranes. *Biochimica et Biophysica Acta*, *559*(4), 399-420.

Dannenberger, D., Nuernberg, G., Scollan, N., Ender, K., & Nuernberg, K. (2007). Diet alters the fatty acid composition of individual phospholipid classes in beef muscle. *Journal of Agricultural and Food Chemistry*, *55*(2), 452-460.

Darras, B. T., Korf, B. R., & Urion, D. K. (2008). Dystrophinopathies. Retrieved May 11, 2015, from GeneReviews Web site: http://www.ncbi.nlm.nih.gov/books/NBK1119/

Deconinck, N., Rafael, J. A., Beckers-Bleukx, G., Kahn, D., Deconinck, A. E., Davies, K. E., & Gillis, J. M. (1998). Consequences of the combined deficiency in dystrophin and utrophin on the mechanical properties and myosin composition of some limb and respiratory muscles of the mouse. *Neuromuscular Disorders, 8*(6), 362-370.

Dellorusso, C., Crawford, R. W., Chamberlain, J. S., & Brooks, S. V. (2001). Tibialis anterior muscles in *mdx* mice are highly susceptible to contraction-induced injury. *Journal of Muscle Research & Cell Motility, 22(5),* 467-475.

Desguerre, I., Arnold, L., Vignaud, A., Cuvellier, S., Yacoub Youssef, H., Gherardi, R. K., & Chazaud, B. (2012). A new model of experimental fibrosis in hind limb skeletal muscle of adult *mdx* mouse mimicking muscular dystrophy. *Muscle & Nerve, 45*(6), 803-814.

DiMario, J. X., Uzman, A., & Strohman, R. C. (1991). Fibre regeneration is not persistent in dystrophic (*mdx*) mouse skeletal muscle. *Developmental Biology, 148*(1), 314-321.

Dorchies, O. M., Wagner, S., Vuadens, O., Waldhauser, K., Buetler, T. M., Kucera, P., & Ruegg, U. T. (2006). Green tea extract and its major polyphenol (−)-epigallocatechin gallate improve muscle function in a mouse model for Duchenne muscular dystrophy. *American Journal of Physiology-Cell Physiology, 290*(2), 616-625.

Duchen, M. R. (2004). Mitochondria in health and disease: perspectives on a new mitochondrial biology. *Molecular Aspects of Medicine*, *25*(4), 365-451.

Dufourc, E. J., Mayer, C., Stohrer, J., Althoff, G., & Kothe, G. (1992). Dynamics of phosphate head groups in biomembranes. Comprehensive analysis using phosphorus-31 nuclear magnetic resonance line shape and relaxation time measurements. *Biophysical Journal*, *61*(1), 42-57.

Durbeej, M., & Campbell, K. P. (2002). Muscular dystrophies involving the dystrophin–glycoprotein complex: an overview of current mouse models. *Current Opinion in Genetics & Development*, *12*(3), 349-361.

Edman, K. A., & Lou, F. A. N. G. (1992). Myofibrillar fatigue versus failure of activation during repetitive stimulation of frog muscle fibres. *The Journal of Physiology*, *457*(1), 655-673.

Emery, A. E. (2002). The muscular dystrophies. *The Lancet*, *359*(9307), 687-695.

Ervasti, J. M., & Campbell, K. P. (1991). Membrane organization of the dystrophin-glycoprotein complex. *Cell*, *66*(6), 1121-1131.

Fajardo, V. A., McMeekin, L., Basic, A., Lamb, G. D., Murphy, R. M., & LeBlanc, P. J. (2013). Isolation of sarcolemmal plasma membranes by mechanically skinning rat skeletal muscle fibres for phospholipid analysis. *Lipids*, *48*(4), 421-430.

Faulkner, J. A. (2003). Terminology for contractions of muscles during shortening, while isometric, and during lengthening. *Journal of Applied Physiology*, *95*(2), 455-459.

Faulkner, J. A., Brooks, S. V., & Opiteck, J. A. (1993). Injury to skeletal muscle fibres during contractions: conditions of occurrence and prevention. *Physical Therapy*, *73*(12), 911-921.

Fiehn, W., & Peter, J. B. (1971). Properties of the fragmented sarcoplasmic reticulum from fast twitch and slow twitch muscles. *Journal of Clinical Investigation*, *50(3)*, 570.

Fiehn, W., & Peter, J. B. (1973). Lipid composition of muscles of nearly homogeneous fibre type. *Experimental Neurology*, *39*(3), 372-380.

Fitts, R. H. (2008). The cross-bridge cycle and skeletal muscle fatigue. *Journal of Applied Physiology*, *104*(2), 551-558.

Folch, J., Lees, M., & Sloane-Stanley, G. H. (1957). A simple method for the isolation and purification of total lipids from animal tissues. *The Journal of Biological Chemistry*, *226*(1), 497-509.

Franco, A., & Lansman, J. B. (1990). Stretch-sensitive channels in developing muscle cells from a mouse cell line. *The Journal of physiology*, *427*(1), 361-380.

Friden, J., Sjöström, M., & Ekblom, B. (1981). A morphological study of delayed muscle soreness. *Experientia*, *37*(5), 506-507.

Garzetti, G. G., Tranquilli, A. L., Cugini, A. M., Mazzanti, L., Cester, N., & Romanini, C. (1993). Altered lipid composition, increased lipid peroxidation, and altered fluidity of the membrane as evidence of platelet damage in preeclampsia. *Obstetrics & Gynecology*, *81*(3), 337-340.

Gissel, H. (2006). The role of Ca^{2+} in muscle cell damage. *Annals of the New York Academy of Sciences*, *1066*(1), 166-180.

Gittings, W. J. (2009). The influence of myosin regulatory light chain phosphorylation on the contractile performance of fatigued mammalian skeletal muscle. Brock University, St. Catharines.

Godt, R. E., & Maughan, D. W. (1981). Influence of osmotic compression on calcium activation and tension in skinned muscle fibres of the rabbit. *Pflügers Archiv, 391*(4), 334-337.

Gordon, A. M., Huxley, A. F., & Julian, F. J. (1966). The variation in isometric tension with sarcomere length in vertebrate muscle fibres. *The Journal of Physiology, 184*(1), 170-192.

Grange, R. W., Gainer, T. G., Marschner, K. M., Talmadge, R. J., & Stull, J. T. (2002). Fast-twitch skeletal muscles of dystrophic mouse pups are resistant to injury from acute mechanical stress. *American Journal of Physiology-Cell Physiology, 283*(4), 1090-1101.

Gregorevic, P., Plant, D. R., & Lynch, G. S. (2004). Administration of insulin-like growth factor-I improves fatigue resistance of skeletal muscles from dystrophic *mdx* mice. *Muscle & Nerve, 30*(3), 295-304.

Grounds, M. D., Radley, H. G., Lynch, G. S., Nagaraju, K., & De Luca, A. (2008). Towards developing standard operating procedures for pre-clinical testing in the *mdx* mouse model of Duchenne muscular dystrophy. *Neurobiology of Disease, 31*(1), 1-19.

Hakim, C. H., & Duan, D. (2012). Gender differences in contractile and passive properties of *mdx* extensor digitorum longus muscle. *Muscle & Nerve, 45*(2), 250-256.

Hakim, C. H., Grange, R. W., & Dongsheng, D. (2011). The passive mechanical properties of the extensor digitorum longus muscle are compromised in 2- to 20-mo-old *mdx* mice. *Journal of Applied Physiology, 110*(6), 1656-1663.

Hamilton, J. A. (2003). Fast flip-flop of cholesterol and fatty acids in membranes: implications for membrane transport proteins. *Current Opinion in Lipidology*, *14*(3), 263-271.

Harper, S. Q., Hauser, M. A., DelloRusso, C., Duan, D., Crawford, R. W., Phelps, S. F., & Chamberlain, J. S. (2002). Modular flexibility of dystrophin: implications for gene therapy of Duchenne muscular dystrophy. *Nature Medicine, 8*(3), 253-261.

Head, S. I., Bakker, A. J., & Liangas, G. (2004). EDL and soleus muscles of the C57BL6J/dy2j laminin-α2-deficient dystrophic mouse are not vulnerable to eccentric contractions. *Experimental Physiology*, *89*(5), 531-539.

Herzog, W., & Leonard, T. R. (2000). The history dependence of force production in mammalian skeletal muscle following stretch-shortening and shortening-stretch cycles. *Journal of Biomechanics*, *33*(5), 531-542.

Hughes, B. P. (1972). Lipid changes in Duchenne muscular dystrophy. *Journal of Neurology, Neurosurgery & Psychiatry*, *35*(5), 658-663.

Hutter, O. F., Burton, F. L., & Bovell, D. L. (1991). Mechanical properties of normal and *mdx* mouse sarcolemma: Bearing on function of dystrophin. *Journal of Muscle Research & Cell Motility*, *12*(6), 585-589.

Jackson, M. J., Jones, D. A., & Edwards, R. H. T. (1984). Experimental skeletal muscle damage: the nature of the calcium-activated degenerative processes. *European Journal of Clinical Investigation*, *14*(5), 369-374.

Keren, K. (2011). Cell motility: the integrating role of the plasma membrane. *European Biophysics Journal*, *40*(9), 1013-1027.

Kometani, K., Tsugeno, H., & Yamada, K. (1989). Mechanical and energetic properties of dystrophic (*mdx*) mouse muscle. *The Japanese Journal of Physiology*, *40*(4), 541-549.

Kriketos, A. D., Pan, D. A., Sutton, J. R., Hoh, J. F., Baur, L. A., Cooney, G. J., Jenkins, A. B., & Storlien, L. H. (1995). Relationships between muscle membrane lipids, fibre type, and enzyme activities in sedentary and exercised rats. *American Journal of Physiology-Regulatory, Integrative and Comparative Physiology*, *269*(5), 1154-1162.

Kunze, D., Reichmann, G., Egger, E., Olthoff, D., & Döhler, K. (1975). Fatty acid pattern of lipids in normal and dystrophic human muscle. *European Journal of Clinical Investigation*, *5*(6), 471-475.

Lieber, R. L., & Friden, J. (1988). Selective damage of fast glycolytic muscle fibres with eccentric contraction of the rabbit tibialis anterior. *Acta physiologica Scandinavica*, *133*(4), 587-588.

Lieber, R. L., Woodburn, T. M., & Friden, J. (1991). Muscle damage induced by eccentric contractions of 25% strain. *Journal of Applied Physiology, 70(6)*, 2498-2507.

Lynch, G. S. (2004). Role of contraction-induced injury in the mechanisms of muscle damage in muscular dystrophy. *Clinical and Experimental Pharmacology and Physiology*, *31*(8), 557-561.

Lynch, G. S., Hinkle, R. T., & Faulkner, J. A. (2001). Force and power output of diaphragm muscle strips from *mdx* and control mice after clenbuterol treatment. *Neuromuscular Disorders*, *11*(2), 192-196.

Macpherson, P. C., Schork, M. A., & Faulkner, J. A. (1996). Contraction-induced injury to single fibre segments from fast and slow muscles of rats by single stretches. *American Journal of Physiology-Cell Physiology*, *271*(5), 1438-1446.

McArdle, A., Edwards, R. H., & Jackson, M. J. (1991). Effects of contractile activity on muscle damage in the dystrophin-deficient mouse. *Clinical Sciences*, *80*(4), 367-371.

McArdle, A., Edwards, R. H., & Jackson, M. J. (1994). Time course of changes in plasma membrane permeability in the dystrophin-deficient *mdx* mouse. *Muscle & Nerve*, *17*(12), 1378-1384.

McCully, K. K., & Faulkner, J. A. (1985). Injury to skeletal muscle fibres of mice following lengthening contractions. *Journal of Applied Physiology*, *59*(1), 119-126.

Mendell, J. R., Sahenk, Z., & Prior, T. W. (1995). The childhood muscular dystrophies: diseases sharing a common pathogenesis of membrane instability. *Journal of Child Neurology*, *10*(2), 150-159.

Mitchell, T. W., Buffenstein, R., & Hulbert, A. J. (2007). Membrane phospholipid composition may contribute to exceptional longevity of the naked mole-rat (Heterocephalus glaber): a comparative study using shotgun lipidomics. *Experimental Gerontology*, *42*(11), 1053-1062.

Moss, R. L., Diffee, G. M., & Greaser, M. L. (1995). Contractile properties of skeletal muscle fibres in relation to myofibrillar protein isoforms. *Reviews of Physiology, Biochemistry and Pharmacology, 126*, 1-63.

Nikolaidis, M. G., & Mougios, V. (2004). Effects of exercise on the fatty-acid composition of blood and tissue lipids. *Sports Medicine, 34*(15), 1051-1076.

Ohlendieck, K., & Campbell, K. P. (1991). Dystrophin-associated proteins are greatly reduced in skeletal muscle from *mdx* mice. *The Journal of Cell Biology, 115*(6), 1685-1694.

Okinaka, S., Sugita, H., Momoi, H., Toyokura, Y., Kumagai, H., Ebashi, S., & Fujie, Y. (1959). Serum creatine phosphokinase and aldolase activity in neuromuscular disorders. *Transactions of the American Neurological Association, 84*, 62.

Owen, O. E., Reichard, G. A., Boden, G., Patel, M. S., & Trapp, V. E. (1978). Interrelationships among key tissues in the utilization of metabolic substrate. *Advances in Modern Nutrition, 2*, 517-550.

Owens, K., & Hughes, B. P. (1970). Lipids of dystrophic and normal mouse muscle: whole tissue and particulate fractions. *Journal of Lipid Research, 11*(5), 486-495.

Ozawa, E., Nishino, I., & Nonaka, I. (2001). Sarcolemmopathy: muscular dystrophies with cell membrane defects. *Brain Pathology, 11*(2), 218-230.

Palacio, J., Gāldiz, J. B., Alvarez, F. J., Orozco-Levi, M., Lloreta, J., & Gea, J. (2002). Procion orange tracer dye technique vs. identification of intrafibrillar fibronectin in the assessment of sarcolemmal damage. *European Journal of Clinical Investigation, 32*(6), 443-447.

Pasternak, C., Wong, S., & Elson, E. L. (1995). Mechanical function of dystrophin in muscle cells. *The Journal of Cell Biology, 128*(3), 355-361.

Pastoret, C., & Sebille, A. (1993). Time course study of the isometric contractile properties of *mdx* mouse striated muscles. *Journal of Muscle Research & Cell Motility, 14*(4), 423-431.

Pearce, P. H., & Kakulas, B. A. (1980). Skeletal muscle lipids in normal and dystrophic mice. *Australian Journal of Experimental Biology in Medical Science, 58*(4), 397-408.

Pelley, J. W. (2011). *Elsevier's Integrated Review Biochemistry*. Elsevier Health Sciences.

Petrof, B. J., Shrager, J. B., Stedman, H. H., Kelly, A. M., & Sweeney, H. L. (1993). Dystrophin protects the sarcolemma from stresses developed during muscle contraction. *Proceedings of the National Academy of Sciences*, *90*(8), 3710-3714.

Prado, L. G., Makarenko, I., Andresen, C., Krüger, M., Opitz, C. A., & Linke, W. A. (2005). Isoform diversity of giant proteins in relation to passive and active contractile properties of rabbit skeletal muscles. *The Journal of General Physiology*, *126*(5), 461-480.

Radley, H. G., De Luca, A., Lynch, G. S., & Grounds, M. D. (2007). Duchenne muscular dystrophy: focus on pharmaceutical and nutritional interventions. *The International Journal of Biochemistry & Cell Biology*, *39*(3), 469-477.

Ramstedt, B., & Slotte, J. P. (2002). Membrane properties of sphingomyelins. *FEBS Letters*, *531*(1), 33-37.

Rando, T. A. (2001). Role of nitric oxide in the pathogenesis of muscular dystrophies: a "two hit" hypothesis of the cause of muscle necrosis. *Microscopy Research and Technique*, *55*(4), 223-235.

Reeve, J. L., McArdle, A., & Jackson, M. J. (1997). Age-related changes in muscle calcium content in dystrophin-deficient *mdx* mice. *Muscle & Nerve*, *20*(3), 357-360.

Ritov, V. B., Menshikova, E. V., & Kelley, D. E. (2006). Analysis of cardiolipin in human muscle biopsy. *Journal of Chromatography B, 831*(1), 63-71.

Roberts, R.G. (2001). Protein family review. *Genome Biology*, 2: 3006.1-3006.

Rose, A. J., & Richter, E. A. (2005). Skeletal muscle glucose uptake during exercise: how is it regulated? *Physiology*, *20*(4), 260-270.

Ruegg, M. A., & Meinen, S. (2014). Histopathology in Masson Trichrome stained muscle sections [cited 2015 May 09]. *TREAT. NMD*. Retrieved from http://www.treatnmd.eu/downloads/file/sops/cmd/MDC1A_M.1.2.003.pdf

Rybakova, I. N., Patel, J. R., & Ervasti, J. M. (2000). The dystrophin complex forms a mechanically strong link between the sarcolemma and costameric actin. *The Journal of Cell Biology*, *150*(5), 1209-1214.

Sacco, P., Jones, D. A., Dick, J. R. T., & Vrbova, G. (1992). Contractile properties and susceptibility to exercise-induced damage of normal and *mdx* mouse tibialis anterior muscle. *Clinical Science*, *82(2)*, 227-236.

Salminen, A., & Vihko, V. (1983). Endurance training reduces the susceptibility of mouse skeletal muscle to lipid peroxidation in vitro. *Acta Physiologica Scandinavica*, *117*(1), 109-113.

Schiaffino, S., Sandri, M., & Murgia, M. (2007). Activity-dependent signaling pathways controlling muscle diversity and plasticity. *Physiology*, *22*(4), 269-278.

Schiaffino, S., & Reggiani, C. (2011). Fibre types in mammalian skeletal muscles. *Physiological Reviews, 91*(4), 1447-1531.

Scott, W., Stevens, J., & Binder–Macleod, S. A. (2001). Human skeletal muscle fibre type classifications. *Physical Therapy*, *81*(11), 1810-1816.

Sicinski, P., Geng, Y., Ryder-Cook, A. S., Barnard, E. A., Darlison, M. G., & Barnard, P. J. (1989). The molecular basis of muscular dystrophy in the *mdx* mouse: a point mutation. *Science*, *244*(4912), 1578-1580.

Singer, S. J., & Nicolson, G. L. (1972). The fluid mosaic model of the structure of cell membranes. *Science*, 175, 720-731.

Smith, L. R., & Barton, E. R. (2014). Collagen content does not alter the passive mechanical properties of fibrotic skeletal muscle in *mdx* mice. *American Journal of Physiology-Cell Physiology*, *306*(10), 889-898.

Smith, I. C., Gittings, W., Huang, J., McMillan, E. M., Quadrilatero, J., Tupling, A. R., & Vandenboom, R. (2013). Potentiation in mouse lumbrical muscle without myosin light

chain phosphorylation: Is resting calcium responsible?. *The Journal of General Physiology*, *141*(3), 297-308.

Song, J. H., Fujimoto, K., & Miyazawa, T. (2000). Polyunsaturated (n-3) fatty acids susceptible to peroxidation are increased in plasma and tissue lipids of rats fed docosahexaenoic acid–containing oils. *The Journal of nutrition*, *130*(12), 3028-3033.

Sorichter, S., Puschendorf, B., & Mair, J. (1998). Skeletal muscle injury induced by eccentric muscle action: muscle proteins as markers of muscle fiber injury. *Exercise Immunology Review*, *5*, 5-21.

Spurney, C. F., Gordish-Dressman, H., Guerron, A. D., Sali, A., Pandey, G. S., Rawat, R., Van Der Meulen, J. H., Cha, H. J., Pistilli, E. E., Partridge, T. A., Hoffman, E. P., & Nagaraju, K. (2009). Preclinical drug trials in the *mdx* mouse: assessment of reliable and sensitive outcome measures. *Muscle & nerve*, *39*(5), 591-602.

Stedman, H. H., Sweeney, H. L., Shrager, J. B., Maguire, H. C., Panettieri, R. A., Petrof, B., Kelly, A. M. (1991). The *mdx* mouse diaphragm reproduces the degenerative changes of Duchenne muscular dystrophy. *Nature*, *352*(6335), 536-539.

Stefanyk, L. E., Coverdale, N., Roy, B. D., Peters, S. J., & LeBlanc, P. J. (2010). Skeletal muscle type comparison of subsarcolemmal mitochondrial membrane phospholipid fatty acid composition in rat. *Journal of Membrane Biology*, *234*(3), 207-215.

Steinbrecht, R. A., & Zierold, K. (1984). A cryoembedding method for cutting ultrathin cryosections from small frozen specimens. *Journal of Microscopy*, *136*(1), 69-75.

Tahallah, N., Brunelle, A., De La Porte, S., & Laprévote, O. (2008). Lipid mapping in human dystrophic muscle by cluster-time-of-flight secondary ion mass spectrometry imaging. *Journal of Lipid Research*, *49*(2), 438-454.

Terrill, J. R., Radley-Crabb, H. G., Iwasaki, T., Lemckert, F. A., Arthur, P. G., & Grounds, M. D. (2013). Oxidative stress and pathology in muscular dystrophies: focus on protein thiol oxidation and dysferlinopathies. *FEBS Journal*, *280*(17), 4149-4164.

Tidball, J. G., & Wehling-Henricks, M. (2007). The role of free radicals in the pathophysiology of muscular dystrophy. *Journal of Applied Physiology*, *102*(4), 1677-1686.

Tsalouhidou, S., Argyrou, C., Theofilidis, G., Karaoglanidis, D., Orfanidou, E., Nikolaidis, M. G., Mougios, V. (2006). Mitochondrial phospholipids of rat skeletal muscle are less polyunsaturated than whole tissue phospholipids: implications for protection against oxidative stress. *Journal of Animal Science*, *84*(10), 2818-2825.

Turner, P. R., Fong, P. Y., Denetclaw, W. F., & Steinhardt, R. A. (1991). Increased calcium influx in dystrophic muscle. *The Journal of Cell Biology*, *115*(6), 1701-1712.

Turner, P. R., Westwood, T., Regen, C. M., & Steinhardt, R. A. (1988). Increased protein degradation results from elevated free calcium levels found in muscle from *mdx* mice. *Nature*, *335*(6192), 735-738.

Tutdibi, O., Brinkmeier, H., Rüdel, R., & Föhr, K. J. (1999). Increased calcium entry into dystrophin-deficient muscle fibres of *MDX* and ADR-*MDX* mice is reduced by ion channel blockers. *The Journal of Physiology*, *515*(3), 859-868.

Voet, V. (2004). Biochemistry (3rd ed.). Pennsylvannia: John Wiley and Sons, Inc.

Wehling, M., Spencer, M. J., & Tidball, J. G. (2001). A nitric oxide synthase transgene ameliorates muscular dystrophy in *mdx* mice. *The Journal of Cell Biology*, *155*(1), 123-132.

Whitehead, N. P., Streamer, M., Lusambili, L. I., Sachs, F., & Allen, D. G. (2006). Streptomycin reduces stretch-induced membrane permeability in muscles from *mdx* mice. *Neuromuscular Disorders*, *16*(12), 845-854.

Whitney, E. N., Cataldo, C. B., & Rolfes, S. R. (1998*). Understanding Normal and Clinical Nutrition*. Wadsworth Publishing Company, Inc.

Yamaguchi, M., Izumimoto, M., Robson, R. M., & Stromer, M. H. (1985). Fine structure of wide and narrow vertebrate muscle Z-lines: a proposed model and computer simulation of Z-line architecture. *Journal of Molecular Biology*, *184*(4), 621-643.

Yeagle, P. L., Albert, A. D., Boesze-Battaglia, K., Young, J., & Frye, J. (1990). Cholesterol dynamics in membranes. *Biophysical Journal*, *57*(3), 413-424.

Yeung, E. W., Balnave, C. D., Ballard, H. J., Bourreau, J. P., & Allen, D. G. (2002). Development of T-tubular vacuoles in eccentrically damaged mouse muscle fibres. *The Journal of Physiology*, *540*(2), 581-592.

Yeung, E. W., Ballard, H. J., Bourreau, J. P., & Allen, D. G. (2003). Intracellular sodium in mammalian muscle fibres after eccentric contractions. *Journal of Applied Physiology*, *94*(6), 2475-2482.

Yeung, E. W., Whitehead, N. P., Suchyna, T. M., Gottlieb, P. A., Sachs, F., & Allen, D. G. (2005). Effects of stretch-activated channel blockers on [Ca2+]i and muscle damage in the *mdx* mouse. *The Journal of Physiology*, *562*(2), 367-380.

Zhao, Y., & Kawai, M. (1994). Kinetic and thermodynamic studies of the cross-bridge cycle in rabbit psoas muscle fibres. *Biophysical Journal*, *67*(4), 1655-1668.

APPENDIX A
Supplementary results

Stiffness

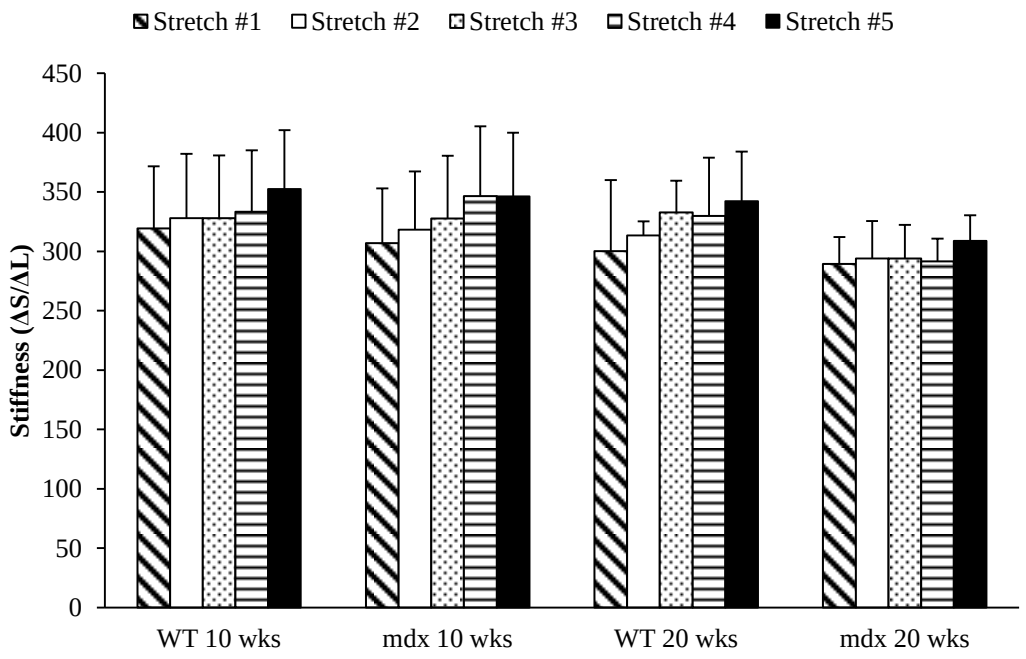

Fig.A.1. Stiffness responses for each of 5 stretches in 10 and 20 week *mdx* and WT EDL. Values are mean ± SEM. Lack of significant changes in stiffness from stretch 1 to 5 within and between groups.

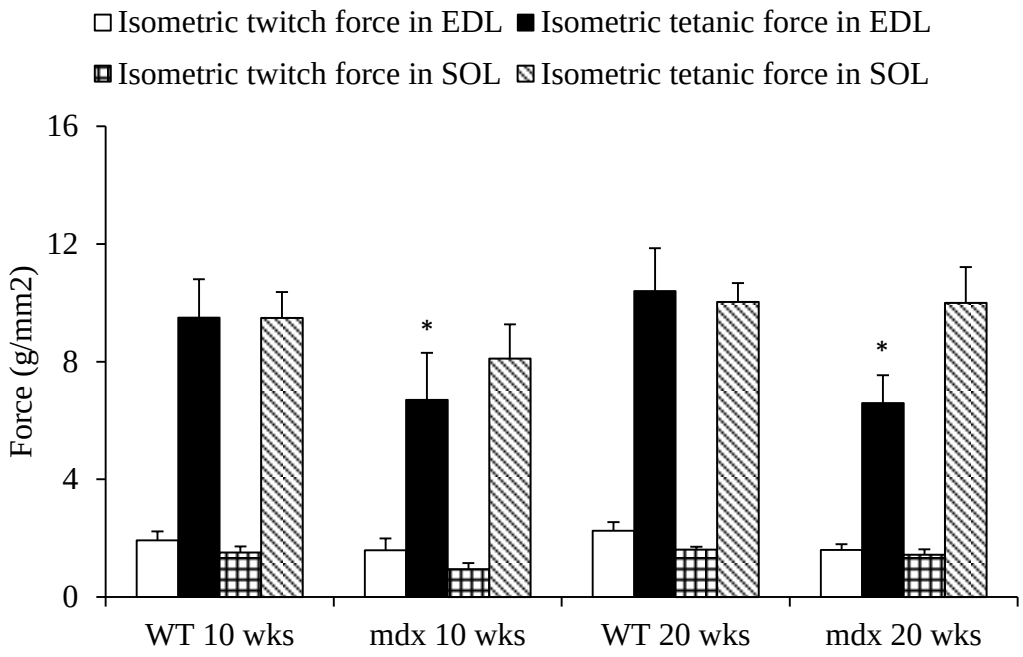

Fig A.2. Representative force outputs of extensor digitorum longus (EDL) and solues (SOL) at mdx and WT at 20 and 20 weeks. Values are mean ± SEM. * denotes significance from WT.

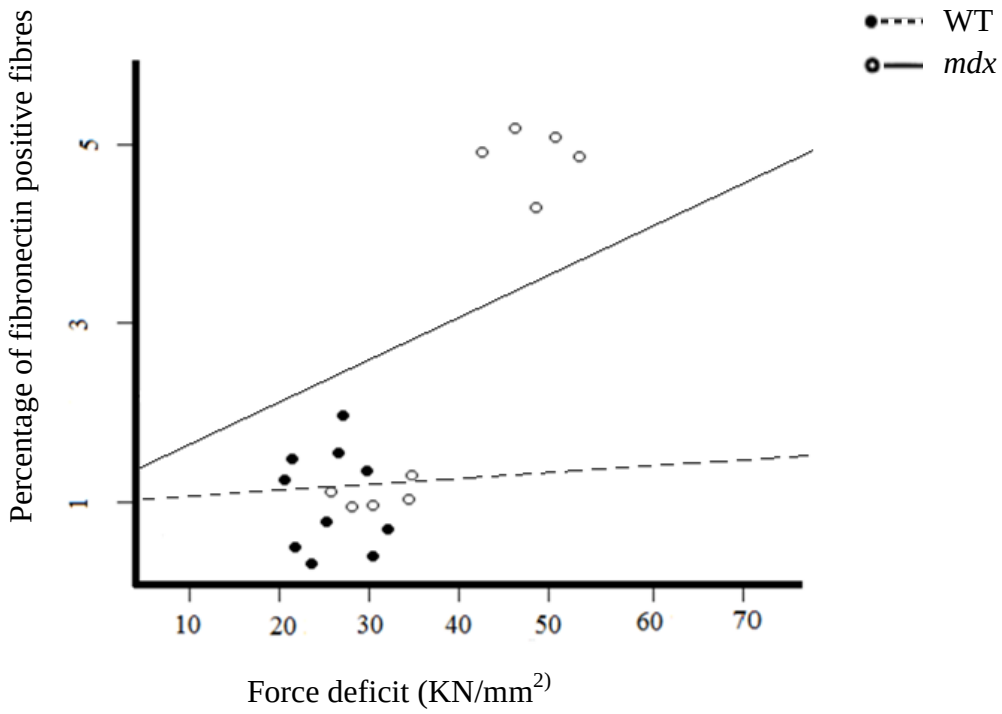

Fig A.3. Linear fitted regression model of percentage of fibronectin positive fibres after eccentric induced damage with force deficit in extensor digitorum longus (WT, r:0.22, $p<0.05$; *mdx*,r: 0.48, $p<0.05$).

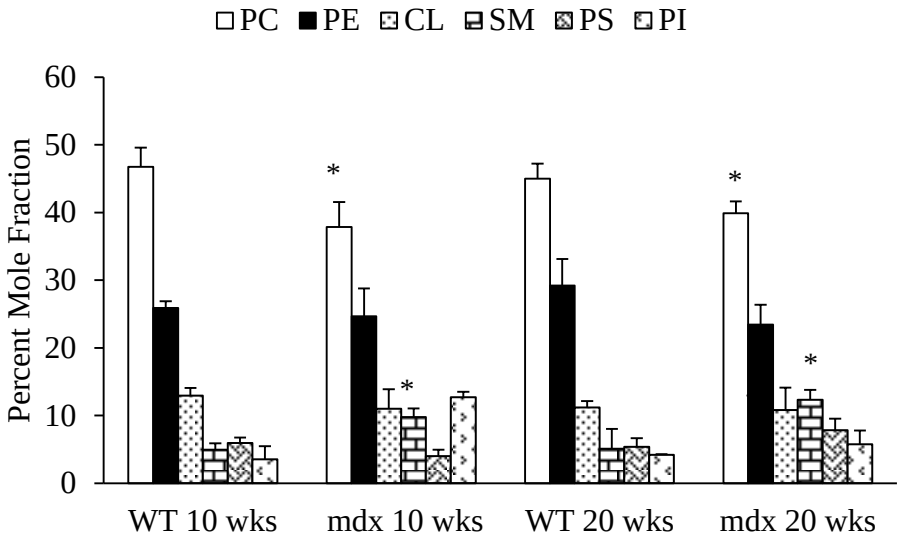

Fig. A.4. Phospholipid species from WT and *mdx* mice EDL in 10 and 20 week of age. Values are means ± SEM. * denotes significance from WTs. † denotes significance from 10 wks old.

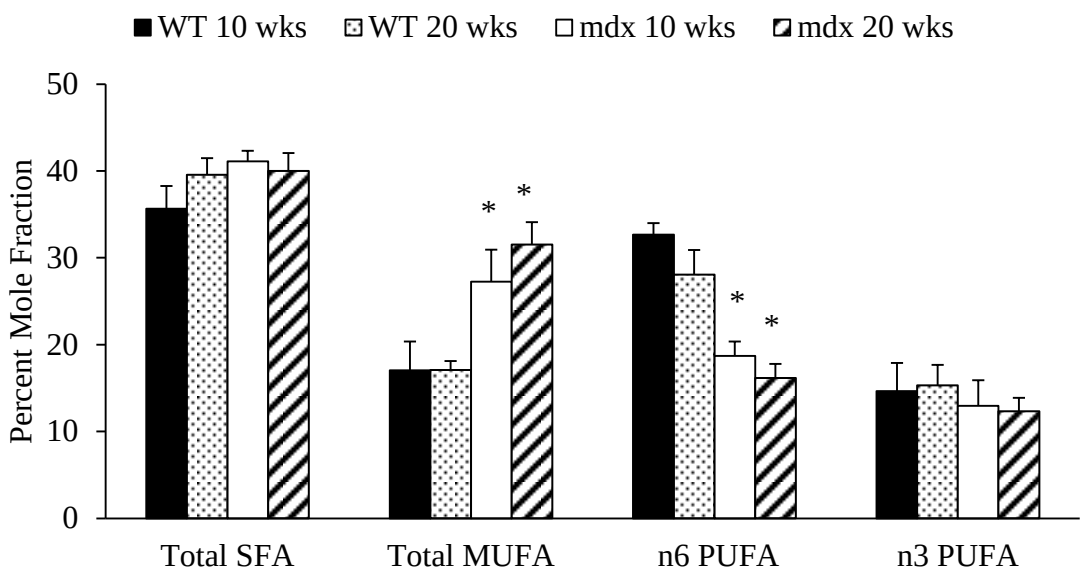

Fig. A.5. Four major fatty acid classes of EDL obtained from 10 and 20 wks old WT and *mdx* mice. Values are mean ± SEM. * denotes significance from WT within same age group.

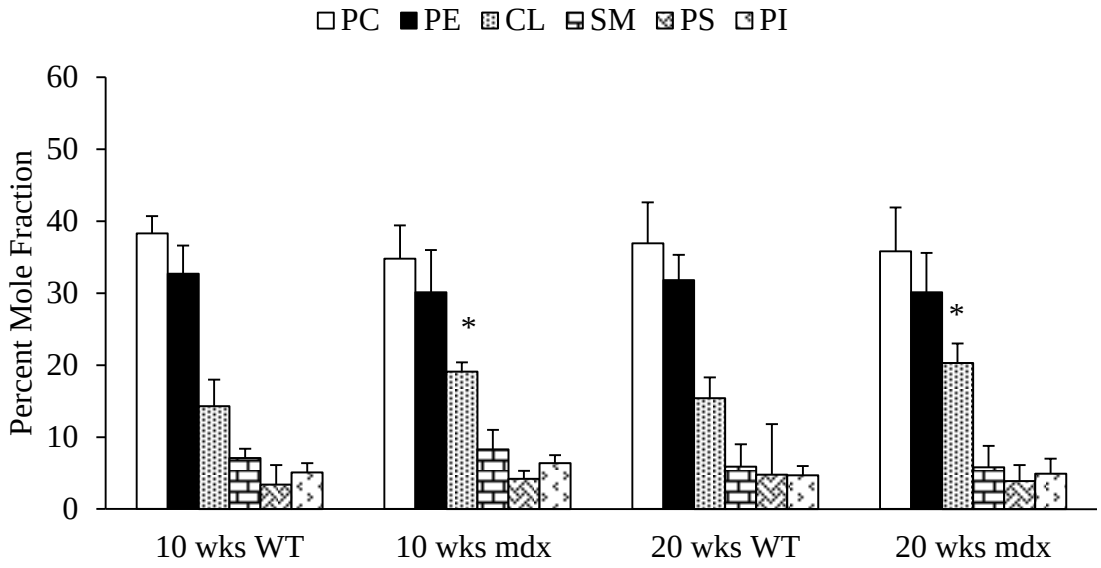

Fig.A.6. Phospholipid species from WT and *mdx* mice SOL in 10 and 20 weeks of age. Values are means ± SEM. * denotes significance from WTs.

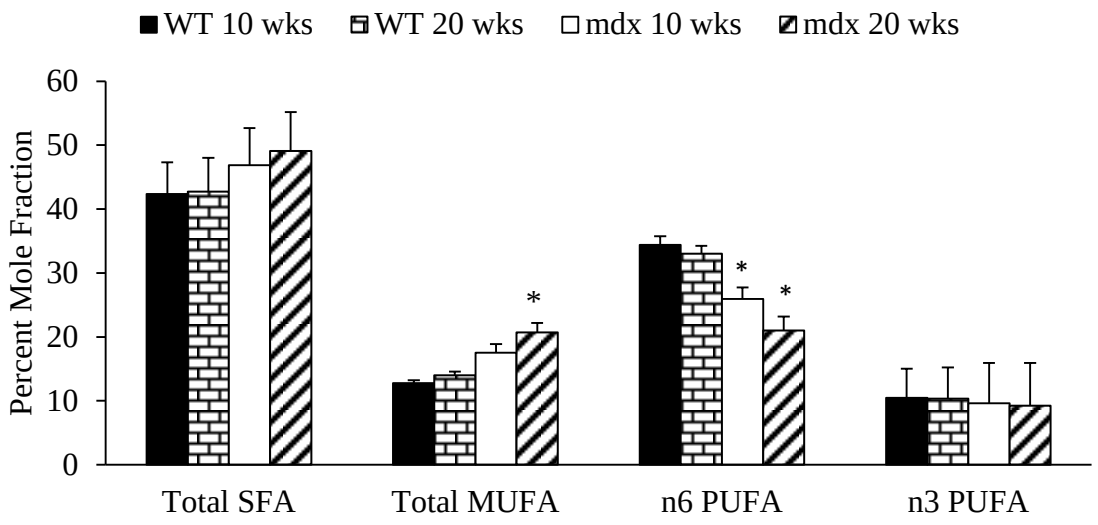

Fig. A.7. Four major fatty acid classes of SOL obtained from 10 and 20 wks old WT and *mdx* mice. Values are mean ± SEM. * denotes significance from WT within same age group.

Table A.1. Percent mole fraction of phosphatidylcholine of extensor digitorum longus muscles from *mdx* and wild type mice at 10 and 20 weeks old.

Fatty	WT		*mdx*	
acid	10 wks	20 wks	10 wks	20 wks
12:0	1.4 ± 0.5	1.4 ± 0.8	1.3 ± 0.8	1.5 ± 0.7
14:0	3.3 ± 1.2	3.3 ± 2.9	1.8 ± 0.7	2.1 ± 0.8
15:0	1.4 ± 0.7	1.3 ± 0.7	1.7 ± 1.0	1.9 ± 0.7
16:0	17.2 ± 2.9	18.6 ± 6.1	18.9 ± 9.3	19.7 ± 10.6
17:0	2.9 ± 1.7	3.9 ± 1.3	3.1 ± 1.1	2.7 ± 1.0
18:0	12.4 ± 3.6	11.6 ± 2.8	21.7 ± 9.6*	23.2 ± 5.6*
20:0	1.7 ± 0.8	2.5 ± 1.2	2.1 ± 1.3	2.3 ± 0.7
22:0	2.7 ± 0.7	2.8 ± 1.5	2.1 ± 1.4	1.9 ± 1.1
23:0	0.9 ± 0.4	1.2 ± 0.8	0.9 ± 0.7	1.1 ± 0.8
15:1	0.5 ± 0.3	0.7 ± 0.3	1.9 ± 0.5	2.3 ± 0.5
16:1	3.1 ± 1.7	3.2 ± 1.4	5.7 ± 2.4	6.9 ± 0.8
17:1	0.8 ± 0.2	1.1 ± 0.4	1.4 ± 0.9	1.7 ± 0.4
18:1	9.2 ± 3.7	10.6 ± 3.2	16.2 ± 5.3*	21.1 ± 8.1*
20:1	1.2 ± 0.4	1.3 ± 0.7	1.2 ± 0.5	1.1 ± 0.4
22:1	nd	nd	1.4 ± 0.7	1.7 ± 0.6
18:3n3	1.1 ± 0.6	1.3 ±0.6	0.9 ± 0.4	1.1 ± 0.4
20:3n3	10.3 ± 3.6	9.2 ± 2.7	7.6 ± 1.3	7.0 ± 1.5
20:5n3	2.1 ± 0.9	1.9 ± 0.8	1.1 ± 0.1	1.1 ± 0.6
22:6n3	4.8 ± 1.2	4.1 ± 1.5	3.9 ± 1.2	4.0 ± 1.3
18:2n6	9.3 ± 1.2	9.2 ± 1.3	3.3 ± 0.5*	2.2 ± 1.3*
18:3n6	1.1 ± 0.3	1.3 ± 0.5	1.1 ± 0.4	0.7 ± 0.4
20:2n6	1.3 ± 0.8	1.1 ± 0.3	0.9 ± 0.6	0.8 ± 0.3
20:3n6	3.3 ± 1.2	3.1 ± 1.5	1.8 ± 1.2	1.6 ± 1.1
20:4n6	7.6 ± 1.2	7.3 ± 3.1	3.1 ± 2.3	1.9 ± 0.6
22:2n6	0.9 ± 0.6	1.2 ± 0.8	nd	nd
Total saturates	47.1 ± 8.3	48.1 ± 6.7	45.2 ± 3.6	38.7 ± 10.2
Total monoenes	16.1 ± 5.2	16.5 ± 1.4	38.9 ± 6.5*	44.9 ± 4.8*
n3 polyenes	13.3 ± 2.9	12.2 ± 2.7	10.2 ± 1.4	7.2 ± 1.7
n6 polyenes	23.5 ± 5.1	23.2 ± 3.2	5.7 ± 3.8*	5.0 ± 1.4*
UI	137 ± 6	131 ± 5	110 ± 7	95 ± 4*†

Values are expressed as means ± SEM, percent mole fractions of fatty acids below 1% across all genotypes and ages are not shown. * denotes significant main effect for genotype; † denotes significant main effect for age; UI, unsaturation index = $\sum m_i \times n_i$ where m_i is the mole percentage and n_i is the number of carbon-carbon double bonds of the fatty acid.

Table A.2. Percent mole fraction of sphingomyelin of extensor digitorum longus muscles from *mdx* and wild type mice at 10 and 20 weeks old.

Fatty	WT		*mdx*	
acid	10 wks	20 wks	10 wks	20 wks
12:0	1.1 ±0.4	1.1 ± 0.4	0.9 ± 0.3	0.7 ± 0.2
14:0	1.9 ±0.7	1.7 ± 0.8	1.6 ± 0.7	1.6 ± 0.5
15:0	2.5 ± 0.9	2.6 ± 0.4	2.3 ± 0.5	2.2 ± 0.6
16:0	18.7 ± 5.6	18.3 ± 3.9	16.9 ± 1.3	16.8 ± 3.4
17:0	3.9 ± 1.0	3.5 ± 1.2	3.1 ± 1.0	2.9 ± 0.4
18:0	13.9 ± 2.5	13.7 ± 9.1	12.9 ± 4.3	12.3 ± 3.9
20:0	2.9 ± 0.8	2.8 ± 5.3	2.6 ± 1.2	2.4 ± 0.7
22:0	8.3 ± 2.4	8.3 ± 3.2	7.9 ±3.5	7.4 ± 2.4
23:0	1.6 ± 0.5	1.3 ± 0.8	1.1 ± 0.4	1.1 ± 0.1
15:1	1.3 ± 0.4	1.5 ± 0.4	2.1 ± 0.8	2.9 ± 0.7
16:1	2.7 ± 0.9	3.1 ± 1.3	4.9 ±1.3	5.6 ± 1.3
17:1	0.7 ± 0.2	1.2 ± 0.4	2.6 ± 0.8	3.7 ± 1.0
18:1	4.1 ± 1.2	4.9 ± 2.1	5.3 ± 1.8	6.7 ± 1.1*
20:1	1.3 ± 0.5	1.5 ± 0.5	2.4 ± 0.7	2.5 ± 0.8
22:1	1.1 ± 0.3	1.3 ± 0.7	1.7 ± 0.5	2.1 ± 0.6
24:1	7.5 ± 3.1	7.8 ± 1.4	12.3 ± 2.9	14.8 ± 2.3
18:3n3	0.9 ± 0.2	0.9 ± 0.1	0.8 ± 0.2	0.7 ± 0.1
20:3n3	1.5 ± 0.6	1.2 ± 0.6	1.0 ± 0.3	0.9 ± 0.3
20:5n3	1.1 ± 0.3	1.0 ± 0.3	nd	nd
22:6n3	5.3 ± 1.2	5.1 ± 2.3	4.7 ± 2.1	4.3 ± 1.7
18:2n6	2.8 ± 2.4	2.6 ± 0.3	2.3 ± 0.8	1.9 ± 0.4
18:3n6	1.2 ± 0.7	1.1 ± 0.5	0.9 ± 0.1	0.7 ±0.3
20:2n6	0.7 ± 0.3	0.7 ± 0.4	nd	nd
20:3n6	2.9 ± 1.1	2.7 ± 1.2	1.9 ± 0.5	1 ± 0.7
20:4n6	1.9 ± 0.2	1.7 ± 0.6	1.4 ±0.9	0.9 ± 0.2
22:2n6	8.6 ± 3.6	8.4 ± 2.5	6.1 ± 3.1	4.1 ± 1.0
Total saturates	54.8 ± 3.6	53.3 ± 9.5	49.3 ± 2.4	47.4 ± 4.1
Total monoenes	18.7 ± 2.5	21.3 ± 4.8	31.3 ± 9.5 *	38.3 ± 5.3 *
n3 polyenes	8.8 ± 1.6	8.2 ± 0.9	6.5 ± 1.2	6.3 ± 0.8
n6 polyenes	18.1 ± 6.4	17.2 ± 4.2	12.9 ± 1.4	8.0 ± 1.3 * †
UI	107 ± 3 *	104 ± 8	95 ± 7	89 ± 6 *

Values are expressed as means ± SEM, percent mole fractions of fatty acids below 1% across all genotypes and ages are not shown. * denotes significant main effect for genotype; † denotes significant main effect for age; WT, wild type; UI, unsaturation index = $\sum m_i \times n_i$ where m_i is the mole percentage and n_i is the number of carbon-carbon double bonds of the fatty acid.

Table A.3. Percent mole fraction of phosphatidylethanolamine of extensor digitorum longus muscles from *mdx* and wild type mice at 10 and 20 weeks old.

Fatty	WT		*mdx*	
acid	10 wks	20 wks	10 wks	20 wks
14:0	1.0 ± 0.2	1.1 ± 0.5	1.2 ± 0.2	0.9 ± 0.4
15:0	1.5 ± 0.4	1.4 ± 0.3	1.3 ± 0.6	2.1 ± 0.8
16:0	0.8 ± 0.2	0.7 ± 0.4	0.9 ± 0.3	1.1 ± 0.6
17:0	9.7 ± 3.2	10.2 ± 3.6	10.7 ± 5.3	11.2 ± 0.5
18:0	1.4 ± 0.4	1.3 ± 0.7	1.8 ± 0.5	1.9 ± 0.4
20:0	18.9 ± 5.2	19.2 ± 6.8	20.1 ± 5.3	20.5 ± 6.2
14:1	1.3 ± 0.4	1.5 ± 0.5	1.4 ± 0.3	2.2 ± 0.5
15:1	1.3 ± 0.5	1.4 ± 0.3	1.2 ± 0.4	1.5 ± 0.6
16:1	4.8 ± 1.1	4.7 ± 1.1	4.5 ± 1.1	4.7 ± 3.4
17:1	0.5 ± 0.2	0.7 ± 0.2	2.6 ± 0.6	3.1 ± 1.9
18:1	1.4 ± 0.4	1.5 ± 0.6	4.5 ± 2.3*	4.7 ± 1.5*
20:1	0.7 ± 0.3	1.1 ± 0.3	1.0 ± 0.2	1.1 ± 0.4
18:3n3	8.2 ± 2.1	8.8 ± 3.6	14.7 ± 4.3	14.8 ± 3.4
20:3n3	1.2 ± 0.9	1.0 ± 0.4	0.8 ± 0.4	1.0 ± 0.4
22:6n3	1.9 ± 0.5	2.1 ± 0.6	1.8 ± 0.5	1.7 ± 0.3
18:2n6	13.5 ± 2.7	11.7 ± 4.9	7.2 ± 3.6 *	5.9 ± 3.1 *†
18:3n6	0.8 ± 0.2	0.9 ± 0.3	1.2 ± 0.4	1.9 ± 0.4
20:3n6	4.6 ± 2.1	4.2 ± 2.2	3.1 ± 1.8	2.2 ± 0.7
Total saturates	1.9 ± 0.4	1.4 ± 0.3	0.5 ± 0.2	0.6 ± 0.2
Total monoenes	40.8 ± 9.8	41.5 ± 11.6	43.1 ± 8.2	46.1 ± 13.1
n3 polyenes	12.1 ± 3.6	13.1 ± 2.9	23.6 ± 6.9	26.6 ± 5.8
n6 polyenes	20.9 ± 12.7	18.3 ± 6.7	12.1 ± 0.5*	10.7 ± 4.1*
UI	172 ± 5	169 ± 9	142 ± 5	131 ± 6

Values are expressed as means ± SEM, percent mole fractions of fatty acids below 1% across all genotypes and ages are not shown. * denotes significant main effect for genotype; † denotes significant main effect for age; WT, wild type; UI, unsaturation index = $\sum m_i \times n_i$ where m_i is the mole percentage and n_i is the number of carbon-carbon double bonds of the fatty acid.

Table A.4. Percent mole fraction of phosphatidylserine of extensor digitorum longus muscles from *mdx* and wild type mice at 10 and 20 weeks old.

Fatty	WT		*mdx*	
acid	10 wks	20 wks	10 wks	20 wks
14:0	1.1 ± 0.5	1.2 ± 0.4	1.1 ± 0.6	1.1 ± 0.4
15:0	1.2 ± 0.8	1.6 ± 0.8	1.4 ± 0.5	1.7 ± 0.8
16:0	1.9 ± 0.8	2.1 ± 0.8	1.6 ± 0.6	1.9 ± 1.0
17:0	15.8 ± 6.5	16.1 ± 6.5	20.9 ± 6.7	14.4 ± 6.4
18:0	23.7 ± 11.2	23.1 ± 11.8	16.5 ± 3.7*	15.8 ± 4.6*
20:0	0.9 ± 0.6	1.3 ± 0.4	1.3 ± 0.8	1.7 ± 0.4
14:1	2.5 ± 1.1	2.7 ± 1.1	2.4 ± 0.7	2.1 ± 0.8
15:1	0.8 ± 0.2	0.9 ± 0.3	1.5 ± 0.8	1.8 ± 0.3
16:1	1.1 ± 0.5	1.3 ± 0.4	1.7 ± 0.4	1.7 ± 0.7
17:1	2.1 ± 0.4	2.4 ± 1.1	7.8 ± 3.4	6.5 ± 1.1
18:1	0.9 ± 0.3	1.7 ± 0.5	3.9 ± 1.2*	4.3 ± 2.1*
20:1	6.3 ± 3.0	6.9 ± 3.4	18.4 ± 9.2	25.3 ± 5.8
18:3n3	3.1 ± 1.2	3.3 ± 1.0	5.6 ± 2.1	4.2 ± 1.9
20:3n3	1.0 ± 0.3	nd	nd	1.1 ± 0.7
20:5n3	1.8 ± 0.5	1.8 ± 0.4	1.3 ± 0.4	1.1 ± 0.4
22:6n3	6.2 ± 3.1	5.8 ± 2.2	4.8 ± 2.2	3.1 ± 1.3
18:2n6	4.4 ± 2.1	3.8 ± 1.3	3.5 ± 1.1	2.4 ± 1.1
18:3n6	9.3 ± 1.5	9.2 ± 3.1	3.3 ± 1.3	2.2 ± 0.6
20:2n6	1.1 ± 0.4	1.3 ± 0.6	1.1 ± 0.6	0.7 ± 0.4
20:3n6	1.3 ± 0.6	1.1 ± 0.5	0.9 ± 0.3	0.8 ± 0.3
20:4n6	7.6 ± 2.3	7.3 ± 2.1	3.1 ± 1.1	1.9 ± 0.8
Total saturates	47.1 ± 11.5	48.1 ± 6.7	45.2 ± 14.0	38.7 ± 12.7
Total monoenes	16.1 ± 3.8	16.5 ± 3.8	38.9 ± 11.3	44.9 ± 11.9
n3 polyenes	13.3 ± 2.4	12.2 ± 4.8	10.2 ± 9.8	7.2 ± 3.1*
n6 polyenes	23.5 ± 3.8	23.2 ± 5.8	5.7 ± 1.8*	5.0 ± 1.5*
UI	137 ± 6	131 ± 5	110 ± 7	95 ± 4*

Values are expressed as means ± SEM, percent mole fractions of fatty acids below 1% across all genotypes and ages are not shown. * denotes significant main effect for genotype; † denotes significant main effect for age; WT, wild type; UI, unsaturation index = $\sum m_i \times n_i$ where m_i is the mole percentage and n_i is the number of carbon-carbon double bonds of the fatty acid.

Table A.5. Percent mole fraction of phosphatidylinositol of extensor digitorum longus muscles from *mdx* and wild type mice at 10 and 20 weeks old.

Fatty	WT		*mdx*	
acid	10 wks	20 wks	10 wks	20 wks
14:0	1.2 ± 0.5	1.1 ± 0.4	0.9 ± 0.4	0.9 ± 0.4
15:0	3.8 ± 1.1	3.7 ± 1.1	3.6 ± 1.2	3.3 ± 1.1
16:0	1.4 ± 0.5	1.4 ± 0.8	1.1 ± 0.3	0.9 ± 0.3
17:0	9.4 ± 3.4	8.9 ± 2.1	7.8 ± 1.5	6.3 ± 2.4
18:0	27.1 ± 11.8	25.4 ± 9.7	23.8 ± 12.0	22.3 ± 6.7
20:0	1.4 ± 0.8	1.3 ± 0.8	1.6 ± 0.7	1.1 ± 0.6
14:1	0.8 ± 0.4	0.7 ± 0.2	0.7 ± 0.3	0.7 ± 0.4
15:1	0.8 ± 0.3	0.6 ± 0.2	0.9 ± 0.3	1.1 ± 0.4
16:1	1.2 ± 0.6	1.3 ± 0.5	1.7 ± 1.0	2.3 ± 1.0
17:1	4.6 ± 1.2	5.5 ± 1.5	8.9 ± 3.7	9.3 ± 3.1
18:1	nd	nd	1.2 ± 0.5	1.7 ± 1.0
20:1	3.5 ± 2.1	4.9 ± 1.3	17.1 ± 9.4	20.1 ± 5.9
18:3n3	0.8 ± 0.4	1.0 ± 0.6	1.6 ± 0.4	2.9 ± 1.4
20:3n3	nd	nd	1.3 ± 0.4	1.5 ± 0.6
20:5n3	1.3 ± 0.4	1.6 ± 0.5	1.2 ± 0.4	0.9 ± 0.4
22:6n3	13.9 ± 6.7	14.1 ± 7.8	10.5 ± 3.1	9.8 ± 3.8
18:2n6	5.3 ± 1.1	4.9 ± 1.8	2.1 ± 0.4	1.9 ± 0.6
18:3n6	10.3 ± 2.3	10.4 ± 3.5	6.3 ±2.1	5.8 ± 1.8
20:2n6	1.3 ± 0.8	1.2 ± 0.4	0.8 ± 0.3	0.9 ± 0.6
20:3n6	4.7 ± 1.8	4.8 ± 2.1	2.4 ± 1.0	2.3 ± 1.8
20:4n6	2.7 ± 1.1	2.8 ± 1.1	0.7 ± 0.3	0.7 ± 0.3
Total saturates	46.8 ± 11.0	43.9 ± 12.8	41.0 ± 16.7	37.2 ± 11.8
Total monoenes	10.9 ± 2.7	13.3 ± 6.3	32.7 ± 6.1*	38.9 ± 8.2*
n3 polyenes	20.5 ± 3.7	20.6 ± 3.4	13.8 ± 8.1	12.1 ± 4.1
n6 polyenes	21.8 ± 5.9	22.2 ± 7.0	12.5 ± 6.4*	11.8 ± 3.0*
UI	139 ±8	142 ±3	108 ± 8*	109 ± 4*

Values are expressed as means ± SEM, percent mole fractions of fatty acids below 1% across all genotypes and ages are not shown. * denotes significant main effect for genotype; † denotes significant main effect for age; WT, wild type; UI, unsaturation index = $\sum m_i \times n_i$ where m_i is the mole percentage and n_i is the number of carbon-carbon double bonds of the fatty acid.

Table A.6. Percent mole fraction of cardiolipin of extensor digitorum longus muscles from *mdx* and wild type mice at 10 and 20 weeks old.

Fatty	WT		*mdx*	
acid	10 wks	20 wks	10 wks	20 wks
16:0	2.8 ± 1.1	4.3 ± 2.1	5.1 ± 2.1	4.6 ± 2.1
18:0	6.1 ± 1.5	6.6 ± 2.8	8.0 ± 3.1	8.3 ± 1.7
16:1	2.1 ± 1.0	2.2 ± 1.0.	7.5 ± 2.2	8.3 ± 2.1
17:1	1.0 ± 0.5	1.3 ± 0.5	1.3 ± 0.8	1.4 ± 0.4
18:1	9.2 ± 3.4	9.8 ± 3.0	18.3 ± 6.2	20.6 ± 11.8
20:1	0.7 ± 0.3	1.3 ± 0.4	3.2 ± 1.1	3.8 ± 1.5
20:3n3	1.1 ± 0.3	1.3 ± 0.5	1.1 ± 0.4	1.6 ± 0.4
22:6n3	3.3 ± 2.1	3.5 ± 1.2	1.2 ± 0.6	1.3 ± 0.5
18:2n6	63.5 ± 9.6	60.4 ± 8.0	41.9 ± 9.3*	37.9 ± 10.7*
20:2n6	2.7 ± 1.3	2.3 ± 1.8	1.8 ± 0.7	1.5 ± 0.8
20:3n6	3.4 ± 1.4	1.0 ± 0.3	0.9 ± 0.5	0.8 ± 0.3
20:4n6	1.3 ± 0.6	1.1 ± 0.7	1.7 ± 0.4	1.4 ± 0.4
Total saturates	9.1 ± 2.1	11.5 ± 3.1	14.1 ± 6.2	14.3 ± 2.0
Total monoenes	13.3 ± 2.4	15.3 ± 4.0	31.7 ± 3.4*	36.2 ± 11.8*
n3 polyenes	4.4 ± 1.2	4.8 ± 3.1	2.3 ± 0.4	2.9 ± 1.0
n6 polyenes	70.9 ± 20.3	64.8 ± 11.5	46.3 ± 11.0*	41.6 ± 12.8*
UI	184 ± 2	173 ± 5	139 ± 1*	135 ± 6*

Values are expressed as means ± SEM, percent mole fractions of fatty acids below 1% across all genotypes and ages are not shown. * denotes significant main effect for genotype; † denotes significant main effect for age; WT, wild type; UI, unsaturation index = $\sum m_i \times n_i$ where m_i is the mole percentage and n_i is the number of carbon-carbon double bonds of the fatty acid.

Table A.7. Percent mole fraction of cardiolipin in soleus muscles from *mdx* and wild type mice at 10 and 20 weeks old.

Fatty	WT		*mdx*	
acid	10 wks	20 wks	10 wks	20 wks
14:0	1.3 ± 0.5	1.4 ± 0.3	1.4 ± 0.4	1.6 ± 0.4
15:0	0.9 ± 0.3	0.9 ± 0.2	1.1 ± 0.4	1.1 ± 0.6
16:0	5.3 ± 1.7	5.5 ± 1.3	5.8 ± 1.8	5.9 ± 0.8
17:0	2.9 ± 0.5	3.2 ± 0.9	3.2 ± 1.1	3.4 ± 1.1
18:0	8.9 ± 3.6	9.1 ± 1.7	10.0 ± 2.6	9.8 ± 1.2
20:0	1.1 ± 0.3	1.4 ± 0.4	1.5 ± 0.4	1.3 ± 0.5
14:1	nd	nd	nd	1.3 ± 0.2
15:1	3.1 ± 0.2	2.7 ± 1.0	2.8 ± 0.4	3.4 ± 1.3
16:1	0.9 ± 0.1	1.3 ± 0.5	1.4 ± 0.3	1.8 ± 0.4
17:1	2.9 ± 0.4	3.1 ± 0.9	3.2 ± 1.9	3.2 ± 1.4
18:1	4.8 ± 1.6	5.1 ± 1.5	5.6 ± 2.1	5.9 ± 2.3
20:1	1.2 ± 0.4	1.1 ± 0.5	0.9 ± 0.3	1.0 ± 0.3
18:3n3	1.9 ± 0.4	1.6 ± 0.9	1.4 ± 0.9	1.5 ± 0.5
20:3n3	4.3 ± 1.7	4.2 ± 1.8	3.9 ± 1.5	3.8 ± 1.2
20:5n3	1.8 ± 0.9	1.8 ± 0.7	1.9 ± 0.6	1.4 ± 0.5
22:6n3	3.2 ± 1.6	3.3 ± 1.2	3.1 ± 0.9	3.2 ± 1.4
18:2n6	43.7 ± 9.7	43.1 ± 12.1	42.9 ± 8.7	39.8 ± 5.8
18:3n6	4.5 ± 2.3	4.3 ± 3.1	4.0 ± 1.3	3.8 ± 1.1
20:2n6	1.9 ± 0.9	1.7 ± 0.9	0.8 ± 0.3	0.7 ± 0.2
20:3n6	2.7 ± 0.9	2.8 ± 0.8	2.4 ± 0.7	2.5 ± 1.1
20:4n6	1.2 ± 0.4	1.0 ± 0.5	1.1 ± 0.6	1.0 ± 0.2
Total saturates	21.1 ± 5.4	22.1 ± 4.7	23.8 ± 2.9	24.1 ± 2.7
Total monoenes	12.9 ± 2.1	13.3 ± 3.2	13.9 ± 1.7	17.4 ± 4.0 *†
n3 polyenes	11.2 ± 4.5	10.9 ± 3.0	10.3 ± 1.7	9.9 ± 2.7
n6 polyenes	54.8 ± 3.2	53.7 ± 12.1	52.0 ± 4.9	48.6 ± 11.7 *
UI	178 ± 7	176 ± 4	170 ± 5	165 ± 7

Values are expressed as means ± SEM, percent mole fractions of fatty acids below 1% across all genotypes and ages are not shown. * denotes significant main effect for genotype; † denotes significant main effect for age. WT, wild type; UI, unsaturation index = $\sum mi \times ni$ where mi is the mole percentage and ni is the number of carbon-carbon double bonds of the fatty acid.

Table A.8. Percent mole fraction of sphingomyelin in soleus muscles from *mdx* and wild type mice at 10 and 20 weeks old.

Fatty	WT		*mdx*	
acid	10 wks	20 wks	10 wks	20 wks
12:0	1.6 ± 0.5	1.9 ± 0.4	2.1 ± 0.8	2.4 ± 1.1
14:0	1.1 ± 0.6	1.5 ± 0.6	1.9 ± 0.6	2.1 ± 0.9
15:0	2.8 ± 1.1	3.2 ± 1.1	3.7 ± 2.4	4.2 ± 2.1
16:0	10.5 ± 2.5	11.8 ± 2.5	12.5 ± 3.4	13.8 ± 3.8
17:0	3.7 ± 1.1	4.1 ± 1.2	4.0 ± 1.5	3.6 ± 1.7
18:0	23.6 3.1	23.8 ± 6.5	26.7 ± 3.7	26.9 ± 9.2
20:0	1.6 ± 0.8	1.9 ± 0.4	2.3 ± 0.8	3.1 ± 0.8
22:0	2.2 ± 1.1	2.0 ± 0.6	2.7 ± 1.1	2.9 ± 1.1
23:0	1.8 ± 0.9	1.6 ± 0.5	1.6 ± 0.8	1.7 ± 0.8
14:1	0.9 ± 0.2	1.6 ± 0.8	1.6 ± 0.5	2.1 ± 1.4
15:1	0.6 ± 0.3	1.2 ± 0.6	1.3 ± 0.4	1.3 ± 0.8
16:1	1.7 ± 0.6	1.6 ± 0.8	2.1 ± 0.7	2.7 ± 1.0
17:1	0.8 ± 0.4	1.0 ± 0.4	1.3 ± 0.8	1.3 ± 0.8
18:1	3.6 ± 1.1	3.7 ± 1.1	5.1 ± 2.2	5.6 ± 2.8
20:1	1.1 ± 0.6	1.3 ± 0.6	1.6 ± 0.7	1.9 ± 0.8
24:1	2.9 ± 1.1	2.6 ± 1.0	2.9 ± 1.0	3.5 ± 1.8
18:3n3	1.7 ± 0.8	1.8 ± 0.6	1.9 ± 0.7	1.3 ± 0.9
20:3n3	3.5 ± 2.1	3.4 ± 1.0	2.3 ± 1.1	2.1 ± 1.0
20:5n3	nd	nd	nd	nd
22:6n3	5.7 ± 2.1	4.9 ± 1.5	4.7 ± 1.4	4.2 ± 1.8
18:2n6	11.3 ± 3.1	11.6 ± 3.0	9.8 ± 3.4	6.8 ± 2.2
18:3n6	5.7 ± 2.2	5.1 ± 1.5	3.2 ± 1.4	2.7 ± 1.1
20:2n6	2.3 ± 1.0	2.0 ± 0.7	1.3 ± 0.8	1.0 ± 0.8
20:3n6	4.9 ±1.0	3.6 ± 0.9	2.7 ± 0.7	`2.1 ± 0.8
20:4n6	1.8 ± 0.8	1.2 ± 0.7	nd	nd
22:2n6	1.7 ± 0.6	1.6 ± 0.8	nd	nd
Total saturates	48.9 ± 11.0	51.8 ± 11.7	57.6 ± 4.7	60.7 ± 11.7
Total monoenes	11.6 ± 6.8	13.0 ± 2.8	16.5 ± 3.8*	19.1 ± 9.7*
n3 polyenes	10.9 ± 5.2	10.1 ± 3.7	8.9 ± 1.7	7.6 ± 3.1
n6 polyenes	28.6 ± 9.0	25.1 ± 6.5	17.0 ± 6.4*	12.6 ± 3.4*
UI	131 ± 7	119 ±3	97 ± 2*	84 ± 5*†

Values are expressed as means ± SEM, percent mole fractions of fatty acids below 1% across all genotypes and ages are not shown. * denotes significant main effect for genotype; † denotes significant main effect for age; WT, wild type; UI, unsaturation index = $\sum m_i \times n_i$ where m_i is the mole percentage and n_i is the number of carbon-carbon double bonds of the fatty acid.

Table A.9. Percent mole fraction of phosphatidylethanolamine in soleus muscles from *mdx* and wild type mice at 10 and 20 weeks old.

Fatty	WT		*mdx*	
acid	10 wks	20 wks	10 wks	20 wks
12:0	0.9 ± 0.3	1.1 ± 0.3	0.7 ± 0.3	1.7 ± 0.4
14:0	1.1 ± 0.6	1.7 ± 0.4	1.6 ± 0.5	3.0 ± 0.9
15:0	2.3 ± 1.1	1.3 ± 0.5	0.9 ± 0.4	2.2 ± 0.7
16:0	12.3 ± 6.2	11.9 ± 4.0	14.3 ± 3.8	14.9 ± 2.8
17:0	2.3 ± 1.2	2.9 ± 0.5	2.0 ± 0.8	1.5 ± 0.7
18:0	19.9 ± 6.8	18.6 ± 6.1	18.9 ± 5.7	20.8 ± 6.8
20:0	2.3 ± 0.6	1.7 ± 0.4	0.9 ± 0.3	0.6 ± 0.3
22:0	1.3 ± 0.9	0.8 ± 0.3	1.0 ± 0.4	nd
23:0	0.8 ± 0.4	0.8 ± 0.2	0.9 ± 0.3	0.5 ± 0.3
14:1	1.1± 0.3	0.9 ± 0.4	1.0 ± 0.2	1.3 ± 0.6
15:1	0.9 ± 0.2	1.1 ± 0.5	1.3 ± 0.4	0.9 ± 0.4
16:1	2.1 ± 0.8	2.3 ± 0.9	2.6 ± 1.1	3.1 ± 1.9
17:1	0.7 ± 0.3	0.7 ± 0.4	0.9 ± 0.5	1.2 ± 0.8
18:1	5.3 ± 1.7	5.9 ± 2.5	9.3 ± 2.0*	9.1 ± 2.4*
20:1	1.3 ± 0.2	1.0 ± 0.4	1.0 ± 0.4	1.1 ± 0.4
24:1	0.6 ± 0.2	0.9 ± 0.2	1.1 ± 0.5	1.0 ± 0.3
18:3n3	1.2 ± 0.5	1.1 ± 0.5	0.9 ± 0.2	0.9 ± 0.4
20:3n3	2.3 ± 1.4	2.1 ± 0.8	0.8 ± 0.3	0.9 ± 0.3
20:5n3	0.9 ± 0.6	0.8 ± 0.3	1.1 ± 0.5	1.2 ± 0.5
22:6n3	8.3 ± 2.1	7.8 ± 2.5	7.9 ± 1.2	8.2 ± 2.8
18:2n6	24.6 ± 10.1	25.9 ± 6.3	23.1 ± 6.1	20.3 ± 9.7
18:3n6	2.3 ± 0.5	3.2 ± 1.1	2.9 ± 1.1	2.1 ± 1.0
20:2n6	3.5 ± 2.0	1.2 ± 0.7	1.3 ± 0.7	1.0 ± 0.4
20:3n6	1.9 ± 0.6	1.2 ± 0.9	1.1 ± 0.4	0.8 ± 0.3
20:4n6	3.1 ± 1.2	1.9 ± 0.5	1.8 ± 0.5	1.1 ± 0.4
22:2n6	43.2 ± 6.9	40.8 ± 13.5	41.2 ± 11.2	45.2 ± 9.7
Total saturates	43.2 ± 6.9	40.8 ± 13.5	41.2 ± 11.2	45.2 ± 9.7
Total monoenes	12.8 ± 3.7	13.7 ± 6.4	17.9 ± 8.4	18.3 ± 6.5
n3 polyenes	12.7 ± 4.3	11.8 ± 3.4	10.7 ± 3.4	11.2 ± 5.6
n6 polyenes	31.3 ± 7.1	33.8 ± 9.7	30.2 ± 10.0	25.3 ± 9.8*
UI	152 ± 6	145 ± 3	140 ± 4	132 ± 4*

Values are expressed as means ± SEM, percent mole fractions of fatty acids below 1% across all genotypes and ages are not shown. * denotes significant main effect for genotype; † denotes significant main effect for age; WT, wild type; UI, unsaturation index = $\sum m_i \times n_i$ where m_i is the mole percentage and n_i is the number of carbon-carbon double bonds of the fatty acid.

Table A.10. Percent mole fraction of phosphatidylcholine in soleus muscles from *mdx* and wild type mice at 10 and 20 weeks old.

Fatty	WT		*mdx*	
acid	10 wks	20 wks	10 wks	20 wks
12:0	1.3 ± 0.2	1.2 ± 0.7	1.9 ± 0.8	2.1 ± 0.5
14:0	1.6 ± 0.4	1.9 ± 1.2	2.3 ± 1.1	2.4 ± 1.1
15:0	0.8 ± 0.3	0.7 ± 0.3	1.3 ± 0.5	1.5 ± 0.6
16:0	20.3 ± 5.6	19.3 ± 6.8	21.3 ± 9.8	22.3 ± 11.0
17:0	2.3 ± 1.2	1.9 ± 0.5	2.8 ± 1.1	2.1 ± 0.5
18:0	11.8 ± 3.8	10.7 ± 5.1	14.9 ± 6.5	15.7 ± 4.9
20:0	0.8 ± 0.2	0.8 ± 0.3	1.3 ± 0.7	1.9 ± 0.8
23:0	1.3 ± 0.8	1.1 ± 0.8	1.4 ± 0.7	1.5 ± 0.4
14:1	0.7 ±0.4	1.1 ± 0.6	1.2 ± 0.3	1.3 ± 0.7
16:1	5.7 ± 2.1	6.1 ± 2.1	7.1 ± 2.9	7.2 ± 5.1
17:1	1.1 ± 0.4	1.2 ± 0.5	2.6 ± 0.4	2.5 ± 1.1
18:1	2.3 ± 1.1	2.6 ± 2.5	9.3 ± 2.9*	10.2 ± 6.9*
20:1	1.5 ± 0.5	1.8 ± 0.4	1.9 ± 0.7	2.1 ± 0.9
18:3n3	0.6 ± 0.3	0.7 ± 0.3	0.9 ± 0.6	1.1 ± 0.5
20:3n3	8.3 ± 2.1	8.4 ± 4.6	9.1 ± 4.0	10.7 ± 3.9
22:6n3	4.8 ± 2.1	4.7 ± 2.0	5.5 ± 3.4	5.9 ± 3.5
18:2n6	24.7 ± 12.1	24.9 ± 6.7	9.1 ± 5.3	5.3 ± 2.2
18:3n6	3.6 ± 1.8	3.9 ± 1.2	1.1 ± 0.4	0.8 ± 0.4
20:2n6	1.1 ± 0.6	1.6 ± 0.7	0.9 ± 0.6	0.7 ± 0.3
20:3n6	3.5 ± 1.1	3.5 ± 1.8	1.8 ± 0.4	1.2 ± 0.7
22:2n6	3.6 ± 1.8	3.9 ± 1.2	1.1 ± 0.4	0.8 ± 0.4
Total saturates	40.9 ± 9.8	38.2 ± 13.8	47.8 ± 14.9	50.2 ± 22.3
Total monoenes	11.8 ± 5.1	13.5 ± 5.7	23 ± 8.5*	24.2 ± 6.8*
n3 polyenes	14.4 ± 6.1	14.4 ± 6.0	16.3 ± 3.8	17.6 ± 8.5
n6 polyenes	32.9 ± 7.9	33.9 ± 10.5	12.9 ± 4.2*	8 ± 2.2*†
UI	143 ± 7	147 ± 2	118 ± 7*	117 ±5*

Values are expressed as means ± SEM, percent mole fractions of fatty acids below 1% across all genotypes and ages are not shown. * denotes significant main effect for genotype; † denotes significant main effect for age; WT, wild type; UI, unsaturation index = $\sum m_i \times n_i$ where m_i is the mole percentage and n_i is the number of carbon-carbon double bonds of the fatty acid.

Table A.11. Percent mole fraction of phosphatidylinositol in soleus muscles from *mdx* and wild type mice at 10 and 20 weeks old.

Fatty	WT		*mdx*	
acid	10 wks	20 wks	10 wks	20 wks
12:0	1.9 ± 0.2	1.3 ± 0.5	2.3 ± 0.5	2.4 ± 1.1
14:0	2.6 ± 1.1	2.8 ± 0.8	3.6 ± 0.9	3.3 ± 2.0
15:0	1.7 ± 0.5	1.6 ± 0.7	1.4 ± 0.4	1.6 ± 0.4
16:0	12.1 ± 5.6	13.3 ± 5.1	14.9 ± 3.7	15.9 ± 6.8
17:0	4.9 ± 3.0	3.5 ± 2.3	3.7 ± 2.4	4.1 ± 2.7
18:0	24.6 ± 12.8	28.8 ± 9.2	29.3 ± 6.2	31.2 ± 10.2
22:0	nd	0.8 ± 0.4	1.2 ± 0.5	1.5 ± 0.6
23:0	0.9 ± 0.3	1.3 ± 0.8	1.8 ± 0.5	nd
14:1	1.3 ± 0.5	1.1 ± 0.3	1.3 ± 0.6	2.4 ± 0.6
15:1	1.6 ± 0.8	1.7 ± 0.4	1.5 ± 0.4	1.6 ± 0.4
16:1	2.0 ± 0.5	2.3 ± 0.9	2.5 ±1.1	3.6 ± 1.8
17:1	1.4 ± 0.4	1.7 ± 0.8	2.1 ± 0.9	4.2 ± 2.4
18:1	4.3 ± 2.2	4.9 ± 2.2	5.3 ± 2.8	6.8 ± 3.7
20:1	0.8 ± 0.6	1.3 ± 0.9	1.2 ± 0.4	1.7 ± 0.4
24:1	nd	0.6 ± 0.2	0.9 ± 0.6	1.3 ± 0.6
18:3n3	2.9 ± 1.1	3.0 ± 1.3	3.4 ± 1.7	3.9 ± 1.1
20:3n3	1.2 ± 0.5	1.2 ± 0.5	0.9 ± 0.4	0.6 ± 0.3
20:5n3	1.9 ± 1.0	1.4 ± 0.4	1.5 ± 0.8	1.3 ± 0.9
22:6n3	0.8 ± 0.3	1.3 ± 0.6	1 ± 0.4	0.8 ± 0.4
18:2n6	9.4 ± 3.5	6.3 ± 2.4	4.1 ± 1.7*	3.6 ± 1.6*
18:3n6	4.3 ± 2.7	3.6 ± 1.2	2.9 ± 2.4	2.3 ± 1.1
20:2n6	1.3 ± 0.4	1.1 ± 0.8	1.6 ± 0.8	1.1 ± 0.5
20:3n6	6.3 ± 2.6	4.9 ± 2.5	3.8 ± 0.3	0.6 ± 0.2
20:4n6	3.7 ± 2.9	3.9 ± 1.3	3.4 ± 2.2	1.6 ± 0.5
22:2n6	4.8 ± 2.0	4.1 ± 2.4	3.1 ± 0.4	1.5 ± 0.5
Total saturates	49.4 ± 14.0	53.4 ± 14.0	58.2 ± 17.2	60.0 ± 11.5
Total monoenes	14.3 ± 6.7	16.6 ± 5.7	18.2 ± 6.3	25.5 ± 3.9*
n3 polyenes	6.5 ± 2.7	6.1 ± 2.3	4.7 ± 1.8	3.8 ± 1.5
n6 polyenes	29.8 ± 9.4	23.9 ± 10.7	18.9 ± 6.0*	10.7 ± 5.1*
UI	120 ± 8	108 ±2	89 ±58	69 ± 3*†

Values are expressed as means ± SEM, percent mole fractions of fatty acids below 1% across all genotypes and ages are not shown. * denotes significant main effect for genotype; † denotes significant main effect for age; WT, wild type; UI, unsaturation index = $\sum m_i \times n_i$ where m_i is the mole percentage and n_i is the number of carbon-carbon double bonds of the fatty acid.

Table A.12. Percent mole fraction of phosphatidylserine in soleus muscles from *mdx* and wild type mice at 10 and 20 weeks old.

Fatty	WT		*mdx*	
acid	10 wks	20 wks	10 wks	20 wks
12:0	1.7 ± 0.5	1.6 ± 0.5	1.5 ± 0.5	1.7 ± 0.5
14:0	1.6 ± 0.4	1.5 ± 0.6	1.7 ± 0.9	2.1 ± 0.5
15:0	0.9 ± 0.6	1.2 ± 0.4	1.4 ± 0.5	1.5 ± 0.4
16:0	6.3 ± 2.5	6.2 ± 3.2	6.7 ± 3.4	6.9 ± 2.3
17:0	3.4 ± 0.7	3.2 ± 1.1	3.5 ± 1.1	3.4 ± 1.1
18:0	30.1 ± 11.2	29.7 ± 13.2	30.5 ± 12.6	32.8 ± 11.3
20:0	1.4 ± 0.4	1.5 ± 0.7	1.8 ± 0.6	0.9 ± 0.4
22:0	0.9 ± 0.3	0.8 ± 0.3	0.9 ± 0.3	1.2 ± 0.5
23:0	4.3 ± 2.2	4.4 ± 2.1	4.7 ± 1.2	3.8 ± 1.1
14:1	2.1 ± 0.4	1.9 ± 0.7	2.1 ± 0.9	2.3 ± 0.8
16:1	1.7 ± 0.3	1.5 ± 0.4	1.8 ± 0.7	2.5 ± 1.3
18:1	6.6 ± 2.2	7.1 ± 3.4	8.1 ± 1.4	10.7 ± 6.8*
24:1	0.8 ± 0.4	0.7 ± 0.4	0.9 ± 0.3	1.2 ± 0.4
18:3n3	1.4 ± 0.8	1.8 ± 0.7	1.8 ± 1.0	2.2 ± 1.0
20:3n3	0.6 ± 0.2	0.8 ± 0.3	0.6 ± 0.4	0.7 ± 0.3
20:5n3	3.2 ± 1.1	3.4 ± 1.4	2.9 ± 1.2	2.1 ± 1.1
18:2n6	7.4 ± 2.2	7.1 ± 3.2	6.9 ± 2.4	6.4 ± 1.8
18:3n6	6.5 ± 3.1	6.6 ± 3.0	5.2 ± 2.0	4.9 ± 2.4
20:2n6	1.8 ± 0.8	1.7 ± 0.6	2.1 ± 1.2	1.8 ± 1.0
20:3n6	7.9 ± 2.1	7.6 ± 2.4	6.5 ± 3.4	5.4 ± 3.2
20:4n6	3.9 ± 2.4	3.5 ± 1.6	2.9 ± 1.1	1.7 ± 0.8
22:2n6	1.5 ± 0.4	1.1 ± 0.3	1.2 ± 0.8	0.6 ± 0.2
Total saturates	50.6 ± 11.1	50.1 ± 12.5	52.7 ± 9.7	54.3 ± 11.7
Total monoenes	13.2 ± 6.8	13.8 ± 6.4	15.6 ± 3.4	19.6 ± 6.8*
n3 polyenes	7.2 ± 2.4	8.5 ± 2.7	6.9 ± 1.9	5.3 ± 1.8
n6 polyenes	29.0 ± 12.5	27.6 ± 8.2	24.8 ± 11.08	20.8 ± 7.5
UI	124 ± 7	127 ± 9	112 ±9	97 ± 7*

Values are expressed as means ± SEM, percent mole fractions of fatty acids below 1% across all genotypes and ages are not shown. * denotes significant main effect for genotype; † denotes significant main effect for age; WT, wild type; UI, unsaturation index = $\sum m_i \times n_i$ where m_i is the mole percentage and n_i is the number of carbon-carbon double bonds of the fatty acid.

APPENDIX B

Laboratory procedures

Part I: Stretch injury

Functional testing of mouse skeletal muscles requires a minimum of four components: a force transducer to monitor force production, a stimulator and electrodes to excite the muscle, a bath to superfuse the muscle with oxygenated Ringer's solution, and a device to record force production. The system used at Brock University included the Aurora Scientific (Aurora, ON) that has been optimized for monitoring function in small tissues. Force transducer for isometric and lengthening contractions was a dual Mode (Force/Position) Servomotor that was able to control muscle length. The stimulator was an internal stimulator provided by Data Acquisition Controller hardware to deliver square wave (0.2 ms) electrical pulses.

After muscle dissections, the excised muscle was placed immediately into oxygenated Ringer solution (maintained at 25 $^{\circ}$C) and equilibrated for 5-10 min. silk suture was tied to the proximal and distal tendons during dissection and used as anchors to maintain resting length in the dish.

Solution:

NaCl (120mM), KCl (5 mM), $CaCl_2$ (2mM), KH_2PO_4 (1mM), $MgSO_4$ (1mM), Glucose (5mM), pH (7.3)

EDL stretch injury:

1- Attach muscle to apparatus (one end of the muscle is tied to the lever arm of the position feedback servomotor and tie the other end of the muscle to a force transducer).

2- Establish optimum length (L_0).

3- Subject the muscle to another series of isomeric and tetanic twitch 3 min apart.

4- Control measurement of P_0 and $P_{t:}$ Stimulate the muscle at 150 Hz for 0.5 ms to establish the control P_t. To minimize muscle fatigue rest the muscles for 3 min, then stimulate at 150 Hz for 500 ms to establish control P_o.

5- Stimulated the muscle at 80 Hz for 700 ms. During the first 500 ms, contraction is isometric at L_0, whereas during the final 200 ms the muscle stretch the muscle at 0.5 L_0/s to yield a total displacement of 0.1 L_0.

6- Repeat the stretch for total 5 times with intervals of 4 min rest.

7- Immediately after the final stretch measure the twitch and tetani tensions. Re-measure in 15 min to minimize muscle fatigue.

SOL stretch injury:

1- Mount muscle to apparatus (one end of the muscle is tied to the lever arm of the position feedback servomotor and tie the other end of the muscle to a force transducer).

2- Establish optimum length ($L_{o)}$.

3- Subject the muscle to another series of isomeric and tetanic twitch 3 min apart.

4- Control measurement of P_t and $P_{0:}$ Stimulate the muscle at 150 Hz for 0.5 ms to establish the control P_t. To minimize muscle fatigue rest the muscles for 3 min, then stimulate at 150 Hz for 500 ms to establish control P_0.

5- Immediately after the isometric tetanus adjust the muscle length from L_o to 0.9 L_0, and have the muscle rest for 4 min.

8- For eccentric contraction stretch the muscle from 0.9 L_o to 1.1 L_o with the velocity of 1.5 L_0/S.

9- Immediately stretching the muscle from 0.9 L_0 to 1.1 L_0 with the velocity of 1.5 L_0/S @ 125 Hz.

10- Repeat the eccentric contractions for total of 10 times, after each 4 min of rest.

11- After the last stretch measure post Stretch P_t and P_0. Re-measure after 15 min of rest.

Part II: Membrane lipid analysis from whole muscle

Solution:

Tris HCl buffer, pH: 8

Lipid Extraction (Bligh & Dyer, 1959)

1- Put at least 5 mg of whole muscle in 1voulme of buffer.

2- Use eppendorf plunger to homogenize the muscle in the tubes.

3- Transfer the homogenized muscle into kimex tubes

4- Add 3.75 ml of Chloroform:Methanol (1:2) with 0.1% BHT and vortex well for 2 min.

5- Add 1.25 ml of chloroform and vortex for 10 seconds.

6- Add 1.25 ml of double distilled water and vortex until white colour change (~2 sec).

7- Centrifuge at 2000 RPM for 6 min.

8- Collect the chloroform phase (bottom phase) carefully, not collecting any of the aqueous layer.

9- Either freeze at - 20 or prepare for solid phase extraction.

Thin Layer Chromatography (Mahadevappa and Holub, 1987)

Solutions:

DCF Solution (for 4 L):

1) To 4 L methanol:water (1:1), add about 2g (saturating) 2',7'-dichloroflourescein.

2) Stir for about 7-8 hours in fume hood or covered (parafilm).

3) Filter out precipitate.

4) Wash filtrate with petroleum ether (about 500mL) in separatory funnel.

5) Remove lower phase (DCF) and store in dark bottle.

6% H_2SO_4:

1) For 100 mL use 94 mL methanol, cool on ice.

2) Carefully drip 6 mLs H_2SO_4 into methanol slowly (use a large beaker and drip the H_2SO_4 down the sides of the beaker).

TLC Procedure:

1- Using clean pointed object (e.g. pipette tip), press chromatography paper into corners of tank.

2- Make up solvent system with Chloroform: methanol: acetic acid: water (100: 75: 7: 4 mL)

3- Pour into bottom of tank, cover and let sit ~ ½ hour.

4- Transfer 2 mL sample into mini vial and dry down under N2.

5- Add 200 µL C:M (2:1) w/ BHT (50µg/ml), vortex, transfer into GC vial and dry down under N2.

6- Add 100 µL C:M (2:1) w/ BHT (50µg/ml), vortex and dry down under liquid N2.

7- In a fume hood, using template, mark off 4 lanes (4 divisions wide) on plate. Leave a lane (2 divisions wide) on each side and one at the top (1 division wide) to stop solvent.

8- Resuspend sample in 15 µL of C:M (2:1).

9- Spot the 15 µL sample onto plate using microsyringe.

10- Add an additional 15 µL of C:M (2:1) to sample vial, vortex, spot over sample.

11- Rinse syringe x5 in C:M (2:1) after each sample.

12- For blank, spot 15 µL C:M (2:1).

13- For STD, spot 10 µL C:M (2:1).

14- Place plate in chamber (leaning against back) with silica side up.

15- Takes about 2 2/1 hours to run (solvent should reach top).

16- Remove plate from tank and let dry in fume hood for several minutes.

17- Set plate in spraying chamber.

18- Spray evenly with DCF solution.

19- Set plate in chamber containing 25% ammonium hydroxide, for about 5 minutes.

20- View plate under UV light: Band separation expected:

Solvent front: *CL PE PI PS PC SM Origin*

21- Use pencil to mark bands.

22- Remove excess silica with razor blades (rinse with C:M between uses).

23- Scrape each band into a kimex tube.

Methylation – Fatty Acid Methyl Esters

Methylation of fatty acids is a crucial step before gas chromatography. Without prior methylation the fatty acids are not volatile substances, and thus will not enter gaseous state easily (which is imperative for gas chromatography). By the addition of the methyl group with an ester linkage the fatty acids are easily put into gaseous state, when heated at high temperatures.

1- To each kimex tube with silica scrapings, add 2mL of 6% H_2SO_4 in methanol.
2- As accurately as possible, add 10uL of 13:0 (External Standard; 1mg/mL hexane) then rinse syringe in hexane.
3- Close tightly, and incubate for 2hrs at 80°C.
4- Cool for 10 min, then break seal.
5- Add 1mL DDW.
6- Add 2mL petroleum ether, then vortex.
7- Centrifuge for 6min at 2000 RPM.
8- Extract petroleum ether phase (top) into mini vial.
9- Seal cap with parafilm and store at -20°C for future Gas chromatography analysis.

Gas Chromatography

Gas chromatography includes a stationary phase and a mobile phase. The stationary phase is via a column packed with diamataceous earth and the mobile phase is helium gas. When the fatty acid methyl esters enter into gaseous state (depending on what temperature is needed for them to do this), they will be dissolved into the helium gas. Depending on size of the fatty acid and stability into gaseous state, they may be held by the solid phase, whereby they must wait for higher temperatures to enter into gaseous

state. Then a flame ionizing detector, will blow up the fatty acids into ions that is read by the detector, and we are then left with peaks, where the concentration is related to the area under the curve.

1- Transfer FAMEs to GC vials.
2- Dry down under gaseous nitrogen.
3- Reconstitute in 10uL of hexane or dichloromethane.
4- Seal cap very well (otherwise the samples will evaporate). Use 1ul injection method.
5- Calibrate the standard. This calibration involves having the 13:0 matching the 13:0 of the samples in terms of retention time.
6- Inject only 1 ul of FAME mix (or any volume to make sure that the peak heights will be as close to the heights of the sample peak heights).

Part III: Embedding of muscle

1- After dissection, the muscles (e.g. EDL and SOL) are mounted on a small mound of cryomatrix that is placed on a cork disc.
2- Ensure that the muscles are totally covered by the cryomatrix (Use the minimum amount of cryomatrix possible to cover the muscles, thus allowing rapid freezing to occur).
3- Place a cold-resistant beaker of isopentane into liquid nitrogen and allow cooling to -150°C (When the correct temperature is attained “sludge” will appear in the bottom of the isopentane).
4- Freeze the embedded muscle by placing it into the cooled isopentane for 20-40 seconds (longer contact times can result in the formation of cracks in the samples; insufficient time can result in freezing artifacts).

5- Cover the embedded muscle in aluminium foil.

6- For short-term or long-term storage keep the samples in -20°C or -80°C freezer, respectively.

Cryosectioning

1- To achieve a thermal equilibration before cryosectioning, store the samples overnight in the -20°C freezer and place them into the cryostat for at least 20 minutes before further processing.

2- Mount the sample on the round metallic mount of the cryostat with cryomatrix. The knife should be pre-cooled to -20°C and the muscle sample to -22°C.

3- Make 12, 10 and 5 µm-thick sections for fibre typing, masson trichorom staining and immunohistochemistry and collect them on warm (RT) Superfrost colorfrost Plus slides.

4- Let the sections dry at RT for 1hr and then store the unstained slides at -20°C or -80°C for short term and long term storage, respectively.

Part IV: Masson trichorom staining (Meinen *et al.*, 2007)

Weigert's iron hematoxylin stains the nuclei in black, Biebrich scarlet-acid fuchsin stains cytoplasm & muscle fibres in red and after treatment with phosphotungstic and phosphomolybdic acid, collagen is stained in blue with aniline blue.

Staining procedure:

1- Preparation: Bring the slides to room temperature

2- For 1° Fixation fix the cryosections in 10% Formalin at RT for 1hr in the fume hood.

3- For 2° Fixation re-fix sections in Bouin's solution at RT overnight to intensify the colors and increase the contrast between the tissue components.

4- Wash slides for 1-2 minutes under running tap water (18–26°C) to remove yellow color from sections. Then rinse briefly in DDW.

5- Weigert's Hematoxilin Staining: Mix equal parts of Hematoxylin Solution A and Solution B (stable for 10 days). Incubate the sections for 5 minutes with Weigert's Iron Hematoxylin Solution to stain the nuclei dark. Discard the Hematoxilin solution.

6- Blueing: Put the slides in a glass chamber and wash under warm running tap water for ~10 minutes to remove excess of Hematoxylin and to intensify the black color. Rinse 1 minute in DDW.

7- Cytoplasm Staining: Incubate the sections for 5 minutes with Biebrich Scarlet-Acid Fuchsin Solution to stain the fibres red. Discard the Solution.

8- Washing: Wash 3x 1minute with DDW.

9- Collagen Staining: To prepare the uptake of the aniline blue stain, incubate the sections with Phosphotungstic/Phosphomolybdic Acid Solution for 3-4x 3minutes. For preparation of Phosphotungstic/Phosphomolybdic Acid Solution (Discard after use) add 1 volume of Phosphotungstic Acid Solution, 1 volume Phosphomolybdic Acid Solution, 2 volumes DDW.

10- After incubation, drain the slides on a tissue before proceeding and directly (without rinsing) incubate the slides for 5 minutes with the Aniline Blue Solution to stain collagen in blue.

11- Washing: Wash 3x 1 minute with DDW.

12- Differentiation: Incubate the sections for 2 minutes with 1% of Acetic Acid to render the shades of color more delicate and transparent. Discard this solution after use.

13- Washing: Wash 2x 1minute with DDW.

14- Dehydration: Drain successively in

-70% EtOH for 3 minutes

-90% EtOH for 3 minutes

-100% EtOH for 3 minutes

-Xylol for 5 minutes

-Drain the slides on a tissue

15- Mounting: Mount the slides with 1-2 drops of a xylene-based mounting media and cover with cover slides, avoid bubbles.

16- Press the slides under heavy weight for 10 minutes at room temperature.

17- Store the slides at room temperature.

Part V: Fibre typing

The principle relies on the ability of the enzyme to remove the terminal phosphate from the ATP, which then combines with calcium in the incubation solution to form an insoluble calcium phosphate. Cobalt is then exchanged for the calcium, which, after reaction with ammonium sulphide, forms a black, insoluble cobalt sulphide at the site of enzyme activity.

Reagents:

1% calcium chloride:

Calcium chloride	5.0 g
Distilled water	500ml

2% Cobalt chloride:

Cobalt chloride	10.0 g
Distilled water	500 ml

1% Ammonium sulphide:

20% ammonium sulphide	0.5 ml
Distilled water	9.5 ml

Alkaline Stock:

7.05% Glycine	2ml
7.5% Calcium Chloride	2ml
5.625% Sodium Chloride	2ml
3.5% Sodium Hydroxide	2ml

Distilled water 42ml

ATP Incubating Medium:

Alkaline Stock 25 ml

ATP (Sigma A-7699) 40 mg

Adjust to pH 9.4 - 9.5 with 0.1M HCl

Staining procedure:

1- Place one slide from each sample in a separate, labelled Coplin jar for each pre-incubation solution.
2- Incubate in the solution with the pH of 10.20 for 15 minutes.
3- After the incubation time period, pour out the solution and rinse one time with DDW for 3 min.
4- Pour the ATP solution into the staining jar and leave for 15 minutes.
5- Wash staining jars with 3 changes of 1% calcium chloride for a total of about 10 minutes (~3min each).
6- Add 2% cobalt chloride to each jar for 10 minutes.
7- Rinse 3 x 3min with DDW
8- Incubate with 1% Ammoniumsulfide for 1 min at room temp until the color develops.
9- Rinse 3 x 3min with DDW.
10- Drain successively in

- 70% EtOH for 3 minutes

- 90% EtOH for 3 minutes

- 100% EtOH for 3 minutes

- Xylol for 5 minutes

-Drain the slides on a tissue

11- Mount the slides with 1-2 drops of a xylene-based mounting media and cover with cover slides, avoid bubbles.

12- Press the slides under heavy weight for 10 minutes at room temperature.

13- Store the slides at room temperature.

Pre-incubation PH	Fibre type 1	Fibre type 2
10.2	Light	Dark

Part VI: Immunohistochemistry

Reagents

TBS:

To Prepare 1 L add 24.2 g Trizma base (C4H11NO3) and 80 g sodium chloride (NaCl) to 1 L dH2O. Adjust pH to 7.6 with concentrated HCl. To prepare 1 L of TBS add 100 ml 10X TBS to 900 ml dH2O

*Blocking buffer***:** 5% BSA, 0.3% Triton X100 in 9.5 ml TBS

1X BSA from 100X: 10 micro BSA in 990 micro TBS.

TBS/0.3% triton: 997 ml TBS+3 ml triton

Blocking buffer: 50 ml BSA to 950 ml TBS/0.3% triton to 4750 micro 1X TBST and add 250 µl BSA

DAB preparation of stock Solutions:

1% DAB (20x) in Distilled Water: Add 0.1g of DAB (3, 3'diaminobenzidine, Sigma Cat#D8001 or DAB-tetrahydrocholoride) in 10 ml distilled water. Add 10 N HCl 3-5 drops and solution turns light brown color. Shake for 10 minutes and DAB should dissolve completely. Aliquot and store at –20 °C. DAB Working Solution: Add 250 µl of 1% DAB to 5 ml of PBS, pH 7.2 and mix well. Add 250 µl of 0.3% H_2O_2 and mix well.

Fixation

1- Fix slides by immersion in cold acetone (-20°C) for 2 minutes or other suitable fixative (e.g. alcohol, formal alcohol, formalin, etc.), air dry at RT and proceed to staining. Then Place slides in TBS bath. Gently change TBS bath several times to remove residual acetone.

2- Alternatively, the frozen section slides can be stored for a short period of time at -80°C in a sealed slide box. When ready to stain, remove slides from freezer and warm to -20°C in the cryostat or -20°C freezer, fix for 2 minutes in cold fixative (acetone or other suitable fixative) and allow adjusting to RT to continue with the staining.

3- When staining cryostat sections stored in a freezer, thaw the slides at room temperature for 10-20 minutes to equilibrate.

Staining

1- Quickly transfer the slides to 1 X TBS and wash, dipping in and out of the solution twice for 5 minutes.

2- Incubate for 10 minutes at room temperature in 3% H2O2 diluted in methanol (To prepare, add 10 ml 30% H_2O_2 to 90 ml methanol and Store at -20°C).

3- Transfer to another Coplin jar containing TBS and wash twice for 5 min.

4- Transfer to another Coplin jar for a second wash in TBS for 5 min.

5- After wash in TBS add blocking serum for 30 min to block nonspecific bindings.

6- Remove blocking solution without washing.

7- Apply 250 µl of primary antibody at 1/100 dilution, and incubate for 2 h at room temperature in a humid chamber. To keep the chamber humid, a paper towel soaked with H2O placed at the bottom of the chamber will suffice. To optimize the dilution of antibody use TBS + 1% of BSA or the blocking buffer at the diluent.

8- After incubation with the primary antibody, wash slides two times in TBS for 3 min.

9- Add 250 µl secondary antibody, diluted in blocking solution. Incubate 30 minutes at room temperature.

10- Remove secondary antibody solution and wash sections three times in wash buffer for 5 minutes each.

11- Application of ABC solution: Preform the ABC complex by mixing 10 µL of avidin and 10 µL of biotin-peroxidase in 1 mL of TBS and incubating for 10 min. Apply 100 µL of ABC solution to each tissue section for 30 min at room temperature.

12- Wash slides three times in TBS for 3 min

13- Incubate slides in DAB solution. The DAB solution should be made up fresh for each staining procedure just before use in fumehood (DAB is known to have carcinogenic effects). The DAB development reaction should be monitored closely under the microscope. The usual development reaction takes 10–20 min.

14- As soon as the sections develop, immerse slides in DDW.

15- Counterstain in hematoxylin for 2 min.

16- Wash sections in DDW 2 x 5 minutes each.

17- Dehydrate sections in

- 70% EtOH for 3 minutes
- 90% EtOH for 3 minutes
- 100% EtOH for 3 minutes
- Xylol for 5 minutes
-Drain the slides on a tissue
- Xylol for 5 minutes
-Drain the slides on a tissue

18- Mount the slides with 1-2 drops of a xylene-based mounting media and cover with cover slides, avoid bubbles.

19- Press the slides under heavy weight for 10 minutes at room temperature.

20- Store the slides at room temperature